

The Eocambrian Valdres Group at Rundemellen, Mellane

*Field observations and sedimentpetrographical
analysis*

Kathrine Sørhus



Master Thesis in Geoscience
Petroleum Geology and Petroleum Geophysics
30 credits

Department of Geosciences
Faculty of Mathematics and Natural Science

UNIVERSITY OF OSLO

June 2017

The Eocambrian Valdres Group at Rundemellen, Mellane

Field observations and sedimentpetrographical analysis

Kathrine Sørhus



Master Thesis in Geoscience
Petroleum Geology and Petroleum Geophysics
30 credits

Department of Geosciences
Faculty of Mathematics and Natural Science

UNIVERSITY OF OSLO

June 2017

© Kathrine Sørhus, 2017

Tutor: Prof. Henning Dypvik, UiO

This work is published digitally through DUO – Digitale Utgivelser ved UiO

<http://www.duo.uio.no>

It is also catalogued in BIBSYS (<http://www.bibsys.no/english>)

Trykk: Reprosentralen, Universitetet i Oslo

All rights reserved. No part of this publication may be reproduced or transmitted, in any form or by any means, without permission.

Abstract

Sedimentary rocks from Rundemellen located in Østre Slidre, Valdres have been studied in field. Sedimentary field data in addition to petrographical and mineralogical analysis (thin sections, SEM, XRD and heavy mineral analysis) have been used to interpret depositional environment and provenance.

The Eocambrian Valdres Group at Rundemellen is composed of coarse-clastic sedimentary rocks deposited in a fluvial braided stream environment. Conglomerates and coarse arkosic sandstones make up most of the successions in the Valdres Group, but thin layers of fine-grained sandstones also occur in between the coarser layers. Quartz/total feldspar ratios together with thin section observations, mineralogical composition and heavy minerals suggest either a relatively long transport or texturally mature source rocks for the Valdres Group at Rundemellen.

Sedimentary structures as cross-bedding, trough cross-bedding and imbrication provided information of the transport direction of the river streams and paleocurrent directions were measured. An ESE transport direction was found at Rundemellen, indicating that the river transported sediments from a source area in WNW. These measurements were used to discuss different possibilities of provenance.

Facies were divided into groups (1-4) based on lithology and the sandstone facies were divided into sub-groups based on sedimentary structures observed in field. Facies associations were divided into four groups where three reflects specific depositional environments within a braided river. Facies association 4 (FA 4) is represented by a glacier tillite deposit of Varanger age which is correlated with the Moelv tillite of the Hedmark Group.

Comparison of depositional environment with the Rendalen Formation of the Hedmark Group and the Valdres Group at Rundemellen revealed that the depositional environments were quite similar. Mineralogical correlation with the Ring Formation showed that the main mineral composition is the same and may support the theory of a Sveconorwegian origin for both the Valdres Group and the Hedmark Group.

Acknowledgements

First I want to thank my supervisor Professor Henning Dypvik at the Department of Geosciences at the University of Oslo. Thank you for always being open for questions and discussions. Thank you for your understanding and support this semester.

I would also like to thank my fellow student and partner in crime, Rikke Øya Småkasin, for fun times during fieldwork, valuable discussions and for proofreading my thesis.

Thanks to Salahalldin Akhavan for preparing my thin sections and Andrew C. Morton for doing the heavy mineral analysis. Thanks to Berit Løken Berg for assisting me during SEM. Thanks to Chloé Marcilly for preparing the XRD and to Beyene Girma Haile for running the XRD.

A thank you must also be given to Phd Katrine Fossum for helpful guidance with the software diffract Eva and to Postdoc. Lars Riber for guidance with the software Siroquant. Thank you to Postdoc. Kjetil Indrevær for your helpful guidance with the stereoplot. A big thanks must also be given to Professor Johan Petter Nystuen for valuable discussions. Thank you to Småforsk for financial support during this thesis.

Thanks to Mali Brekken for proofreading my thesis and to my sister, Elisabeth, for support and for motivating me with candy. Thank you to my beloved Lars who has put out with me being stressed about my thesis. Your love and support is very much appreciated. Thanks to my family for supporting and encouraging me through my studies.

Table of Content

1	Introduction	1
1.1	Background	1
1.1.1	Study area	1
1.1.2	Previous studies	2
1.2	Geological framework	4
1.2.1	Tectonostratigraphic development	4
1.2.2	Lithostratigraphy of the Valdres basin and the Hedmark basin	7
1.2.3	Thrust sheet complexes	10
2	Methodology	12
2.1	Fieldwork	12
2.2	Facies and facies association	13
2.3	Petrographical and mineralogical analyses	13
2.3.1	Thin section	13
2.3.2	Point counting and rock characteristics	15
2.3.3	Scanning electron microscope (SEM)	15
2.3.4	X-ray diffraction analyses	16
2.3.5	Heavy mineral analysis	18
3	Results	20
3.1	Field measurements	20
3.2	Facies	20
3.3	Facies associations	28
3.3.1	FA 1	30
3.3.2	FA 2	31
3.3.3	FA 3	31
3.3.4	FA 4	31
3.4	Petrographical analysis	31
3.4.1	Results of thin sections and point counting	31
3.4.2	Results of scanning electron microscope analysis	38
3.5	XRD Results	41
3.6	Heavy mineral analysis	44
4	Discussion	45
4.1	Depositional environment	45
4.1.1	FA 1	46
4.1.2	FA 2	48
4.1.3	FA 3	50
4.1.4	FA 4	50
4.1.5	Braided river depositional environment	50
4.2	Mineralogical observations	52
4.3	Environmental setting	54
4.3.1	Transport and maturity	54
4.3.2	Rift-controlled basin	56
4.3.3	Provenance area	57
4.4	Correlation with Skarvemellen	58
4.5	Correlation with the Hedmark Group	63
4.5.1	Correlation with the Ring Formation	63
4.5.2	Correlation with the Rendalen Formation	65

5 Conclusion.....	67
References	69
Appendix A (Thin sections)	I
Appendix B (Point counting).....	VII
Appendix C (XRD).....	IX
Appendix D (Heavy minerals).....	XIII
Appendix E (Field measurements)	XIV

1 Introduction

1.1 Background

The Valdres Group is one of the least studied and understood sedimentary formations in the southern Norwegian Caledonides. The several hundred meters thick siliciclastic succession was possibly deposited in an alluvial/fluvial environment and probably in a rift setting (Loeschke and Nickelsen, 1968). The sedimentary rocks of the Valdres Group were subjected to low-grade metamorphism during the Caledonian orogeny (Loeschke and Nickelsen, 1968; Bockelie and Nystuen, 1985). They are well exposed, and it is possible to map the sedimentary succession far outside the study area.

This master thesis is based on geological mapping, sedimentological logging, sampling and petrographical analysis of the Rundemellen type sedimentary succession in the Valdres Group at Rundemellen, located in Mellane, Østre Slidre (Figure 1.1). The data for the thesis was gathered during fieldwork in July 2016 by Rikke Øya Småkasin and the author. The aim of this thesis is to improve the understanding of the Valdres Group by analyzing rock sequences and samples from Rundemellen. The focus will be on depositional environment. Correlation with the Ring Formation in the Hedmark Group will also be done, to see if there are any mineralogical relations between the sedimentary formations. Correlation with the Rendalen Formation in the Hedmark Group and the Valdres Group will be done to see if there is any relation between the depositional environments. The Hedmark Group and the Valdres Group were deposited in two different basins located close to each other at the western margin of Baltoscandia, the Hedmark Basin and the Valdres Basin respectively (Figure 1.5). Supervisor for this thesis is Professor Henning Dypvik at the Department of Geoscience, University of Oslo (UiO).

1.1.1 Study area

Rundemellen is located at Mellane in Østre Slidre, Valdres (Figure 1.1). It is the highest of five mountains in Mellane and ranges 1345 m.a.s.l. The area has experienced different tectonic regimes from Late Precambrian to Silurian time (Kumpulainen and Nystuen, 1985; Lamminen et al., 2015). Rifting in Late Precambrian resulted in the formation of the Valdres Basin and compression in Late Cambrian-Early Devonian time

resulted in the Scandinavian Caledonides (Hossack and Cooper, 1986). The Caledonian orogeny generated thrust sheets (Figure 1.7 and 1.8) that were transported for many kilometers from a NNW direction (Figure 1.5) (Nystuen and Lamminen, 2011). During the movement of these thrust sheets, deformation of the sediments within occurred.

The Valdres Group is today seen as an overturned succession situated above the younger Mellseinn Group. The two groups are separated by a breccia believed to have been deposited during the Varanger Glaciation (~ 650 Ma).

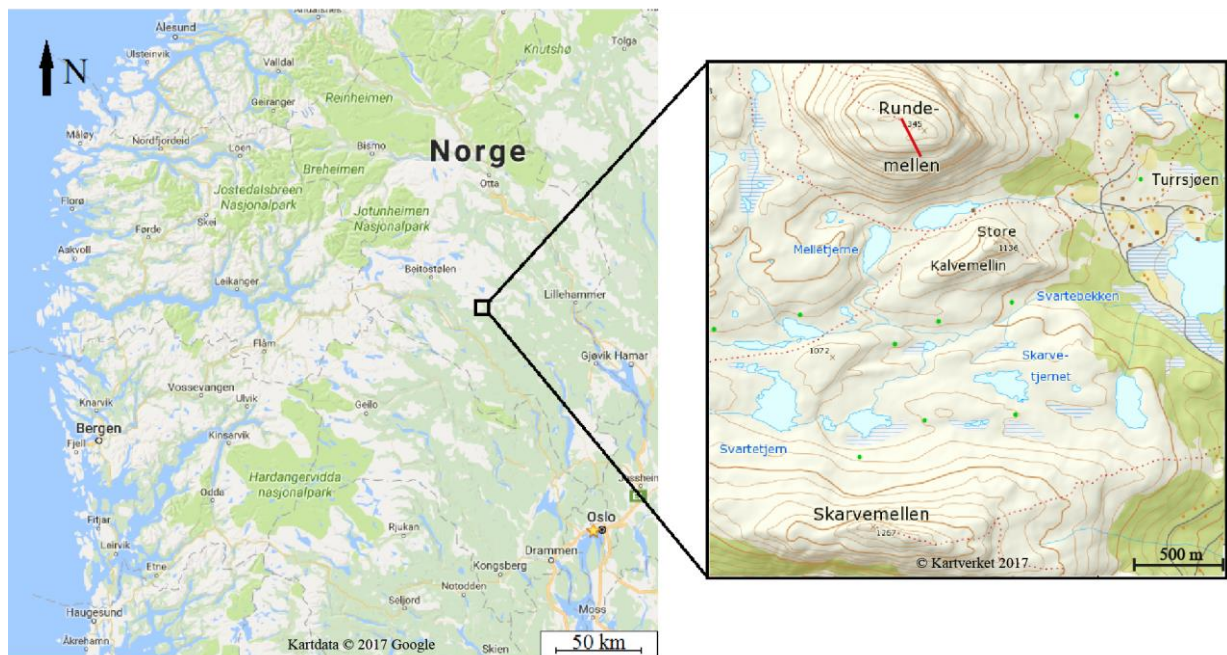


Figure 1.1: Map over southern Norway to the left and the field location (Rundemellen and Skarvemellen) to the right. The red line marks the logged section at Rundemellen (Google Maps, 2017 and Kartverket, 2017).

1.1.2 Previous studies

The geology of the Valdres area has not been studied in great detail since the 1970-80's, when the focus was mainly on structural geology and deformation from the Caledonian orogeny. The bedrock geology was first known in 1855 after published papers and geological maps from Kjerulf (1855-1887), Kjerulf and Dahl (1866) and Törnebohm (1873, 1882). Kjerulf (1879) estimated the relative ages of the Precambrian basement rocks, Upper Proterozoic sparagmites and Silurian strata.

The term sparagmite was first introduced by Esmark (1829) for the coarse-grained feldspatic successions in the Valdres- and Hedmark Basin. This term is no longer used, but remained for the outcrop areas of these successions in southern Norway (Bockelie and Nystuen, 1985). Through a series of profiles, Kjerulf (1873) showed folding characteristic for the Silurian strata in the lower allochthon. Törnebohm (1888) discussed the position of the overthrust and deformed Precambrian successions in the Valdres area (Bockelie and Nystuen, 1985).

In the early 1900's Bjørlykke (1905), Goldschmidt (1916) and Strand (1959) discussed the age and tectonic position of the Valdres Group. They suggested an Upper Ordovician or Lower Silurian age for the Valdres Group. The position of the Valdres Group was interpreted to be above the lower Jotun nappe and below the upper Jotun nappe. In the 1960's Kulling (1961), suggested an Eocambrian age for the Valdres Group, based on his work on similar successions in Sweden. He believed that the Valdres Group formed a separate tectonic unit; The Valdres nappe. Holtedahl (1959) agreed on an Eocambrian age for the Valdres Group, based on his observations at Grønsennknipa to the southwest of Mellane. Today there is an agreement on an Eocambrian age for the Valdres Group (Loeschke, 1967; Nickelsen, 1967; Heim et al., 1977; Nickelsen et al., 1985; Nystuen and Lamminen 2011). The amount of movement of the allochthonous thrust sheets in the Valdres Basin is still a topic of debate.

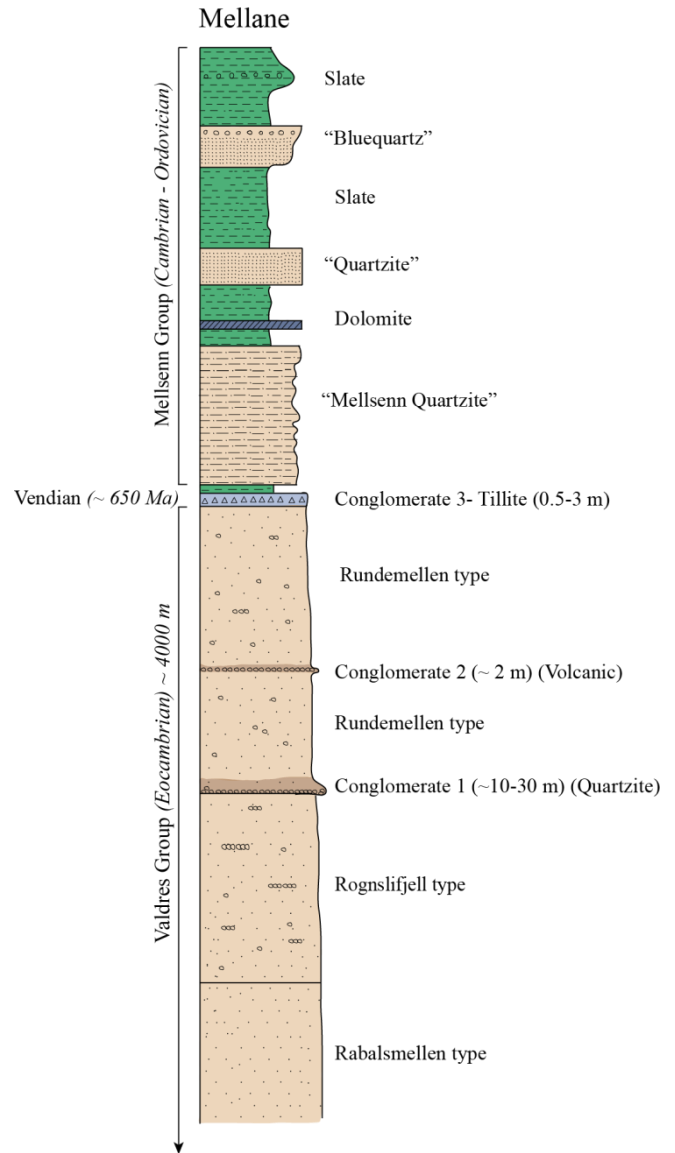


Figure 1.2: Lithostratigraphic column of the Valdres Group and the Mellseinn Group at Mellane. A thin tillite layer separates the Valdres Group from the younger Mellseinn Group. All the sparagmite types are shown in the stratigraphic column. Modified from Hossack et al. (1985) and based on descriptions from Loeschke and Nickelsen (1968).

Loeschke (1967) carried out detailed petrographical analysis at Mellane. Based on observation in field and petrographical analysis, he described the sedimentary successions (Valdres Group and Mellsehn Group) at Rundemellen and Skarvemellen at Mellane.

In the 1980's several papers were published by Nickelsen et al., (1985), Hossack et al., (1985), Kumpulainen and Nystuen (1985), where they discuss the stratigraphy, age and tectonic position of the Valdres Group.

1.2 Geological framework

1.2.1 Tectonostratigraphic development

During Late Precambrian (Figure 1.4), an intracontinental rupture led to the formation of several rift basins within Baltica, from Ukraine in the east and Scandinavia in northwest (Kumpulainen and Nystuen, 1985). This rifting event is related to the break-up of the supercontinent Rodinia (~750-600Ma) (Figure 1.3), where the continent Baltica in west was separated from the continent Laurentia in east during the opening of the Iapetus Ocean (Kumpulainen and Nystuen, 1985).



Figure 1.3: Some parts of the supercontinent Rodinia located close to equator at 750 Ma. The red line marks the position of the Valdres- and Hedmark basins created during the opening of the Iapetus Ocean. Modified from Hartz and Torsvik (2002).

Along the southwestern part of the Baltoscandian margin of Baltica three rift basins were created; The Valdres Basin, Hedmark Basin, and Engerdalen Basin (Figure 1.5), where the Hedmark Basin is the largest (Nystuen and Lamminen, 2011). Further stretching after the basins were formed, led to deeper basins with more accommodation. The Valdres- and Hedmark basin were closely located (Figure 1.5) and it is assumed that the two basins went through a similar geological development from Late Precambrian to Cambrian times (Nystuen, 2013). These two basins will further be described.

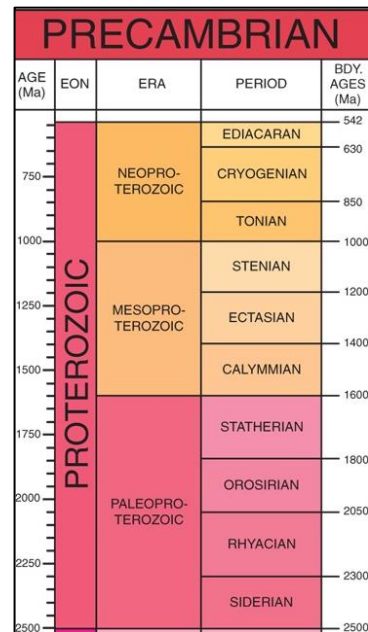


Figure 1.4: Geological time-scale for the Proterozoic (Walker et al., 2012)

The Valdres Basin was located in the western part of Baltoscandia (Figure 1.5) in Neoproterozoic time (Figure 1.3). During the early stages (Precambrian-Cambrian) the area was dominated by shallow depths and coarse clastic sediments from rivers were deposited the basin (Loeschke and Nickelsen, 1968). These sedimentary deposits are today known as the Valdres Group (Figure 1.2 and 1.6). Due to the textural immaturity, lithologic diversities and variable thickness of the Valdres Group sedimentary rocks, Nickelsen et al. (1985) suggested that the Valdres Group was deposited in an area with considerable relief, and possibly near a continental margin during the opening of the Iapetus Ocean. According to Heim et al., (1977), the Eocambrian arkosic sandstones in the Valdres Group were deposited as a result of uplift and erosion. Structural studies have disclosed the Valdres Group to be allochthonous and recumbently folded (Nickelsen, 1967). The Valdres Group lies within the Valdres thrust sheet, which will further be described in chapter 1.2.3.

The Hedmark Basin is the largest of the basins formed at the southwestern part of Baltoscandia (Figure 1.5) during the continental break-up of Rodinia (Figure 1.3). The basin is 200-300 km wide in east-west direction, and a few hundreds of km long in the NNE- SSW direction (Bockelie and Nystuen, 1985). A several thousand meters thick sedimentary sequence was deposited in the Hedmark Basin, known as the Hedmark Group (Figure 1.6). In the western part of the Hedmark Basin, ocean water covered large areas and turbidite sandstones and mud were deposited. In the eastern part of the basin, coarse grained sediments

from rivers were deposited (Bjørlykke et al., 1976). The Hedmark Group occurs in the Osen-Røa thrust sheet complex in the Lower allochthon of the Caledonian thrust sheets.

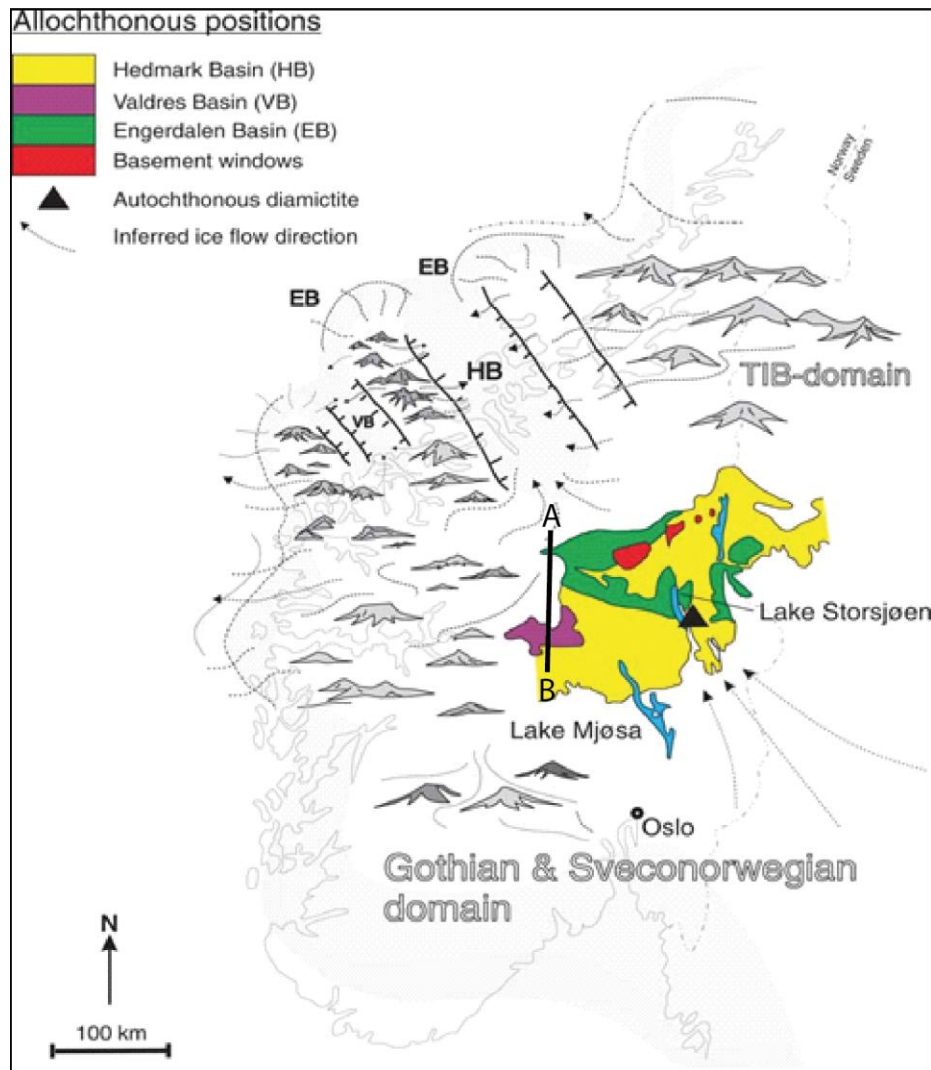


Figure 1.5: The position of the Valdres Basin (VB), Engerdalen Basin and the Hedmark Basin (HB) at the western part of Baltoscandia. The colors indicate the present position of the basin deposits, after they were transported several hundreds of km in SE direction. TIB is the Trans-Scandinavian Igneous Belt. The dotted lines show the movement direction of the ice sheet during the Varanger Glaciation (from Nystuen and Lamminen, 2011). Profile A-B is shown in Figure 1.8.

Seven stages for the structural-sedimentary evolution of the Hedmark Basin have been suggested by Nystuen (1987, p. 404- 412):

1. Pre-rift sedimentation and initial formation of the main graben (Brøttum Fm)
2. Rifting and basin expansion (Rendalen Fm)
3. Rifting, volcanism and basin submergence (Rendalen Fm)
4. Rifting, sub-basin and basin expansion (Biri Fm, Biskopåsen Conglomerate, Ring Fm)

5. Late rifting and glaciation (Moelv Tillite)
6. Late rifting (Ekre Fm)
7. Post rifting and subsidence (Vangsås Fm)

During the Varanger Glaciation (~650 Ma), a glacier ice sheet covered large areas of Baltica (Kumpulainen and Nystuen, 1985). The ice sheet moved towards west and into the western basins of Baltoscandia (Figure 1.5). The main facies of the glacial Varanger Formation comprises a basal tillite which has been observed in the Hedmark Basin by the Moelv Formation. In the Valdres Basin a breccia has been interpreted to represent the glacier Varanger deposit. It occurs as erosional remnants on the continental platform along the front of the Caledonian thrust sheets (Kumpulainen and Nystuen, 1985). It makes up an important surface for regional stratigraphic correlation. According to Kumpluainen and Nystuen (1985) the tillite from the Varanger glaciation is not found east of the Caledonian thrust sheets in Scandinavia.

The Neoproterozoic basinal successions of southwestern Norway were folded and thrust on top of each other during the Caledonian orogeny, when Laurentia and Baltica collided. They were thrust inland from the southwestern margin of Baltoscandia (Figure 1.5), and are today present in thrust sheets and thrust sheet complexes of the Caledonides (Lamminen et al., 2015).

1.2.2 Lithostratigraphy of the Valdres basin and the Hedmark basin

The Mellsenn Group

The Mellsenn Group consists of quartzites and slates that make up a sequence of approximately 240 meter (Figure 1.2 and 1.6). It has previously been described by Loeschke (1967) at the south face at Mellane. A Cambrian-Ordovician age has been suggested for the Mellsenn Group, based on the occurrence of *graptolites* and *dictyonema* in the sedimentary rocks. The Mellsenn Group is overturned and positioned underneath the older Valdres Group sedimentary rocks. A breccia believed to represent a Varanger glacier deposit separates the two sedimentary successions (Figure 1.2) (Nickelsen et al., 1985).

The Valdres Group

The Valdres Group (Figure 1.2 and 1.6) has been interpreted to be allochthonous and occurs as an intermediate thrust sheet underneath the Jotun thrust sheet in northwest and above the Synnfjell thrust sheet (Figure 1.8) in southeast at Mellane (Loeschke and Nickelsen, 1968). The Valdres Group is characterized by coarse clastic arkosic sandstones and conglomerates that make up a sequence of at least 4000 meter (Figure 1.2 and 1.6) (Nickelsen et al., 1985). The coarse grained arkosic sandstones have been interpreted to represent braided streams, possibly on alluvial fans or alluvial flood plains. The conglomerates are thought to have been formed at the base of an alluvial fan, and are pebble- or boulder-bearing (Kumpulainen and Nystuen, 1968).

Two conglomerates occur in the Valdres Group succession; a quartzitic conglomerate (Conglomerate 1, Figure 1.2) and a volcanic pebble conglomerate (Conglomerate 2 in Figure 1.2). Several of the clasts in the conglomerates show evidence of deformation, and has been elongated under the pressure of the Jotun thrust sheet (Hossack, 1968). A breccia thought to represent a Varanger glacier deposit separates the Valdres Group from the younger Mellsenn Group (Conglomerate 3 in Figure 1.2) (Nickelsen et al., 1985). Three different types of feldspathic arenites occur in the Valdres Group, where each has been given a name according to their area of occurrence; Rabaldsmellen type, Rognslifjell type and Rundemellen type (Figure 1.2) (Loeschke, 1967). These feldspathic arkoses will further be described, based on their occurrence in field and petrography.

The Rabaldsmellen type is the oldest of the three types of arkoses at Mellane (Figure 1.2) (Loeschke, 1967). Fine-grained and coarse-grained layers alternate in this succession and the color varies from green and pink towards grey tones. Dark lines or veins rich in heavy minerals can often be seen, and was probably formed in hydrothermal veins of uncertain thickness (Loeschke, 1967). Conglomerates have not been found in the Rabaldsmellen type arkose. The thickness is suggested to be around 1000 meters (Loeschke, 1967).

The Rognslifjell type arkose (Figure 1.2) is very coarse grained, poorly sorted and contains several conglomerate layers. It is known as tricolor arkose because of pink-purple fragments of feldspar and white quartz fragments in a greenish matrix. The Rognslifjell type arkose consist of normal- and quartz greywackes, and show slight foliation in field (Loeschke and Nickelsen, 1968).

The Rundemellen type arkose (Figure 1.2) occupies large areas of Mellane, and is the most common arkose type at Rundemellen and Skarvemellen and the main focus in this thesis. It is more fine-grained than the Rognslifjell type and is light pink to greenish in color. The mineralogical composition of the Rundemellen and Rognslifjell type arkose is the same, but the amount of the different components varies (Loeschke and Nickelsen, 1968). The Rundemellen type is better sorted and contains more quartz, but less feldspar and phyllosilicates than the Rognslifjell type arkose (Loeschke and Nickelsen, 1968). At Rundemellen it is seen as a light pink towards red and purple arkose. The thickness is estimated to be ~ 650 m at Rundemellen, but is probably tectonically reduced (Loeschke, 1967).

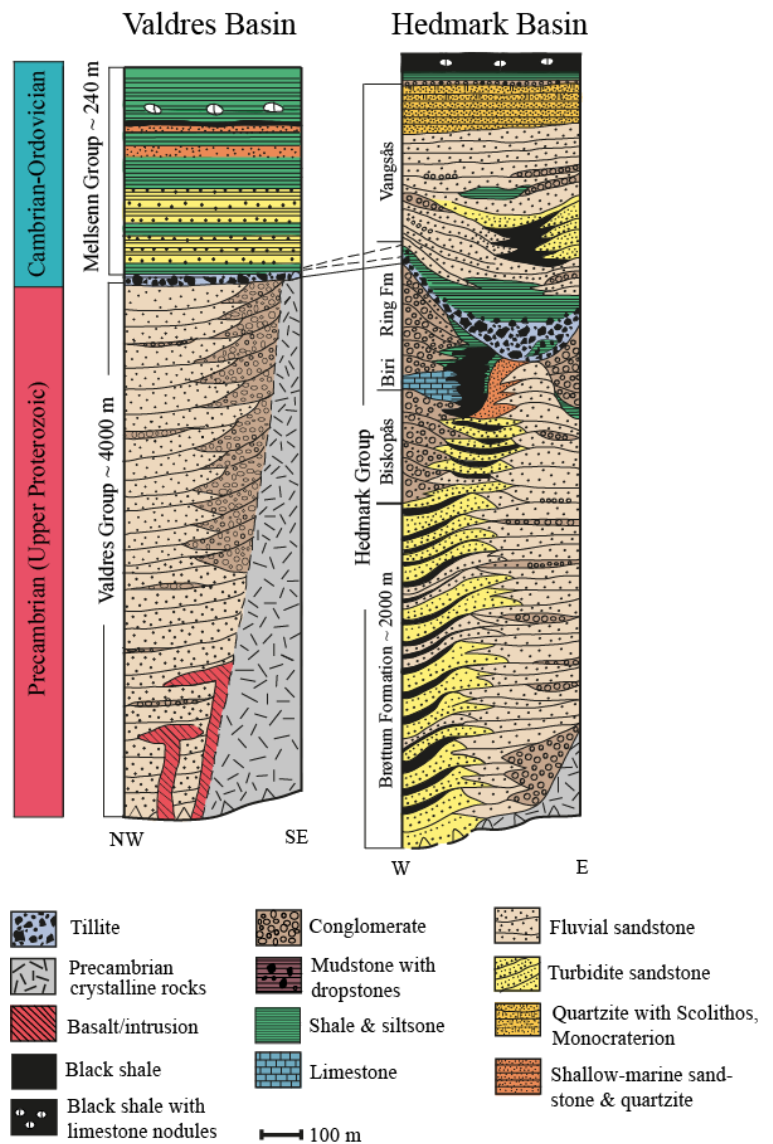


Figure 1.6: Lithostratigraphic column through the Valdres- and Hedmark Basin. Modified from Bockelie and Nystuen (1985) and Kumpulainen and Nystuen (1985).

The Ring Formation

The Ring Formation is a Neoproterozoic (Figure 1.4) sedimentary succession mainly consisting of arkoses and conglomerates, deposited from rivers and as fan deltas in the western part of the Hedmark Basin (Bockelie and Nystuen, 1985). The Ring Formation has in the Moelv area been interpreted to be a part of a submarine fan environment, today called the Ring submarine fan. The subaqueous conglomerate bodies pinches out into Biri shales or Brøttum sandstones (Bockelie and Nystuen, 1985).

The Rendalen Formation

The Rendalen Formation consists of fluvial sandstones and conglomerates deposited in the eastern part of the Hedmark Basin in Late Proterozoic (Figure 1.4). The Rendalen Formation is a sedimentary succession with a thickness of approximately 2500 meters and is composed of red and light grey, coarse-grained arkosic sandstones (Nystuen, 1982). These coarse clastic sedimentary successions were deposited in the continental part of the Hedmark Basin by rivers. Analysis of zircons has been carried out by Bingen et al. (2005a) and showed that the catchment for the Rendalen Formation was dominated by granitic rocks of approximately 1,48 Ga. The Rendalen Formation rests on the allochthonous basement sheets of the Osen-Røa thrust sheet complex with a depositional contact, both east and west of Femunden (Nystuen, 1982). It is believed that the Rendalen Formation is an eastern lateral equivalent to the turbidites of the western Brøttum Formation deposited during Vendian time (Nystuen, 1982).

1.2.3 Thrust sheet complexes

The following chapter will focus on the thrust sheet complexes of the Valdres- and Hedmark area. The Lower allochthon is composed of the Synnfjell thrust sheet and the Osen-Røa thrust sheet complex (Figure 1.7). The Middle allochthon consists of the Kvitvola thrust sheet, the Valdres thrust sheet and the Jotun thrust sheet (Figure 1.7 and 1.8).

Lower allochthon

The Lower Allochthon consists of the Synnfjell thrust sheet and the Osen-Røa thrust sheet complex (Figure 1.7 and 1.8) (Bockelie and Nystuen, 1985). The Synnfjell thrust sheet was thrust over the Osen-Røa thrust sheet (Figure 1.8) and has its roof at the detachment in the base of the Valdres thrust sheet or the

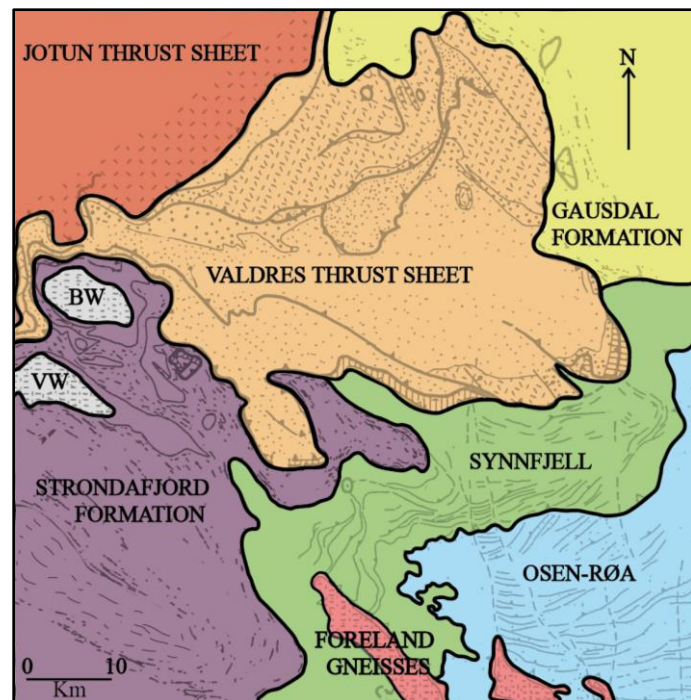


Figure 1.7: Thrust sheets of the Lower Allochthon (Synn timer and Osen-Røa) and the Middle Allochthon (Jotun and Valdres thrust sheets). The basement windows are shown in brown color, where BW is the Beito window and VW is the Vang window (Modified from Nickelsen et al., 1985).

Strondafjord Formation (Hossack et al., 1985). The Synnfjell thrust sheet consists of repeated sections with sedimentary units of the Dalselvi Formation and the Ørneberget Formation. According to Nickelsen et al., (1985), the Dalselvi Formation correlates with the sedimentary rocks of the Valdres Group and the Ørneberget Formation correlates with the sedimentary rocks of the Mellseinn Group. In the Valdres area the Synnfjell thrust sheet rests directly on the autochthon.

The Osen-Røa thrust sheet (Figure 1.7 and 1.8) is interpreted as one tectonic unit that includes the Osen thrust sheet at the thrust sheet front and the Røa thrust sheet towards north in the window region (Figure 1.7) (Bockelie and Nystuen, 1985). Upper Proterozoic to Lowermost Cambrian sedimentary rocks of the Hedmark Group make up the Osen-Røa thrust sheet. West of lake Femunden they make up one tectonic unit, and east of lake Femunden the Røa thrust sheet is thrust over the Osen thrust sheet (Bockelie and Nystuen, 1985).

Middle allochthon

The Middle allochthon consist of the Jotun thrust sheet and the Valdres thrust sheet (Figure 1.7). The Jotun thrust sheet was thrust over the Valdres thrust sheet leading to deformation of the sedimentary rocks of the Valdres Group in the Valdres thrust sheet. There is no agreement on how far

the Jotun thrust sheet was transported during the Caledonian deformation (Hossack et al., 1985). The Jotun nappe consists of basement rocks, where the oldest are basement gneisses, metamorphosed in amphibolite and granulite facies (Hossack et al., 1985). These basement gneisses can also be seen in the Valdres thrust sheet.

The Valdres thrust sheet (Figure 1.7 and 1.8) consists of Precambrian gneisses and the sedimentary rocks of the Valdres- and Mellseinn Group. The gneisses are stratigraphically overlain by the Valdres Group sedimentary rocks, which in turn is stratigraphically overlain by the Mellseinn Group (Hossack et al., 1985). The Valdres thrust sheet in west is an equivalent to the Kvitvola thrust sheet (Figure 1.8) in east.

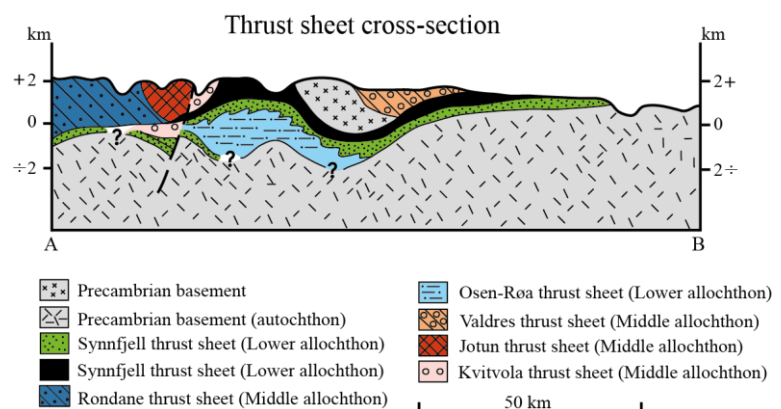


Figure 1.8: Cross-section through profile A-B displaying how the different thrust sheets occur along the profile. The profile is shown in Figure 1.5. Modified from Bockelie and Nystuen (1985).

2 Methodology

2.1 Fieldwork

Fieldwork and sedimentological sampling at Mellane, Østre Slidre were carried out by Rikke Øya Småkasin and the author 18-30th of July 2016, under supervision of Professor Henning Dypvik at the Department of Geoscience, University of Oslo (UiO). The localities visited were Rundemellen and Skarvemellen (Figure 1.1) where the reference name used were “RUND” and “SKA”. The samples were named based on the locality reference together with sample number and the year of collection (e.g. Rund 1-6-16). Approximately 400 meters were in total logged from the two localities (Rundemellen and Skarvemellen) using a logging sheet with scale 1:100, and in areas with greater variations a detailed log with scale 1:20 was made. The Rundemellen section is presented in this thesis while the Skarvemellen section is presented by Småkasin (2017). Samples were collected from the two profiles while logging with close spacing. A grain size chart based on Wentworth’s (1922) grain size classes (Table 2.1) was used during logging to differentiate between the grain sizes.

During two days in September (9th and 10th) 2016, Rikke Øya Småkasin and the author went back to Rundemellen and Skarvemellen to take a few more pictures and samples.

Table 2.1: Wentworth’s (1922) grains size classes given in millimeters and phi values.

Wentworth size classes	Phi (ϕ) units	Size in millimeters (mm)
Boulder	-8	> 256
Cobble	-6	64-256
Pebble	-4	4-64
Granule	-2	2-4
Very coarse sand	-1	1-2
Coarse sand	0	0.5-1
Medium sand	1	0.25-0.5
Fine sand	2	0.125-0.25
Very fine sand	3	0.063-0.125
Silt	4	0.004-0.063
Clay	8	< 0.004

2.2 Facies and facies association

Facies determinations are based on thin section analysis and field observations on the basis of lithology, sedimentary structures, bedding characteristics and texture (Figure 3.2). Facies is the total sum of features that represent the depositional environment under which a given rock is deposited. Facies associations are made up of facies that are genetically related to one another, and reflect a specific sedimentary environment (Reading and Levell, 1996). The facies are grouped together in facies associations (Figure 3.9).

2.3 Petrographical and mineralogical analyses

Petrographical analyses on the collected samples were performed by optical thin-section observations (Appendix A), scanning electron microscopy (SEM), heavy mineral analysis (Appendix D) and X-ray diffraction (XRD) analysis (Appendix C) based on bulk composition of the rock.

2.3.1 Thin section

A total of 19 samples representative of the lithologies at Rundemellen, were prepared by Salahalldin Akhavan at the petro-technical laboratory at the Department of Geoscience, (UiO). The samples were impregnated by blue epoxy and glued onto glass slides of 2,5cm x 4,5cm. Then the samples were polished down to a thickness of 30µm.

A Nikon Labophot-Pol petrographic microscope was used during the thin section study to observe the texture and mineralogical composition of the rock samples. Each of the

selected samples were studied under plane polarized light (ppl) and cross polarized light (cpl) in order to observe the mineralogical composition in detail. Thin section analysis provides information about the mineralogy, lithology, structures, sorting, grain size and shape.

Table 2.2: Thin section samples. Samples marked in bold have been point counted.

Sample	
Rund 1-5-16	Rund 1-15-16
Rund 1-6-16	Rund 2-8A-16
Rund 1-7-16	Rund 2-8-16
Rund 1-8-16	Rund 2-7B-16
Rund 1-9-16	Rund 2-6-16
Rund 1-10-16	Rund 2-5-16
Rund 1-11-16	Rund 2-3-16
Rund 1-12-16	Rund 2-2-16
Rund 1-13-16	Rund 2-1B-16
Rund 1-14-16	

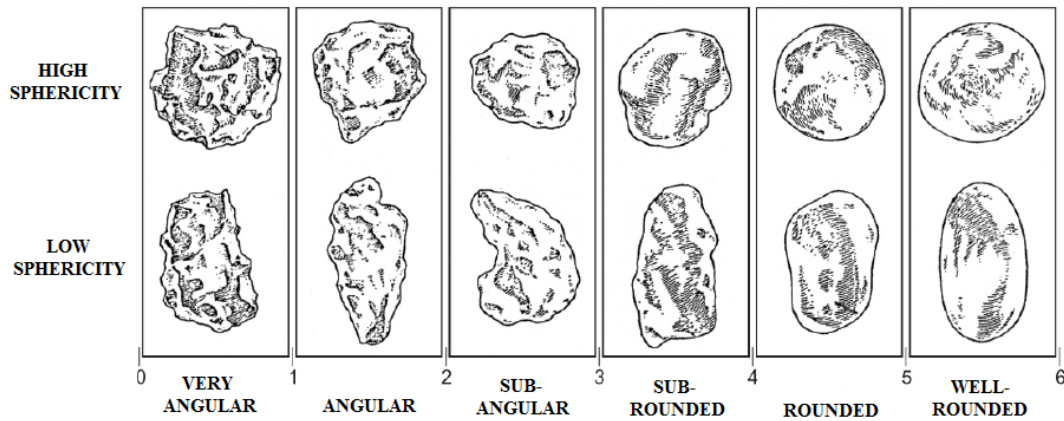


Figure 2.1: The degree of sphericity and roundness on detrital grains (modified from Powers 1953).

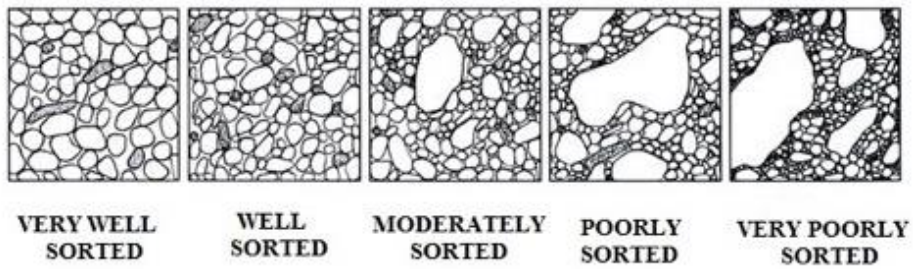
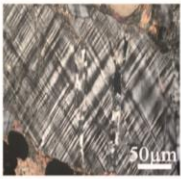
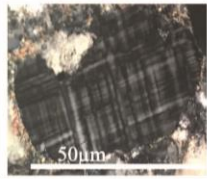
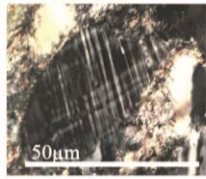
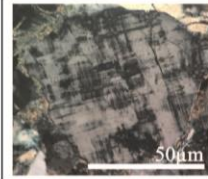
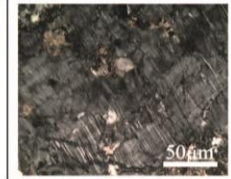


Figure 2.2: Degree of sorting modified from Compton's (1962) classification scheme.

The degree of rounding was determined based on Power's (1953) terminology (Figure 2..1) and the degree of sorting was decided based on Compton's (1962) classification scheme (Figure 2.2).

Preservation of feldspar grains have been identified and described based on five categories of preservation (Table 2.3, Appendix A). Feldspar grains identified in thin sections were assigned to a category I-V based on the degree of weathering. Each of the five categories represent a specific degree of preservation of feldspar grains, where category I is fresh and has not been subjected to weathering. Category V is the end member and the feldspar grains assigned to this category have been subjected to a high degree of weathering and is almost fully dissolved (Table 2.3)

Table 2.3: The degree of weathering on feldspar grains, ranging from category I-V. Modified from Fossum (2012).

Category	I	II	III	IV	V
Description	Fresh, has not been subjected to weathering	Subjected to some weathering. Twins almost fully preserved	Twins starts to look blurry. Grain surface show evidence of roughness	Very rough surface. Twinning might be hard to recognize. Difficult to distinguish K-feldspar	Twins are absent or hard to recognize. difficult to distinguish K-feldspar from quartz.
Example					

2.3.2 Point counting and rock characteristics

A total of 12 samples representing conglomerate-, sandstone-, fine-grained sandstone- and breccia facies were chosen for point counting, to estimate the average mineral composition in each of the chosen samples. 400 points were counted using a Nikon Labophot-Pol petrographic microscope in both plane polarized light (ppl) and cross polarized light (cpl) together with a *Swift* point counter. Quartz grains were divided into undulating and non-undulating grains in addition to monocrystalline and polycrystalline grains. Feldspar grains were separated into plagioclase and K-feldspar while point counting. Rock fragments were also counted and other visible features such as heavy minerals, pore filling cement, iron oxides, porosity and amount of matrix.

2.3.3 Scanning electron microscope (SEM)

The scanning electron microscope (SEM) was used to identify minerals that were difficult to identify or not identified in the optical analysis. 5 thin sections representing several facies were studied in greater detail in SEM, where the focus was on heavy minerals identification, feldspar preservation and zonation, authigenic minerals and feldspar overgrowth. Four samples from Rundemellen and one sample from the Ring Formation in the Hedmark Group were studied in SEM. The analysis was utilized on a HITACHI SU5000 scanning electron microscope, and interpreted in the software *Quantax 800* by Rikke Øya Småkasin and the author under supervision by Berit Løken Berg at the Department of Geoscience, (UiO). The

thin sections were coated with carbon before they were placed in the SEM. The backscatter electron image (BEI) technique was used while studying the thin sections.

2.3.4 X-ray diffraction analyses

X-ray diffractometry (XRD) was used to provide information about the mineralogical composition and the quantitative distribution of the mineral phases in a sample. A total of 19 samples from Rundemellen were selected for X-ray diffraction analyses, and prepared by M.Sc. student Chloé Marcilly at the Department of Geoscience (UiO) and run by Mr. Beyene Girma Haile at the Department of Geoscience (UiO). All of the samples were run on a *Bruker D8 Advanced* (40kV and 40mA) diffractometer, with a *Lynxeye XE High-Resolution Energy Dispersive 1D Detector*, using *CuK α* radiations.

The mineralogical composition is possible to determine from X-ray diffractions due to the mineral's specific atomic structure, giving a distinct distance between two crystallographic planes in the crystal lattice. This distance is referred to as the *d-spacing* and is given in Ångström ($1 \text{ \AA} = 10^{-10} \text{ m}$) (Goldstein et al., 2003). When a mineral is bombarded with X-ray beams it will provide a specific signature in the form of *d-values* and 2θ -values as a function of the crystallographic properties. The 2θ -values represents the diffracted angle of the X-ray beam (Moore and Reynolds, 1997).

The measured peaks of the diffracted X-ray beams are recorded as peaks in a diffractogram, given their specific *d-values* and 2θ - angles. The mineralogical composition of the samples was interpreted with the semi-quantitative *Diffrac Eva software* (Bruker, 2011) and the quantitative software *Siroquant* (Sietronics, 2013).

Bulk analysis preparation

The first step in the bulk preparation was to reduce the grain size by grounding the rock to powder in a slinging mill. In this process some of the grains were reduced to a size of $500\mu\text{m}$, but most grains were reduced to $100\text{-}200\mu\text{m}$. To avoid cross-contamination, the slinging mill was carefully cleaned with ethanol between each sample.

The next step in preparing the samples for XRD was to further reduce the grain size down to $10\mu\text{m}$. This was done by the aid of a *McCrone* micronizer machine. Approximately 5g rock

powder of a sample was mixed with 7-8ml ethanol in a small container filled with pieces of agate. The container was then placed in the micronizer machine and run for 12 minutes. The micronized dispersion was then put in an oven and dried at 50°C over night. The final step in XRD preparation of the samples was to place the micronized powder in small plastic holders by a front-loading technique. This was done carefully to avoid artificial orientation of grains in the rock powder.

DiffraC Eva software

The qualitative *DiffraC Eva* software (Bruker, 2011) was used to interpret and analyze the peaks of the X-ray diffraction data. The software helps to evaluate which mineral phases are present in the diffractogram by identifying representative peaks. The identification of minerals in the diffractogram was done using the d-spacing values and the 2θ -angles. The mineral phases were identified by the values listed in Table 2.4.

Table 2.4: The d-spacing values in Ångström used to identify the different mineral phases in the software *DiffraC Eva*.

Mineral	d-spacing (Å)
Quartz	4.26
K-feldspar	3.24
Plagioclase	3.19
Mica	10.00
Hematite	2.70
Illite	10.00

Siroquant version 4 software

The software *Siroquant* (Sietronics, 2013) was used to quantify the mineral phases that already were identified in *DiffraC Eva* (Bruker, 2011). The main goal is to find mineral phases with as identical peaks as the original diffractogram. When all of the respective mineral phases have been added, several steps need to be done before running the quantification. The method described by Hillier (2000) with a five-stage procedure was then

used. An additional sixth stage with six cycles on orientation and a damping factor of 0, 4 were added.

2.3.5 Heavy mineral analysis

Heavy mineral (HM) analysis is one of the most sensitive and widely used techniques for provenance studies in sandstones (Morton and Hallsworth, 1999). A total of 16 samples (Appendix D) were prepared and analyzed by heavy mineral specialist Andrew C. Morton at the HM Research, Great Britain. 6 of the analyzed samples are from Rundemellen, 6 from Skarvemellen and 4 of the samples are from the Hedmark Group (Appendix D).

Heavy mineral analysis were carried out in five stages; sampling, preparation, separation, counting and data treatment (Morton, 1985). The samples need to be carefully disaggregated by a mortar before separation takes place. High-density liquids are generally used when separating the heavy mineral grains from other grains in the sample, either by centrifuge or gravity-settling. The heavy minerals were then quantified and counted. A minimum of 200-300 counts of detrital grains are commonly considered to give the best estimations (Morton, 1985). When a sample contains few heavy minerals a lower count rate is carried out which leads to higher uncertainties of the results. For a more detailed description of the preparation of samples for heavy mineral analysis, see Morton (1985).

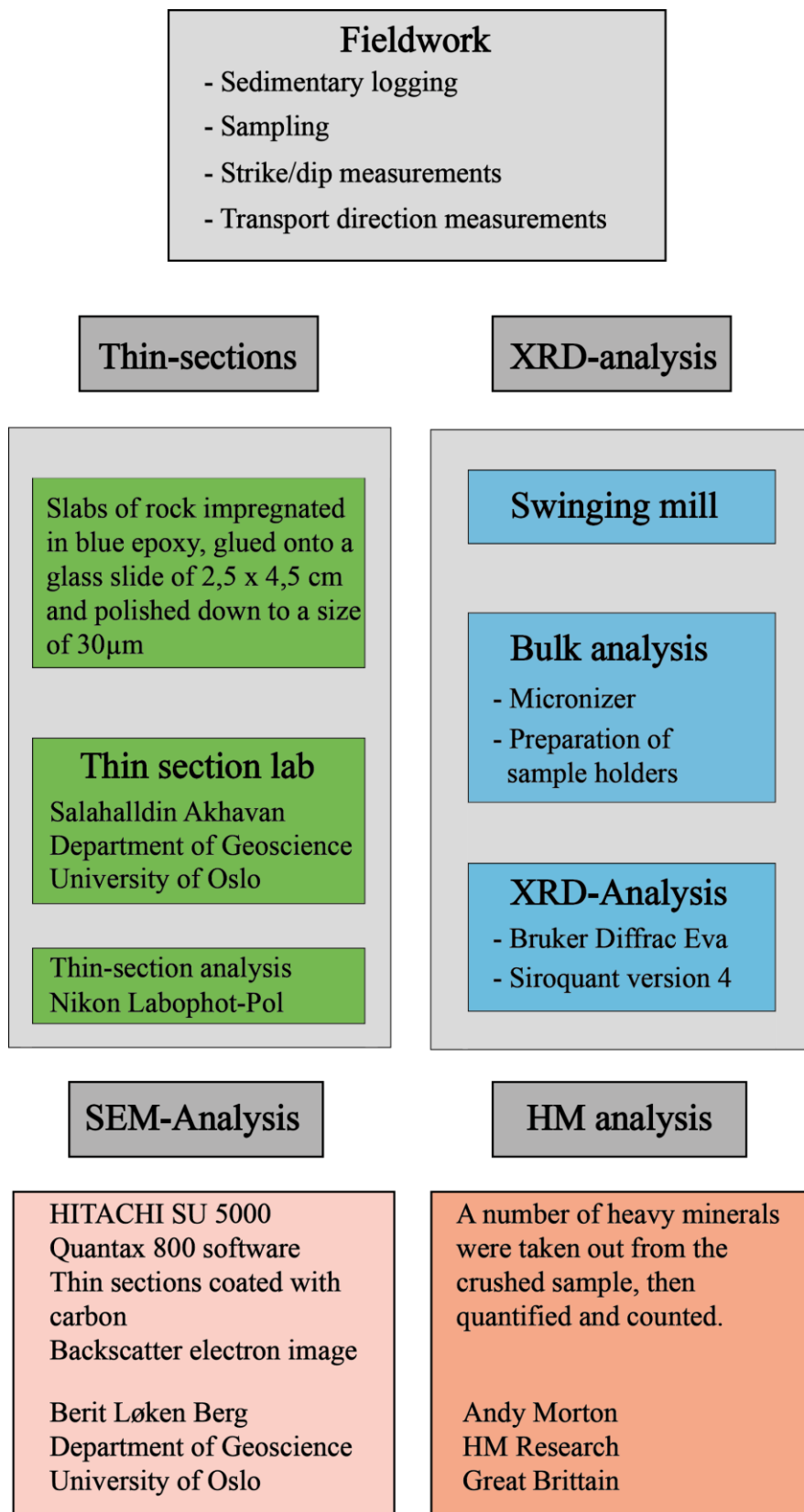


Figure 2.3: Methodology summary, modified from Oberhardt (2013).

3 Results

The results presented in this chapter consist of field observations, sedimentological logs, petrographical analysis and heavy mineral analysis of samples gathered from Rundemellen. Facies analysis based on field observations is described in chapter 3.2, followed by a description of facies associations (FA) in chapter 3.3. Results from the petrographical analysis are described according to facies in chapter 3.4. The final chapter (3.5) presents the results from heavy mineral analysis.

3.1 Field measurements

Paleocurrent data seen in Figure 3.1 include measurements of cross-bedding, imbrication, trough cross-bedding and ripples. Because the sedimentary strata at Rundemellen is overturned, the layers had to be restored back to horizontal in a stereonet in order to end up with correct paleocurrent measurements. The fold axis is assumed to be horizontal. The results strongly indicate an E-SE sedimentary transport direction. Strike/dip measurements are displayed in Appendix E.

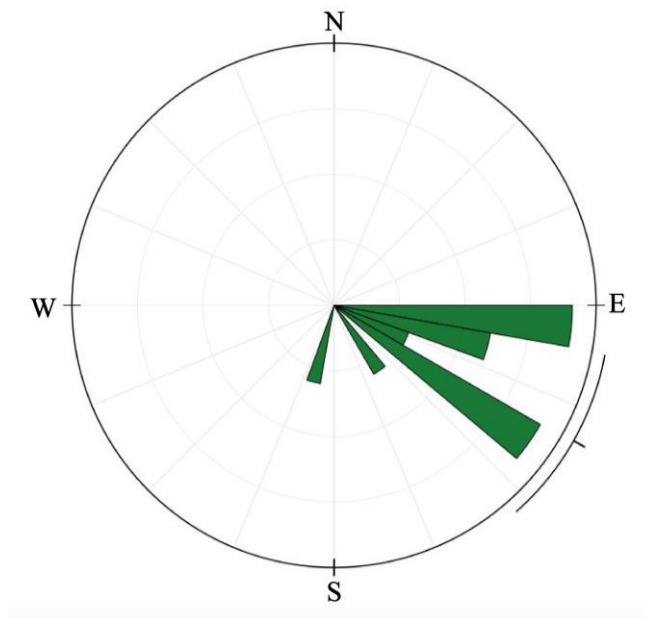


Figure 3.1: Paleocurrent measurements from Rundemellen indicate an ESE sedimentary transport direction.

3.2 Facies

Presented facies are grouped in first order facies based on lithology (Facies 1, 2, 3 and 4). Sandstones contain sedimentary structures and are divided into sub-group based on structures.

Table 3.1: Sedimentary facies found in the logged section at Rundemellen.

Facies number	Facies	Grain size	Description	Sample
1.	Conglomerate	Very coarse sand-gravel	Grain-supported, polymict conglomerate. Light pink towards red and purple matrix. Clasts consist of clay, quartzite, feldspar and volcanic fragments.	Rund 1-13-16 Rund 1-14-16 Rund 1-15-16
2a.	Cross-bedding	Coarse-medium sandstone	Overtuned cross-bedding in light pink towards red and purple sandstone beds.	Rund 2-5-16 Rund 2-6-16 Rund 2-8A-16
2b.	Parallel lamination	Coarse-medium sandstone	Clasts of quartzite and clay have been observed. Mineral precipitation seen as thin bands with a darker pink-color, possibly enriched by iron oxides.	Rund 1-6-16 Rund 1-8-16 Rund 1-9-16 Rund 2-2-16
2c.	Structureless	Coarse-medium sandstone	No sedimentary structures have been observed. Randomly dispersed clasts occur in some beds.	Rund 1-10-16 Rund 1-12-16 Rund 2-1B-16 Rund 2-8-16
2d.	Pebbly sandstone	Medium sandstone	Sandstone with clasts. May include cross bedding, parallel lamination or be structureless.	Rund 2-8-16
2e.	Trough cross-bedding	Coarse-medium sandstone	Tangential trough cross-bedding in a light pink sandstone bed.	
3.	Fine-grained sandstone	Fine-grained sandstone	Alternating red and light brown fine-grained sandstone layers. One contains asymmetrical ripples.	Rund 1-11-16 Rund 2-3-16 Rund 2-7B-16
4.	Breccia	Coarse sand	Matrix supported and poorly sorted. Angular clasts of varying mineralogical composition.	Rund 1-5-16

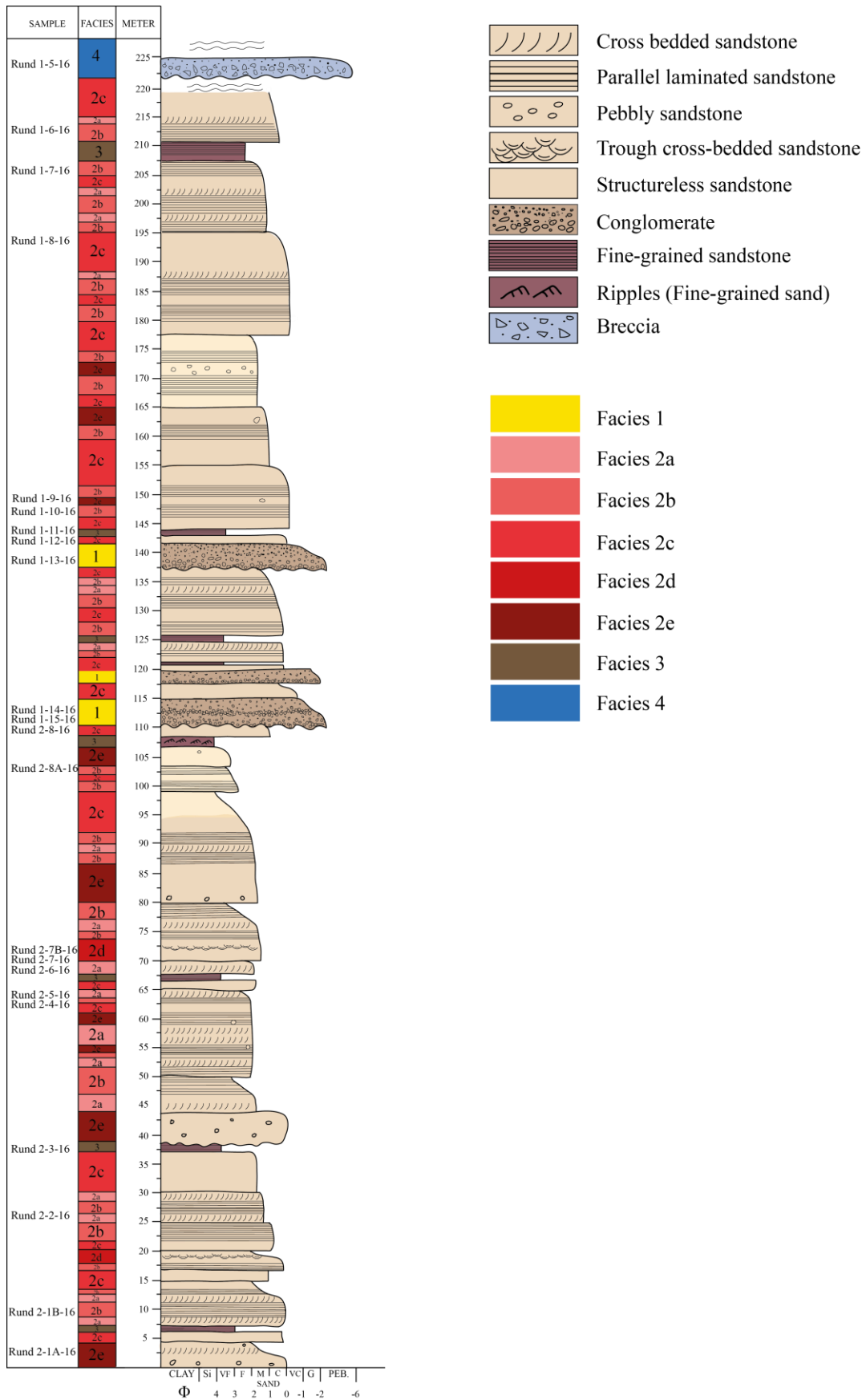


Figure 3.2: Sedimentological log from Rundemellen displaying grain size, structures, facies and samples. The log is in the scale of 1:100.

1. Conglomerate

The conglomerate units (Figure 3.2 and Figure 3.3) representing facies 1 can be observed in the sedimentary log (Figure 3.2).

The thicknesses of the conglomerate units vary from 2-5 meters (Figure 3.2). The conglomerates are grain-supported, poorly to moderately sorted and polymict. All of the conglomerate units display upwards fining matrix, and show normal grading. The matrix in the conglomerates seems to have the same composition as the sandstones, and the grain size ranges from gravel to very coarse sand. The clasts may show imbrication some places and consist mainly of quartzite, feldspar and volcanic clasts, of

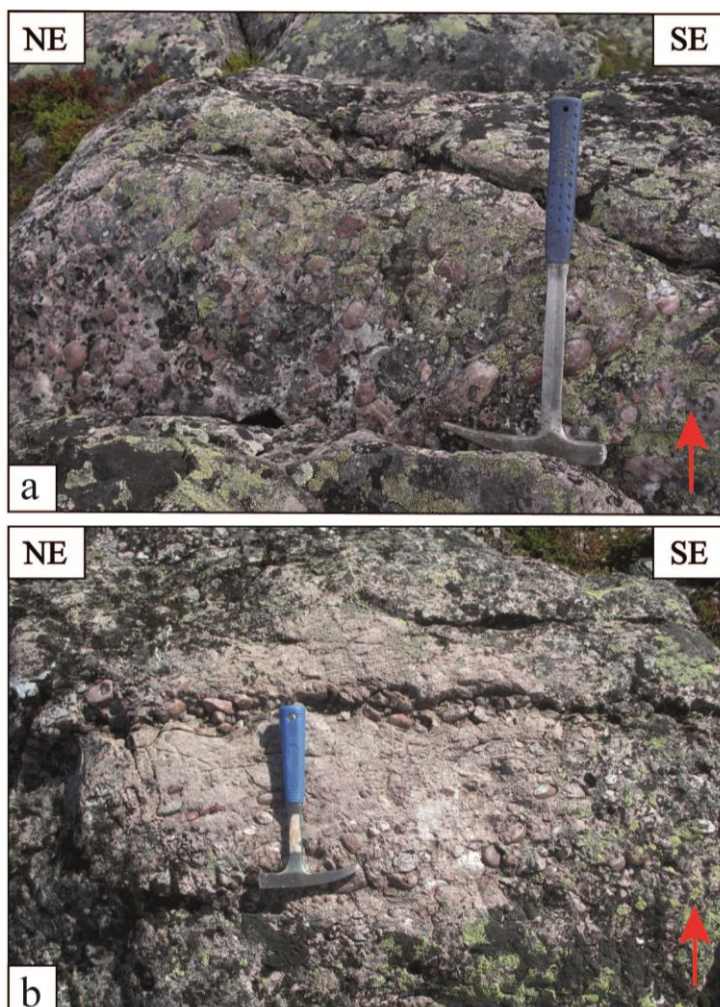


Figure 3.3: Figure a) Conglomerate unit with relatively large clasts. Figure b) Conglomerate unit with an assemblage of clasts along a band. Red arrows indicate stratigraphic up.

varying size. The largest clasts in the conglomerates have size of 7 cm and the average clast size is 4 cm. The quartzite clasts represent the largest (4-7 cm) and most abundant clasts, and are commonly well rounded. The feldspar (mainly K-feldspar) clasts are usually small (1-2 cm) and sub-angular to angular. The rhyolite clasts in the conglomerate are less common than feldspar- and quartzite clasts, and well rounded. They vary in size from 2-5 cm. The conglomerate unit at 110 meters in the sedimentary log (Figure 3.2) has an assemblage of large clasts along a line, seen in Figure 3.3 b. The conglomerate units show great lateral extent and no clear end in lateral extent of the units was observed.

2. Sandstone

Sandstones, representing facies 2 can be observed throughout the entire section, between finer sandstone layers and conglomerate units (Figure 3.2). The transition from sandstone to overlying conglomerate is often marked by an erosional surface, while the transition from conglomerate to sandstone is usually more gradual (Figure 3.2). The transition between sandstone and fine-grained sandstone layers are quite sharp. The grain size varies from coarse- to medium sand. The sandstone facies is divided into five separate facies units based on the sedimentary structures observed in field (Table 3.1 and Figure 3.2).

2a. Cross-bedded sandstone

Cross-bedded sandstone is relatively common in the sedimentary log (Figure 3.2). The cross beds at Rundemellen show evidence of overturning, displayed in Figure 3.4. Both angular and tangential cross bedding have been observed. The transport direction of the cross-beds is stable and show uni-directional flow towards NE (Figure 3.4). The cross-beds are sometimes eroded at the top. The transport direction inferred from cross-bedding appears quite stable. The dominating colors of the cross-bedded sandstone beds are light pink towards red and purple, and the dominating grain size is coarse to medium sand. A gradual change from parallel lamination to cross-bedding and from cross bedding to parallel lamination is often seen. In Figure 3.4 a, parallel lamination truncates the top of the underlying cross-bedding.

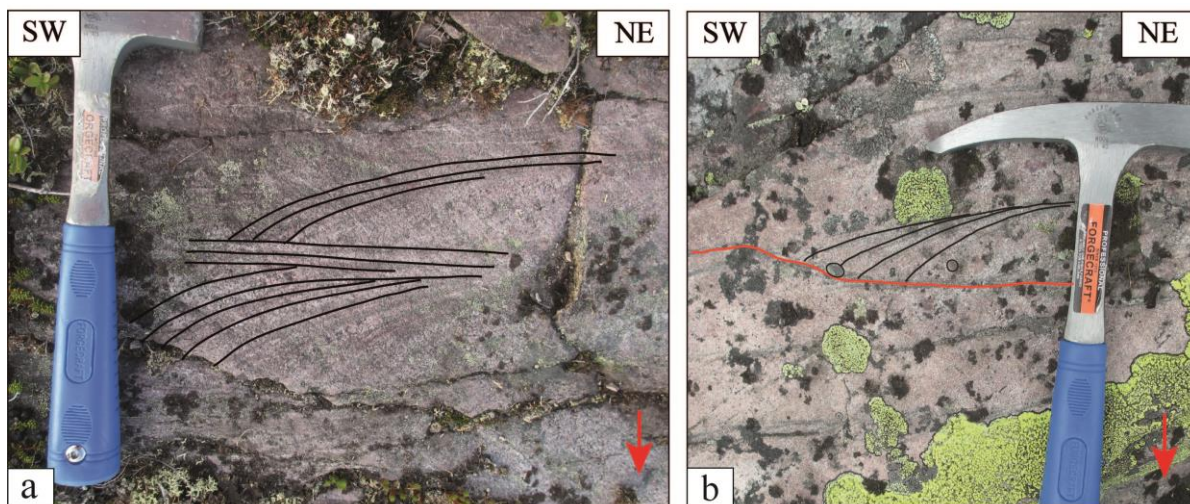


Figure 3.4: a) Coarse sandstone with overturned cross-bedding and parallel lamination between the cross beds. b) Overturned cross-bedding in coarse sandstone containing quartzite clasts. An erosional surface cuts the cross bed at the top, marked by the red line. Red arrows indicate stratigraphic up.

2b. Planar laminated sandstone

Planar lamination (Figure 3.5 a) is frequently observed in the logged section at Rundemellen (Figure 3.2). It is sometimes observed to cut the cross beds (Figure 3.4 a). The dominating grain size is coarse to medium sand and the color of the beds varies from light pink towards red and purple. In some beds mineral precipitation can be observed in the laminations as thin bands with a darker color.

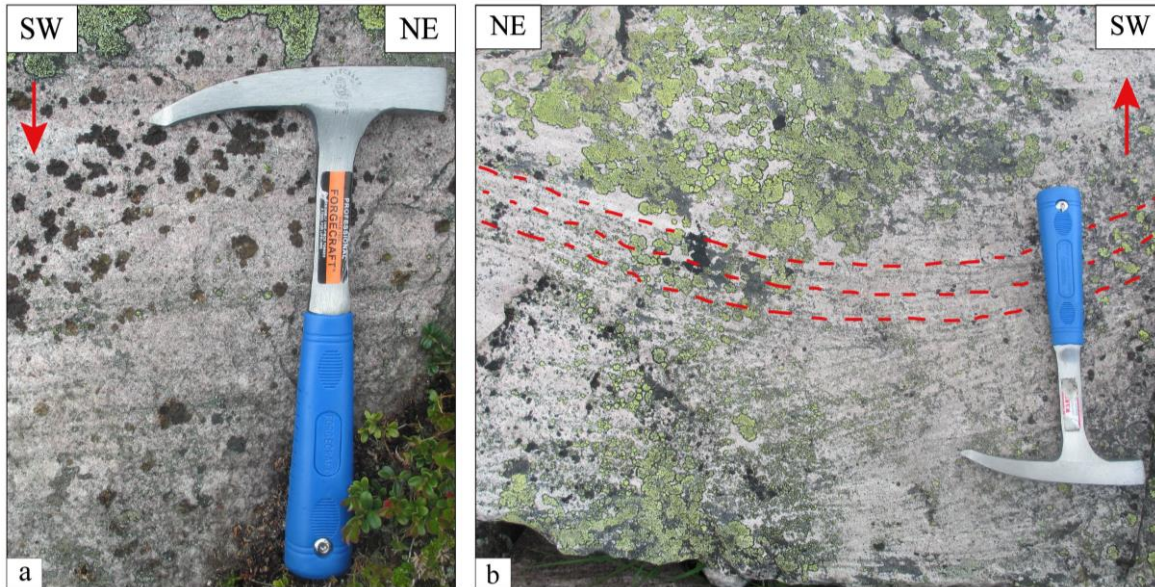


Figure 3.5: a) Parallel lamination in coarse sandstone. b) Trough cross-bedding in coarse –medium grained sandstone, with wavy erosional surface at the top marked in red stippled lines. The red arrows indicate stratigraphic up.

2c. Structureless sandstone

No sedimentary structures have been observed in this facies. The dominating grain size is coarse to medium sand and the dominating color is light pink towards red and purple (Figure 3.6). Mineral precipitation can be observed, and appears as coarser bands of darker color, but is not very common in these structureless sandstones.

2d. Trough cross-bedded sandstone

Through cross bedding occurs in a light pink, medium to coarse-grained sandstone (Figure 3.5 b) seen at 70 m in the sedimentary log (Figure 3.2). The cross bedding has a relatively high angle and may show a tabular relationship towards the base of the set. This is however difficult to determine since large areas are covered by vegetation. The cross bedding is eroded at the top by a curved bounding surface (Figure 3.5).

2e. Pebbly sandstone

This facies consists of medium to coarse-grained sand with randomly distributed clasts (Figure 3.6). The clasts make up less than 50% of the sandstone beds, and consist of quartzite, K-feldspar and clay. The size of the clasts varies from 2-5 cm. The sandstone facies with clasts



occur in structureless sand, parallel laminated sand and cross-bedded sand. In the

Figure 3.6: Coarse sandstone with randomly dispersed clasts. A quartzite clast is seen in the coarse-grained sandstone. The red arrow indicates stratigraphic up.

structureless sandstone beds (facies 2c) clay clasts dominate, whereas in the cross-bedded (facies 2a) and parallel laminated sandstone beds (facies 2b), clasts of quartzite dominate. The quartzite clasts are normally well rounded and have an average size of 4 cm (Figure 3.6). The shape of the red clasts consisting of clay varies from rounded to sub-angular, and are normally smaller than the quartzite clasts (2-3 cm). The feldspar clasts are not as common as quartzite- and clay clasts, and have an average size of 1 cm.

3. Fine-grained sandstone

Facies 3 is represented by fine-grained sandstone beds (Figure 3.7), alternating between light brown and red colored layers. Seven beds of this facies can be observed through the entire log (Figure 3.2). They have a great lateral extent, and no clear end of these layers was observed. The transition between the fine-grained sandstone layers to overlying conglomerates is erosional while the transition to both overlying and underlying sandstones is sharp (Figure 3.2). The thickness of this layer varies from 0.3- 1 meter. No sedimentary structures or parallel lamination were observed in most layers, but one layer had asymmetrical, sinuous crested ripples (Figure 3.2 and Figure 3.7 b). The ripples were 1-2 cm high and 2-3 cm long and were found at the bottom of the fine-grained layer at 107 m in Figure 3.2.

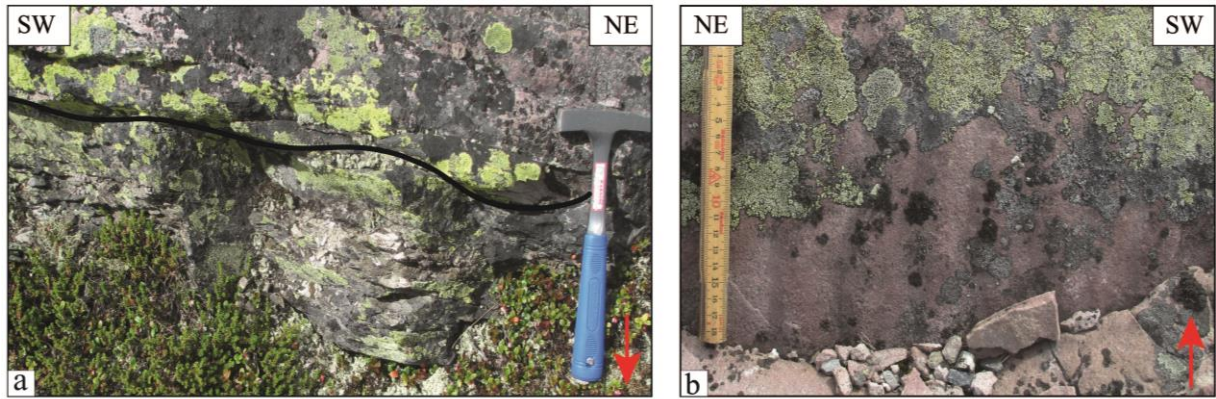


Figure 3.7: a) The figure shows a fine-grained sandstone layer below the black line and red coarse sandstone above. b) Asymmetrical ripples in red fine-grained sandstone. Red arrows indicate stratigraphic up.

4. Breccia

The breccia representing facies 4 is matrix supported and poorly sorted (Figure 3.8). The clasts are angular to sub-rounded and consist of quartzite, feldspar, rock fragments and possibly volcanic fragments of varying grain size. The feldspar clasts are most abundant and vary in size from 1 cm to 6 cm (Figure 3.8). The color of the matrix is dark grey towards green, with coarse sand being the dominant grain size. The breccia has not been observed in any consistent layers, only in loose boulders, and it is therefore difficult to conclude upon the thickness of the layer.



Figure 3.8: Poorly sorted breccia with red K-feldspar clasts found at Skarvemellen in a solid layer, 1050 m.a.s.l. At Rundemellen this breccia looks exactly the same, but was only found in loose boulders. The red arrow indicates stratigraphic up.

3.3 Facies associations

The facies associations (FA) are grouped together based on larger-scale trends than the facies. Each FA reflects a specific depositional environment, which will be discussed in chapter 4.

FA 1: Conglomerate and sandstone association

- Grain supported conglomerate (Facies 1)
- Cross bedded sandstone (Facies 2a)
- Parallel laminated sandstone (Facies 2b)
- Structureless sandstone (Facies 2c)
- Fine-grained sandstone (Facies 3)

FA 2: Upwards fining sandstone association

- Cross bedded sandstone (Facies 2a)
- Parallel laminated sandstone (Facies 2b)
- Structureless sandstone (Facies 2c)
- Trough cross-bedded sandstone (Facies 2d)
- Pebbly sandstone (Facies 2e)
- Fine-grained sandstone (Facies 3)

FA 3: Sandstone association

- Cross bedded sandstone (Facies 2a)
- Parallel laminated sandstone (Facies 2b)
- Structureless sandstone (Facies 2c)
- Trough cross-bedded sandstone (Facies 2d)
- Pebbly sandstone (Facies 2e)

FA 4: Poorly sorted feldspar rich breccia association

- Breccia (Facies 4)

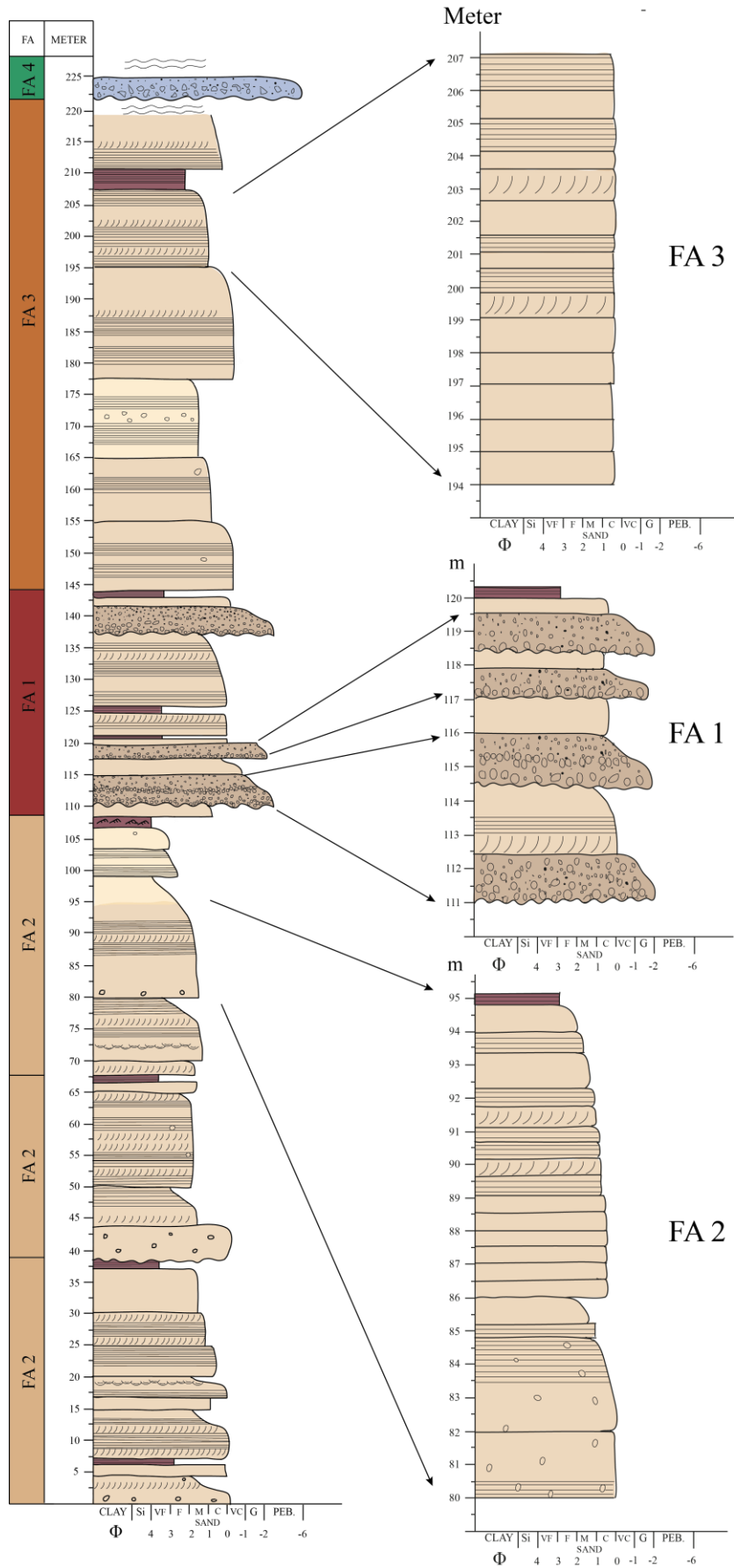


Figure 3.9: Sedimentological log from Rundemellen, with detailed logs of the different facies associations. Legend can be seen in Figure 3.2

3.3.1 FA 1

The FA 1 is composed of upwards fining sequences consisting of alternating units of conglomerates, sandstones and fine-grained sand, where the conglomerate units dominate. The conglomerate units (Facies 1) are upwards fining, and grain supported. Four conglomerate units show normal grading, with larger clasts in the bottom part. However, one conglomerate unit has an assemblage of large clasts along a line (115 m in Figure 3.9 and Figure 3.10 b). There is confined variation within the conglomerate units, but the lowest unit (111 m in Figure 3.10) has larger clasts than the upper three units. The matrix in the conglomerates are light pink towards red and purple, very coarse-grained sandstones, and seem to be comparable to the surrounding sandstone units. The sandstone units separate the conglomerates as seen in Figure 3.9. The sandstone units (Facies 2, Table 3.1) may have minor variation in grain size, but upwards fining (ϕ 0-1) units are also present (Figure 3.10). The sandstone beds have structures of facies 2a and 2b, but can also be structureless (Table 3.1). The transition from sandstone to conglomerate is erosional while the transition from sandstone to fine-grained sandstone layers is often sharp or more gradual. A thin fine-grained sandstone unit at the top of FA 1 contributes to an overall upwards fining trend of FA 1 (Figure 3.10).

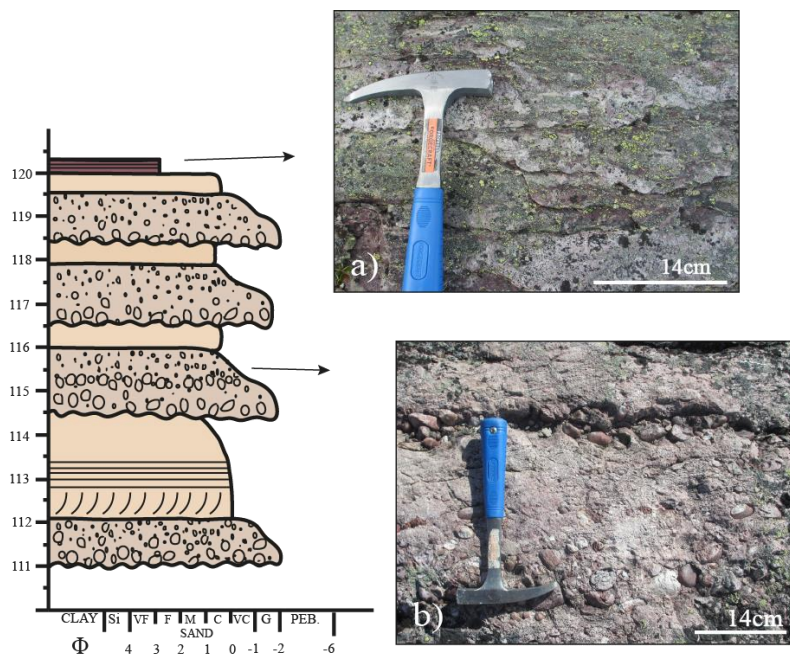


Figure 3.10: Detailed log of FA 1 with pictures taken from Rundemellen displaying facies 1 and 3. Legend can be seen in Figure 3.2. a) Fine-grained sandstone with alternating red and light brown color. b) Conglomerate with an assemblage of clasts along a line.

3.3.2 FA 2

FA 2 is composed of several upwards fining sequences of sandstone units (Facies 2) with a fine-grained sand unit at the top, seen in Figure 3.9. The sandstone units dominate in this sequence and contain sedimentary structures (Facies 2a, 2b, 2d and 2e, seen in Table 3.1), but structureless layers also occur (Facies 2c seen in Table 3.1). The pebbly sandstone of facies 2e occurs only in the lowermost sandstone units of FA 2 (Figure 3.9), and contains mostly clasts of clay. The grain size varies from medium sand to coarse/very coarse sand in the sandstone beds. There is a sharp transition from the sandstones to the overlying fine-grained sandstone unit in the FA 2 sequence (Figure 3.9). The thin fine-grained sandstone bed at the top of FA 2 is mostly parallel laminated, but asymmetrical ripples occur in one layer. The FA 2 sequence is overall upwards fining as seen in Figure 3.9.

3.3.3 FA 3

The FA 3 sequence is composed of several sandstone units (Facies 2) with little or no variation in grain size, as seen in Figure 3.9. The units are often structureless (Facies 2c), but structures of facies 2a, 2b and 2e (Table 3.1) may also occur. The FA 3 sequence is overall massive with coarse sand being the dominant grain size (Figure 3.9).

3.3.4 FA 4

There is no sedimentary log for FA 4, because the breccia was not seen in consistent layers at Rundemellen, only as loose boulders. The FA 4 is the same as Facies 4 and further description of the breccia facies can be found in chapter 3.2.

3.4 Petrographical analysis

3.4.1 Results of thin sections and point counting

The main focus of the thin section analysis was to identify the mineral composition, examine feldspar preservation, measure grain sizes and grain shapes. Grain sizes were measured along the longest axis of the grains and clasts. The main focus during point counting was to figure out the composition of the rock by counting matrix, quartz, plagioclase, K-feldspar, porosity,

rock fragments and opaque grains. A more detailed description of the thin sections can be found in Appendix A, and the point counting results in Appendix B.

Facies 1: Conglomerate

The conglomerate samples (Rund 1-13-16 and Rund 1-14-16) are more representative for the conglomerate matrix than Rund 1-15-16. Sample Rund 1-15-16 contains several large clasts and is more representative for the clasts in the conglomerate rather than the matrix. Large rhyolite clasts are very common in this sample (Rund 1-15-16), whereas quartzite clasts and granite clasts are less common. All of the samples show highly deformed conglomerates, where several grains have been crushed and lost its original form. The samples representative for the matrix will be described under conglomerate matrix below.

Rhyolite clasts

The rhyolite clasts make up the largest clasts in sample Rund 1-15-16 with an average size of 0.8 cm. They all show salt and pepper texture and some of the clasts have phenocrysts ranging in size from medium to coarse sand (Figure 3.11 a) The average size of the phenocrysts are around 1 mm and probably consist of quartz. The rhyolite clasts have a sub-angular to sub-rounded shape.

Granite clasts

The granite clasts consist of quartz grains, feldspar grains and mica (Figure 3.11 b). The quartz grains are both undulatory and non-undulatory, where undulatory quartz grains are most common in sample Rund 1-15-16 (Figure 3.11 b). The feldspar grains are highly weathered and represent preservation category V (Table 2.3). The degree of weathering of the feldspar grains are so high that it is difficult to distinguish between K-feldspar and plagioclase. Most of the grains within the granite clasts are in direct contact and may have concavo-convex, long, sutured or tangential boundaries (boundaries can be observed in Figure 3.13). Some of the grains are surrounded by a thin film of mica, and therefore not in direct contact with other grains. The full size of the granite clast is not measured, since it lies at the edge of the thin section and is cut.

Quartzite clasts

The quartzite clasts consist of small grains of undulating and non-undulating quartz and a few feldspar grains. The feldspar grains are smaller than the quartz grains and ranges in size from

0.2 mm to 0.3 mm. In the quartzite clasts, quartz grains make up approximately 90% and feldspar grains approximately 10% (Appendix B). The clasts are sub-rounded and ranges in size from 0.7 mm to 1 mm. The shape of the mineral grains varies from angular to sub-rounded.

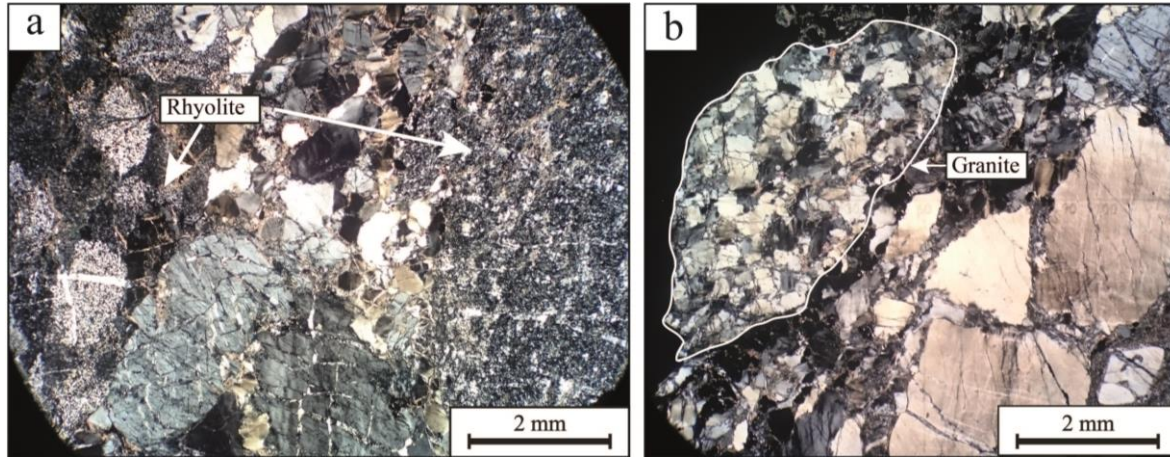


Figure 3.11: Pictures from thin sections displaying clasts in the conglomerates. a) Rhyolite clasts in the conglomerate with salt-and pepper texture and phenocrysts. b) Sub-angular granite clast consisting of K-feldspar, quartz, mica and plagioclase. Both pictures are taken from sample Rund 1-15-16.

Conglomerate matrix

The conglomerate matrices are grain supported and consist mainly of quartz, K-feldspar, plagioclase, sericite and mica (Figure 3.12). The average grain size is coarse sand. The pores are commonly filled with mica and sericite. Most of the grains are covered by a thin film of mica and/or sericite, but some are in direct contact and may have concavo-convex, sutured, tangential or long grain contacts. These grain contacts can be seen in Figure 3.13. Opaque grains are also present in the conglomerate matrix, and mostly represent heavy minerals or iron oxides. These opaque grains make up only 0.5% of the conglomerate matrix seen from point counting (Appendix B), and are normally organized in lines or clusters. The mineral identification of the opaque grains will be discussed further in the SEM results, chapter 3.4.2. The quartz grains represent the largest grains in the conglomerate matrices, with sizes varying between 3 mm and 0.5 mm. Thin sections display average quartz percentage to be 62.7% (Appendix B). Both undulating and non-undulating quartz grains are present, where undulating quartz is most common. The feldspar grains are generally smaller than the quartz grains and the average grain size of feldspar was found to be 1 mm. The largest feldspar

grains are 2.5 mm and the smallest grains have a size of 0.7 mm. The feldspar grains in the matrix were found to make up on average 3.5 %, with dominating K-feldspar (Appendix B). The mica and sericite act as pore filling, and make up an average percentage of 10.5% of the matrix (Appendix B). Rock fragments are also present and make up 2.0% and 5.0% in sample Rund 1-13-16 and Rund 1-14-16, respectively (Appendix B). Some of the grains in the matrix are fractured, and in sample Rund 1-15-16 some grains have been crushed and lost their original grain shape. The fractures in the grains are filled by secondary growth of polycrystalline quartz and sericite.

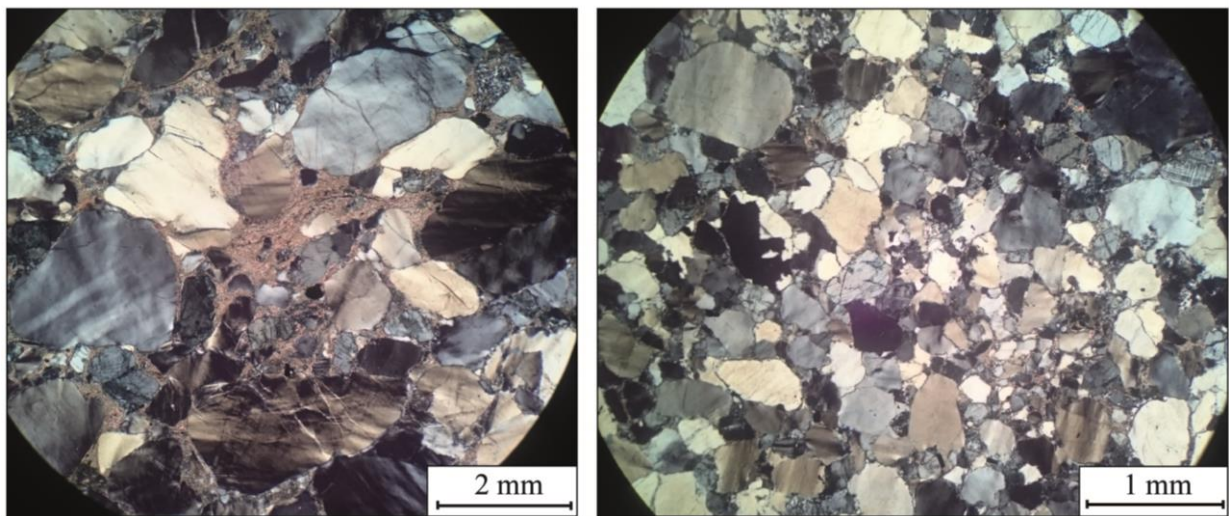


Figure 3.12: Pictures of the conglomerate matrices taken in cpl. The left picture is taken of sample Rund 1-13-16, which has more muscovite and sericite matrix than sample Rund 1-14-16 in the right picture. The matrix of sample Rund 1-14-16 (right picture) consists mostly of small quartz grains.

Facies 2: Sandstone

The sandstones have a grain supported framework consisting of quartz, K-feldspar, plagioclase and rock fragments (Figure 3.13). Opaque grains are also present in varying amounts in the different samples, and are often arranged along lines or in clusters. Mica and sericite make up most of the matrix in the sandstone samples (Figure 3.13 c and Figure 3.13 d). The matrix content varies from sample to sample, where the lowest percentage is 13.0% and the highest 33.2% found from point counting (Appendix B). Quartz is the dominating mineral in all of the sandstone samples and normally represents the largest grains (Appendix A). Both undulatory and non-undulatory quartz occur, undulatory quartz grains being most common. Polycrystalline quartz is also common, but there are great variations in the amount. From point counting the average quartz content is found to be 62.3% (Appendix B). The K-

feldspar grains are often weathered (Figure 3.13 d), but there are great variations in amount of weathering from sample to sample, ranging from preservation category II-III. From point counting the average K-feldspar percentage is found to be almost 9.0% (Appendix B). The plagioclase grains are normally smaller than the K-feldspar grains (0.5 mm), and have an average size of 0.3 mm. The percentage of plagioclase is also lower than K-feldspar and the average was found to be 2.6% from point counting (Appendix B). Intergrowth of plagioclase and feldspar is rare but occurs in most of the samples. Low amounts of plagioclase are present in all sandstone samples, as seen in the point counting results (Appendix B).

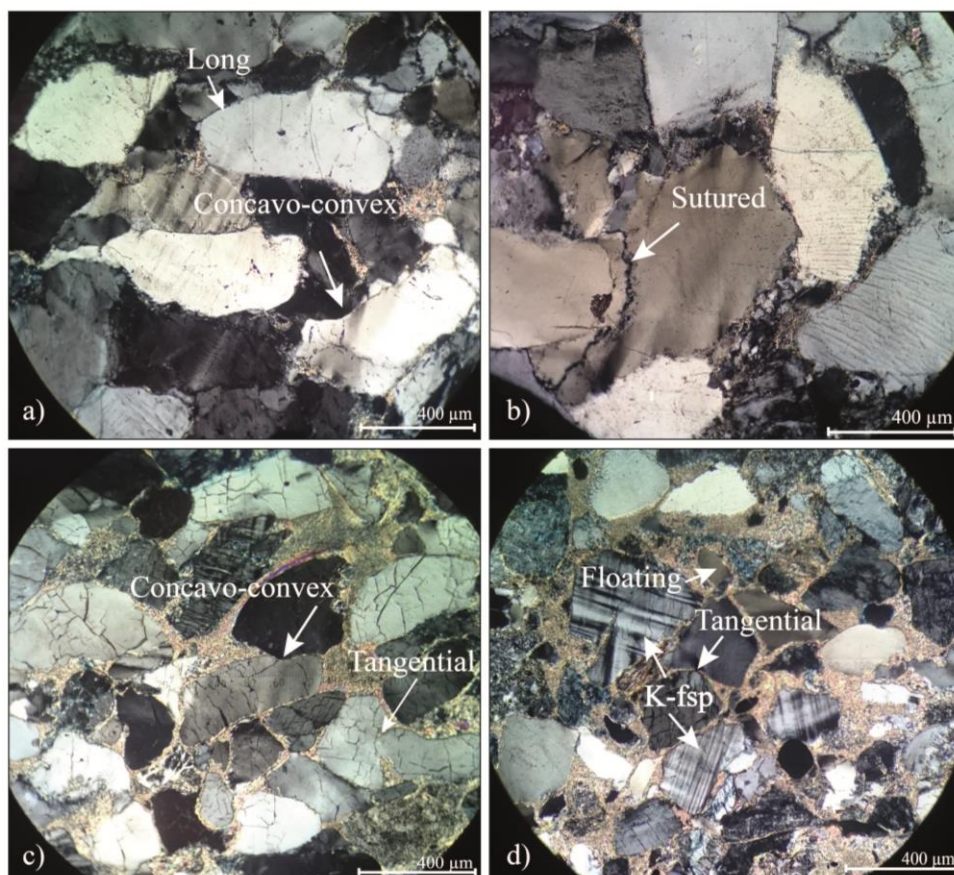


Figure 3.13: Thin section picture of sandstone samples in cpl. a) Quartz grains with long and concavo-convex grain contacts (Sample Rund 2-8-16). b) Quartz grains in sandstone sample with sutured grain contacts (Rund 2-8-16). c) Fractured grains with concavo-convex and tangential grain contacts (Sample Rund 1-6-16). d) Mostly floating grains, but some have tangential grain contacts. K-feldspar grains of preservation category II-III (Rund 1-6-16).

Most of the grains in the sandstone samples are floating in the surrounding matrix, and covered by mica and/or sericite. The grains in direct mutual contact may have long,

tangential, sutured or concavo-convex grain boundaries (Figure 3.13). Some deformation occurs in all samples and is seen as fractures in the grains or crushed grains (Figure 3.13 c). Polycrystalline quartz and sericite are often found within the fractures. The sorting in the sandstone samples range from moderately to very well.

Facies 3: Fine-grained sandstones

The fine-grained sandstone facies is seen in thin sections as alternating layers with high concentration of opaque grains and mica, and coarser layers with less mica, larger grains and almost none opaque grains (Figure 3.14). In point counting the opaque grains were found to be on average 6.3% (Appendix B). Flakes of muscovite are mostly present in the more fine-grained layers, with highest concentration towards the top. The fine-grained sandstones are matrix supported, and the grains are floating in a matrix composed mostly of mica and sericite. From point counting the average matrix content was found to be 68.45% (Appendix B).

The largest grains in the fine-grained sandstones are quartz (0.5-0.7 mm) and the grain shape varies from angular to sub-rounded. Both undulatory and non- undulatory quartz grains occur, with undulatory quartz grains being most common (Appendix B). During point counting the average quartz content was found to be 21.7% (Appendix B). The K-feldspar grains are smaller (0.25 mm) than the quartz grains and have a more rounded shape. Preservation of K-feldspar grains in these samples ranges from category III-IV (Table 2.3). From point counting the average feldspar content was found to be 6.35% (Appendix B). The plagioclase content in these samples is very low and was found to have an average percentage of 0.85% in point counting analysis (Appendix B). Rock fragments also occur and were found to have an average percentage of 0.45% from point counting (Appendix B).

Some of the grains are in direct contact, often with concavo-convex boundaries. Most of the grains are covered by a thin film of mica or sericite. The sorting in the fine-grained samples ranges from moderate to very poorly sorted, where the smallest grains have a size of 0.25 mm and the largest 1mm.

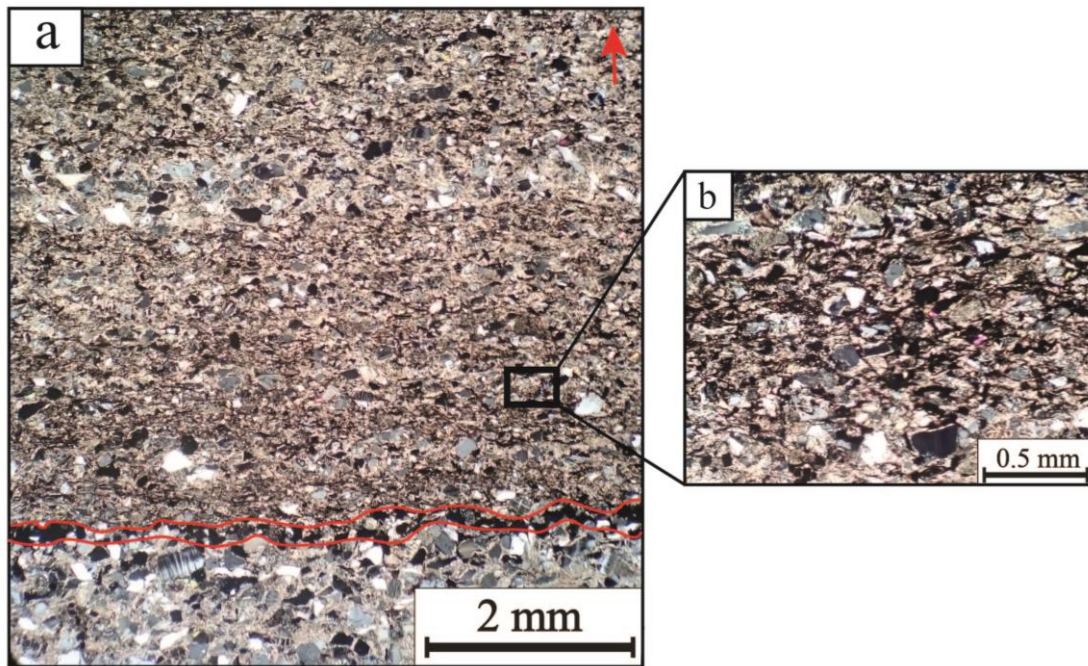


Figure 3.14: Thin section pictures taken in cpl of the fine-grained sandstone (Sample Rund 2-7B-16).
 a) Alternating layers of coarser grains and finer grains. Within the red lines there is an assemblage of opaque grains (black grains). Above the red lines there is a finer-grained zone with increasing mica content towards the top of the figure. Stratigraphic up is shown by the red arrow. b) Close up of the finer-grained zone. The black minerals are xenotime.

Facies 4: Breccia

The breccia matrix consists mainly of quartz, feldspar and mica and the clasts consist mainly of K-feldspar. Low amounts of quartzite clasts are also present in the sample. It is found to be matrix supported, where mica and sericite make up most of the matrix together with smaller grains of feldspar and quartz (Figure 3.15). The opaque grains are often arranged in lines or clusters and were found to make up 9.9% of the total sample (point counting, Appendix B). Quartz grains are the largest grains in the matrix and ranges from 0.5-1 mm. During point counting the quartz content was found to be 33.7% (Appendix B). Polycrystalline quartz is common in this sample, both as cement in the fractures and as grains in the matrix. It was found to make up 12.5% of the sample (Appendix B). The largest clasts in the breccia consist of K-feldspar and ranges from 3 mm to 1 cm. They are more weathered than the smaller clasts and are classified as category IV-V of K-feldspar preservation (Table 2.3). Smaller clasts (1.5-3 mm) were less weathered and interpreted as category I-II of K-feldspar preservation (Table 2.3). Fractures are also present in the feldspar clasts and are filled with polycrystalline quartz or sericite. The largest clasts (3.5 mm-1 cm) are sub-rounded, while the smallest clasts (1 mm) are angular to sub-angular. Most of the grains are surrounded by a thin

film of mica and/ or sericite. Some grains are in direct contact along straight or concavo-convex boundaries (the grain contacts can be seen in Figure 3.13). Plagioclase is not very abundant in the breccia sample and was found to be 2.7% (point counting, Appendix B). Rock fragments are present in small amounts and were found to be 2.5% (point counting, Appendix B). The sample is overall poorly sorted, with grain sizes ranging from 0.5 mm to 1 mm.

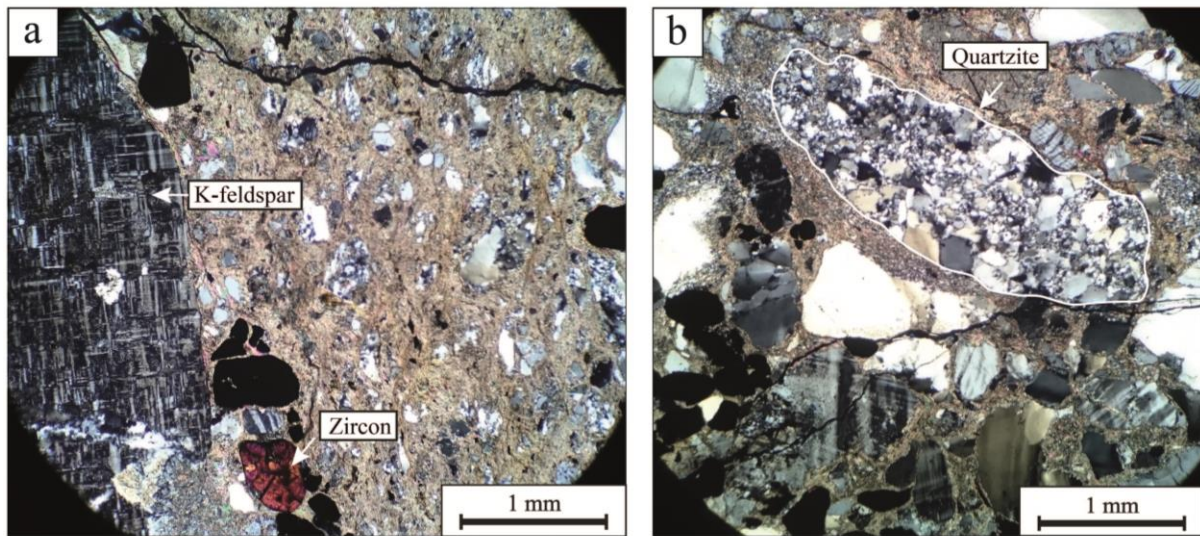


Figure 3.15: Picture taken in cpl of the breccia sample (Rund 1-5-16). a) Sub-rounded K-feldspar clast and a zircon grain floating in matrix. A pressure solution seam is seen at the top of the figure. b) Poorly sorted breccia with a large quartzite clast floating in the matrix.

3.4.2 Results of scanning electron microscope analysis

The main focus when analyzing the samples in scanning electron microscope (SEM) was to identify the mineral composition of the opaque grains seen in thin section, examine possible feldspar overgrowth, feldspar zonation and other features that are possible to detect in SEM. The opaque grains were found to be several different heavy minerals and iron oxides of varying composition between sandstone, fine-grained and breccia samples. None of the conglomerate samples were studied in SEM.

Facies 2

Two sandstone samples were studied in SEM, Rund 2-5-16 and Rund 2-6-16. Several feldspar grains, both K-feldspar and plagioclase, were studied in detail to examine feldspar zonation. None of the samples showed great variations or patterns in chemical composition or feldspar overgrowth. The feldspar grains often display fringy or irregular edges with mica or

sericite surrounding the grains. Mica and sericite seem to make up most of the matrix in the sandstone samples, and acting as both pore filling and cement in fractures. Sericite appeared as a very fine-grained muscovite and has a ductile or floating impression. Microscopic grains of heavy minerals were seen within the sericite (Figure 3.16 b). Several heavy minerals were identified; zircon, apatite, monazite, rutile and thorium phosphate (Figure 3.16 c). They are often randomly scattered in the sandstone samples, but appear also in clusters or veins (Figure 3.16 c). The iron oxides identified are hematite and ilmenite, hematite being the most abundant. Intergrowth of quartz and feldspar were discovered in both of the sandstone samples (Figure 3.16 a). The amount of heavy minerals in the sandstones is much lower than in the fine-grained and breccia samples.

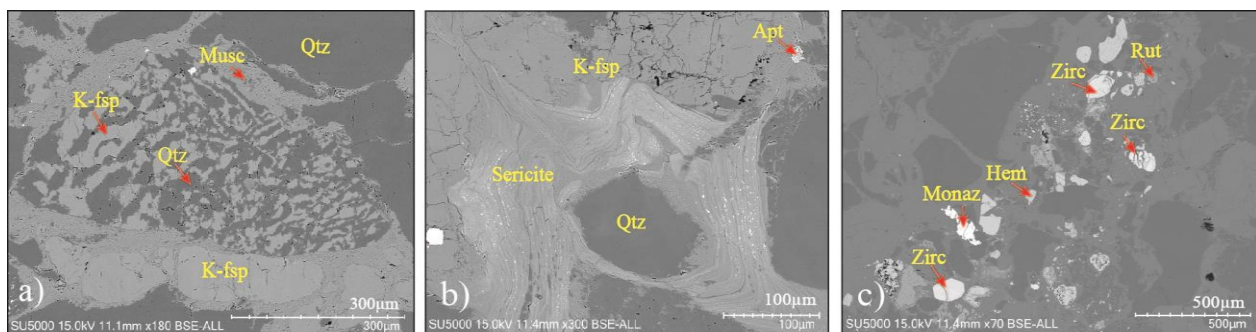


Figure 3.16: Backscatter images of facies 2. a) Intergrowth of quartz and K-feldspar (Rund 2-5-16). b) Sericite with a ductile or floating appearance in the sandstone samples. The quartz grain is completely surrounded by sericite (Rund 2-6-16). c) Assemblage of heavy minerals and iron oxides along a line (Rund 2-6-16). K-fsp (K-feldspar), Musc (muscovite), Qtz (quartz), Apt (apatite), Hem (hematite), Rut (rutile), Monaz (monazite).

Facies 3

One sample of fine-grained sandstone facies was studied in SEM; Rund 2-7B-16. In the sample finer-grained layers alternate with coarser layers. The top of the finer-grained layers display an increase in muscovite content. In between these layers there is a string composed heavy minerals, marking the transition between the coarser layer and the fine-grained layer (Figure 3.17 a). In the fine-grained sample the heavy minerals are usually organized along lines, while the smallest grains often are found scattered. The heavy minerals identified were rutile, zircon, apatite and xenotime. In the sample there is a large amount of microscopic xenotime grains that seem to surround the grains and fill pores (Figure 3.17 b).

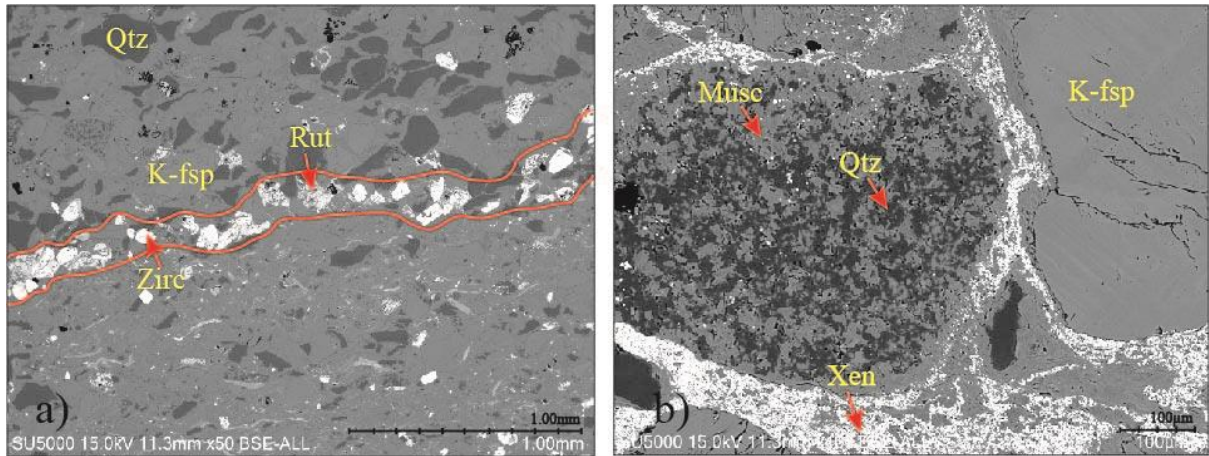


Figure 3.17: Backscatter photo of the fine-grained sandstone (Sample Rund 2-7B-16). a) Alternation of coarser layer and finer-grained layer separated by an assemblage of heavy minerals along a line marked in red. Muscovite content increases upwards in the finer-grained layer. b) Intergrowth of quartz and muscovite with xenotime (white color) surrounding the grains. Qtz (quartz), Rut (rutile), K-fsp (K-feldspar), Zirc (zircon), Musc (muscovite), Xen (xenotime).

Facies 4

One breccia sample was studied in SEM; Rund 1-5-16. In this sample most of the grains were found to be surrounded muscovite. Muscovite act as pore filling and cement in fractures (Figure 3.18 c). The K-feldspar grains were found to have irregular edges surrounded by muscovite needles. Perthite lamellas were discovered in SEM, where K-feldspar is the host grain with albite lamellas. Heavy minerals such as zircon, apatite, rutile, monazite and xenotime were identified (Figure 3.18). The largest heavy mineral grains seem to be organized in clusters or strings, while the smaller ones are more scattered throughout the sample. Zircons may be fractured and have xenotime coating. Iron oxides as ilmenite and hematite were identified, where the ilmenite was found to have lamellas of more iron-rich ilmenite (Figure 3.18 b).

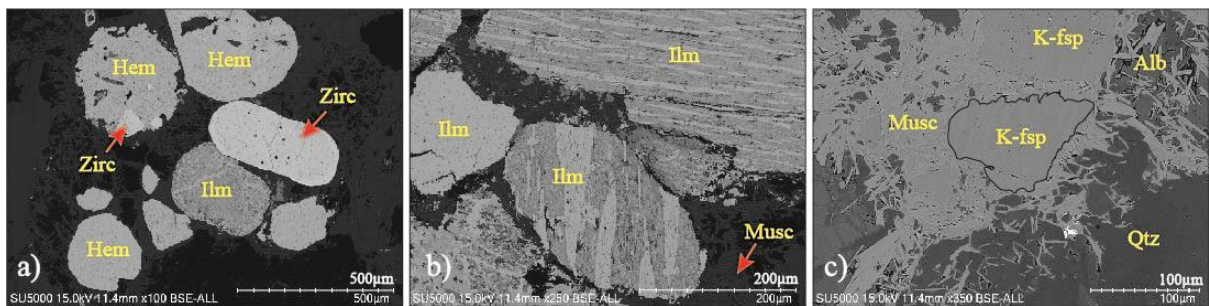


Figure 3.18: Backscatter image of sample Rund 1-5-16. a) Heavy minerals arranged in a cluster. b) Ilmenite with lamellae of more iron-rich ilmenite seen in lighter color. c) K-feldspar grain with irregular edges surrounded by muscovite. Zirc (zircon), Ilm (ilmenite), Hem (hematite), Musc (muscovite), Alb (albite), K-fsp (K-feldspar), Qtz (quartz).

Ring Formation

One sandstone sample of the Ring Formation from the Hedmark Group was studied in SEM; KIN 3-15. In this sample chlorite acts as the pore-filling mineral and (seen in white color in Figure 3.19). Several perthite lamellas were discovered, where K-feldspar is the host grain with irregular lamellas of albite as seen in Figure 3.19 a. Quartz-feldspar intergrowth was also present in this sample, seen in Figure 3.19 b. Some heavy minerals were present, but only monazite and rutile were identified. Iron oxides such as hematite and ilmenite were also identified. Feldspar grains were studied in detail to examine feldspar zonation, but no variations in chemical composition or feldspar overgrowth were observed.

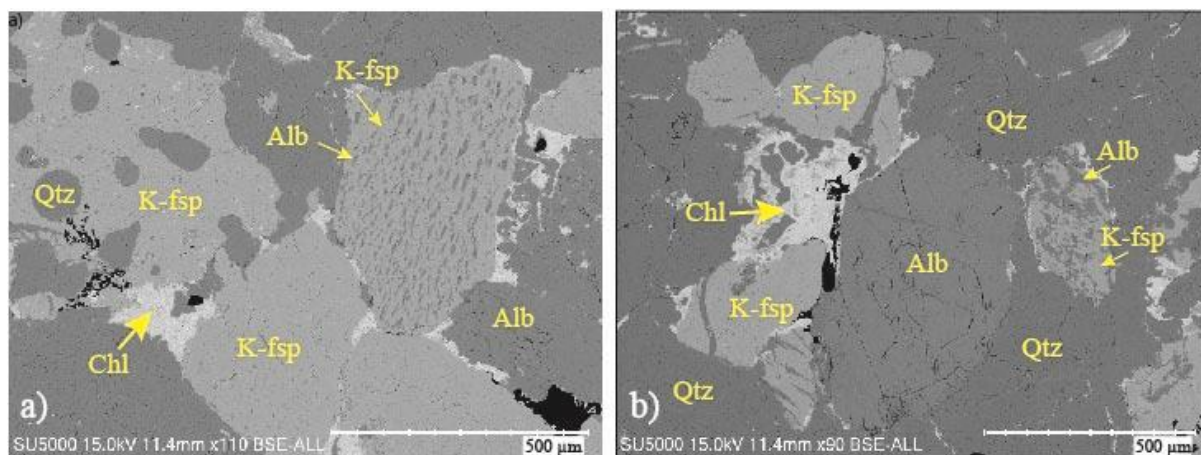


Figure 3.19: Backscatter photo a sandstone from the Ring Formation (sample KIN 3-15). a) Perthite lamellae, K-feldspar is the host grain with irregular lamellae of albite. Quartz intergrowth in a K-feldspar grain is also present. b) General appearance of the sandstone sample from the Ring Formation. Feldspar intergrowth and quartz veins in K-feldspar grains are present. Chlorite acts as pore filling in both a) and b).

3.5 XRD Results

A total of 23 samples were prepared for XRD-analysis, and the resulting diffractograms were interpreted. The results are shown in XRD% (Figure 3.20 and Appendix C).

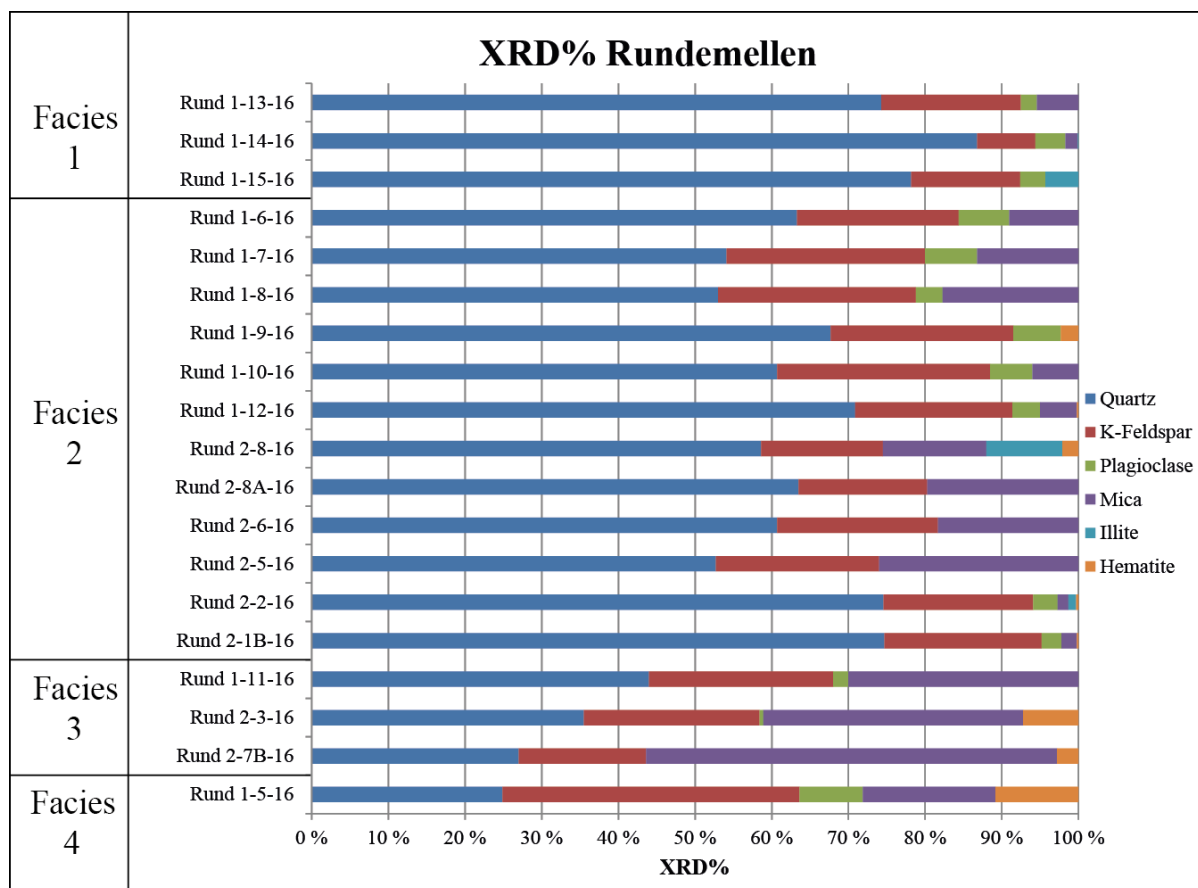


Figure 3.20: Bar plot showing the mineral content extracted from the XRD analysis in XRD% of the samples from Rundemellen. The samples are separated into facies.

Conglomerate matrix (Facies 1)

The minerals in the conglomerate matrix consist mainly of quartz, K-feldspar, plagioclase and mica based on the XRD% shown in Figure 3.20 and Appendix C. Quartz is by far the most abundant mineral and constitutes on average 76.3 XRD% (Figure 3.20, Appendix C). K-feldspar constitute on average of 16.2 XRD% and plagioclase only 2.7 XRD% (Figure 3.20, Appendix C). In the conglomerate matrix, mica is represented by muscovite and sericite and constitute on average 5.4 XRD%. Illite is also present in the conglomerate matrix of sample Rund 1-15-16 and makes up 4.4 XRD% (Appendix C). Traces of hematite are present in the conglomerate matrix. The quartz/total feldspar ratio for the conglomerate samples are shown in Figure 3.20. Sample Rund 1-14-16 has the highest ratio at 11.0, while the sample Rund 1-15-16 has the lowest ratio of 5.5. The average quartz/feldspar ratio of facies 1 is 7.0, where sample Rund 1-14-16 contributes to the high average ratio.

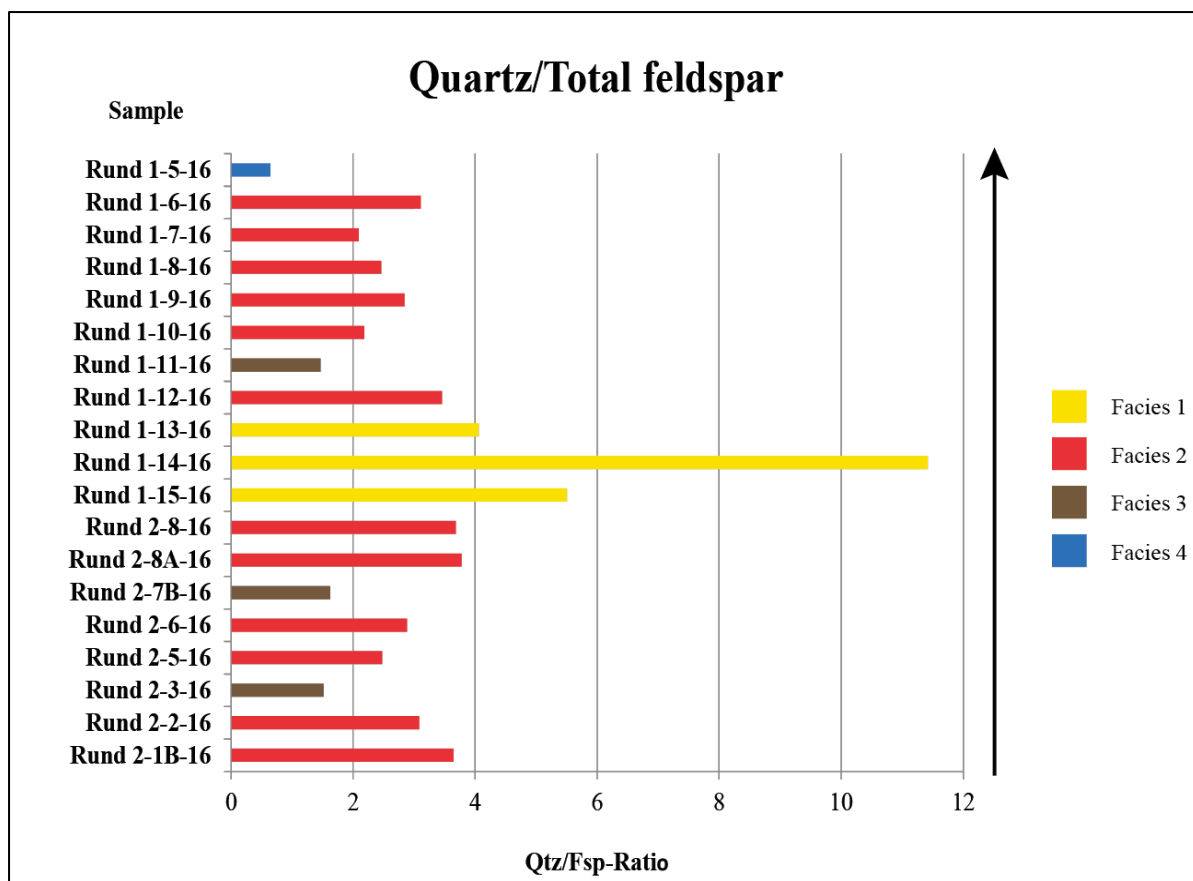


Figure 3.21: Quartz/total feldspar plot of the individual samples from Rundemellen in stratigraphic order. The colors indicate which facies the samples are grouped into and the black arrow indicate stratigraphic up.

Sandstone (Facies 2)

Quartz, K-feldspar, plagioclase and mica make up the most common minerals in the sandstone facies (Figure 3.20 and Appendix C). Quartz is normally the most abundant mineral and constitute on average 62.5 XRD% (Figure 3.20 and Appendix C). Mica constitutes on average 12.0 XRD%, and is represented by muscovite and sericite. While K-feldspar makes up 22.0 XRD%, plagioclase is only present in some samples and makes up on average 4.9 XRD% (Figure 3.20 and Appendix C). Hematite constitutes on average 1 XRD% and is only present in a few samples. Illite is only present in two samples; Rund 2-2-16 and Rund 2-8-16, and make up 1 XRD% and 9.8 XRD%, respectively (Figure 3.20 and Appendix C). The quartz/total feldspar ratio for facies 2 is shown in Figure 3.21. The average quartz/total feldspar ratio for the sandstone samples are 2.9.

Fine-grained sandstone (Facies 3)

Mica, quartz and K-feldspar are the most common mineral groups in the fine-grained sandstones, shown by the XRD% in Figure 3.20. Mica is represented by muscovite and sericite, which together make up on average 39.2 XRD% (Figure 3.20, Appendix C). Quartz makes up an average of 35.5 XRD% (Figure 3.20 and Appendix C). K-feldspar is found in all samples of the fine-grained sandstones, and makes up an average of 21.1 XRD% (Figure 3.20 and Appendix C).

Hematite is present in all the samples of the fine-grained sandstone and make up an average of 3.3 XRD% (Figure 3.20 and Appendix C). The quartz/total feldspar for the fine-grained sandstone samples are shown in Figure 3.21. Rund 2-7B-16 has the highest ratio at 1.62, while Rund 1-11-16 has the lowest ratio of 1.47. The average quartz/feldspar ratio of facies 3 is 1.54.

Breccia (Facies 4)

Quartz, K-feldspar, and mica make up the most common mineral groups in facies 4, based on the XRD% shown in Figure 3.20 and Appendix C. K-feldspar is mainly present as clasts of varying size and make up 38.7 XRD% (Figure 3.20 and Appendix C). Mica is represented by muscovite and sericite, which makes up most of the matrix and together they make up a total of 17.3 XRD%. Quartz make up 24.9 XRD% (Figure 3.20 and Appendix C). Hematite and plagioclase are also present in the sample of the breccia and make up 10.9 XRD% and 8.3 XRD%, respectively (Figure 3.20 and Appendix C). The quartz/total feldspar ratio for the breccia sample is 0.53 and is much lower than ratio of the fine-grained sandstone samples and the sandstone samples (Figure 3.21).

3.6 Heavy mineral analysis

The results of the heavy mineral analysis are shown in Table 3.2. The samples are dominated by stable minerals, but some unstable phases such as amphibole, epidote, and pyroxene are present in minor amounts (Table 3.2 and Appendix D). Zircon is the most common heavy mineral and apatite is abundant in some of the samples (Table 3.2). The zircon grains were often found to be fractured and partially metamict. All of the samples from Rundemellen are very similar and are highly dominated by zircon. Other minerals are present, but in very small

amounts (Table 3.2 and Appendix D). The samples seem to have predominantly felsic igneous/metamorphic origin with only small amounts of rutile, garnet and monazite (Table 3.2 and Appendix D).

Table 3.2: Results from the heavy mineral analysis. R=remnants, Ap (Apatite), Ca (calcium amphibole), Cp (clinopyroxene), Ep (epidote), Gt (garnet), Mo (monazite), Op (orthopyroxene), Ru (rutile), To (Tourmaline).

Sample	Ap	Ca	Cp	Ep	Gt	Mo	Op	Ru	To	Zr
Rund 1-5-16	2.0				0.5			1.5		96.0
Rund 1-7-16		0.5	0.5	1.0		R				98.0
Rund 1-8-16	2.0	1.0					1.0		0.5	95.5
Rund 2-8-16	4.0								0.5	95.5
Rund 2-6-16				2.9	1.0					95.1
Rund 2-5-16				1.8						98.2

4 Discussion

4.1 Depositional environment

An Eocambrian age has been suggested for the sedimentary rock of the Valdres Group (Strand, 1959; Loeschke and Nickelsen, 1968; Hossack et al., 1985). These sedimentary successions were deposited in a rift basin, the Valdres Basin, at the western margin of Baltoscandia (Nystuen and Lamminen, 2011). The Valdres Basin was a continental basin at the time the Valdres Group was deposited, and a dominating fluvial depositional environment has been suggested (Loeschke and Nickelsen, 1968). When comparing the sedimentary logs of the Valdres Group at Rundemellen to the sedimentary logs of the Rendalen Formation in the Hedmark Group, they show great similarities. The sedimentary successions of the Rendalen Formation were deposited in the continental part of the Hedmark Basin and in a braided river environment (Nystuen, 1982).

4.1.1 FA 1

FA1 is composed of grain-supported conglomerates separated by structureless sandstone units or sandstones containing sedimentary structures. FA 1 has a thin layer of fine-grained sandstone at the top, making it an overall upwards fining sequence (Figure 3.9).

The conglomerates are characterized by sub-angular to rounded clasts consisting of quartzite, feldspar, clay and rhyolite. The clasts range in size from granule to pebble, where the largest clasts (quartzite and rhyolite) are usually more rounded than the smaller ones (feldspar and clay). The degree of rounding is mainly a function of grain size, mineralogical composition, transport mechanisms and distance (Reading and Levell, 1996). The variation in degree of rounding may indicate that some of the clasts have been transported for a longer distance than others, or simply that some of the clasts had a larger surface area and is thus easier to erode. Feldspar grains are not as resistant to erosion and weathering as quartz grains and may have been eroded during transport. This could lead to smaller feldspar grains with more angular surfaces than the larger and more rounded quartz grains. Clasts deposited during short-lived floods tend to be more angular and display the greatest immaturity (Nemec and Steel, 1984). This may also be a reason why some grains are more angular than others. The conglomerates are poorly sorted and normally lack sedimentary structures. An overall normal grading was observed in all conglomerate units, however one unit had an assemblage of large clasts in a line horizontal to bedding (Figure 3.9).

The conglomerate matrices are made up of sandstones with grain sizes ranging from very coarse sand to coarse sand. The dominating color of the matrix is light pink, but red and purple color tones also occur. There are differences in the clast composition, clast size and percentage of clasts in the conglomerates. A possible explanation may be that changes in supply and transport distance from the provenance area caused these differences during deposition.

Sandstone units of facies 2 found in FA 1 can be divided into three different sandstone types based on the presence of sedimentary structures. Structureless sandstones are most common within FA 1, but parallel lamination and cross-bedding also occur (Figure 3.9 and 3.10). Structureless sandstone units may indicate rapid deposition of large amounts of sediments in suspension in the area and time of deposition (Collinson et al., 2006). These sandstone units

thus point to a high-energy depositional environment (pers. com. J. P. Nystuen, 2017). The parallel laminated sandstone units may indicate changes or fluctuations in the depositional conditions, since these sedimentary structures are caused either by grain size variations or variations in mineralogical composition. In this case the parallel laminations are most likely caused by grain size variations rather than variations in mineralogical composition, and thus reflect changes in flow velocity (Collinson et al., 2006). The parallel laminations may have been created by sand grains settling from suspension or traction transport in water (Collinson et al., 2006). The cross-bedded sandstones have been deposited by other mechanisms than the structureless and parallel laminated sandstone units. Cross-beds are usually created by migrating dunes, ripples or channel bars, and may indicate a fluvial depositional environment (Collinson et al., 2006). Within braided river channels, traction currents transport sediments in the form of longitudinal and transverse bar systems which deposit cross-bedded sandstones (Selley, 1996).

The fine-grained sandstone of facies 3 found in FA 1 is characterized by a dark red to brown color and contains parallel lamination. The laminations were created by the same mechanism as described above. The transition from coarse sandstone to fine-grained sandstone marks a change in flow conditions, from a high-energy environment to a lower-energy environment. These fine-grained sandstones may be related to overbank conditions where the channel breaks its banks due to increased water level during periods of heavy or increased rainfall. In overbank environments the energy-level decrease abruptly when the stream oversteps its banks. The sediments with the highest density will then settle out of suspension first, in this case fine-grained sand (Selley, 1996). The fine-grained sandstone layers may also be linked to longitudinal bar deposits, where the channel overtops the bar due to heavy rainfall. The energy will then abruptly decrease and the conditions will be quite similar to the overbank conditions. A possible reason for the finest material being fine-grained sand may be that the energy conditions were not sufficiently low for silt and clay to settle out of suspension. Another possibility is that silt and/or clay are not available in the provenance area. However, in braided river systems it is rare that silt and clay are preserved because there is no clearly defined flood plain where these sediments can settle out of suspension (Selley, 1996).

The upwards fining trend of FA 1 reflects fluvial depositional processes, since fluvial deposits generally display a fining upwards grain size trend (Collinson et al., 2006).

According to Reineck and Singh (1975), channel bars in braided rivers are usually made up of coarse or gravelly sediments. However, the formation of different bars in a braided river depends mainly on grain size and sorting (Smith, 1970). Longitudinal bars (Figure 4.1) are formed by coarse and poorly sorted sediments, while finer-grained and better sorted sediments favors the formation of transverse bars (Smith, 1970). Longitudinal bar deposits are essentially characterized by accumulations of coarse-grained to gravelly material with varying composition of sand and finer-grained material (Figure 4.1) (Lunt et al., 2004). During periods of high flow the channel bar may become stabilized by fine-grained sediments deposited on top (Reineck and Singh, 1975). The sedimentary log of FA 1 (Figure 3.9) displays poorly sorted conglomerates, several coarse-grained sandstone units topped by a fine-grained sandstone layer. This suggests that FA 1 may represent a longitudinal bar deposit rather than a transverse bar deposit.

4.1.2 FA 2

FA 2 is composed of several sandstone units of facies 2 and 3, with grain sizes ranging from very coarse sand to fine sand. The sandstones in FA 2 are coarsest at the base with a grain size of very coarse sand, and become finer upwards. A thin fine-grained sandstone layer is found at the top, making FA 2 an overall upwards fining sequence (Figure 3.9).

Sandstone units of facies 2 found in FA 2 can be divided into four different sandstone types based on the presence of sedimentary structures. Both structureless, parallel laminated and cross-bedded sandstones dominate in FA 2, and are created as described in chapter 4.1.1 above. Trough cross-beds also occur, but are less common. They usually form under lower flow regimes when ripples or dunes migrate (Reading and Levell, 1996). Pebbly sandstones of facies 2e are also present in FA 2, and are poorly sorted. They may have been deposited at the channel-floor by saltation. Such deposits are typical for channel systems in braided rivers, and have also been observed in the Rendalen Formation (Hedmark Group) (Nystuen, 1982). The largest clasts in the pebbly sandstones may represent the maximal competence of the river current. Grain size variations can also be a result of the sediments available from the provenance area and not necessarily the stream competency (pers. com. J. P. Nystuen, 2017).

Fine-grained sandstone layers of facies 3 occur at the top of FA 2 and are parallel laminated or contain asymmetrical ripples (Figure 3.9). Deposition of parallel laminated sandstone beds

has been described above in chapter 4.1.1. Ripples are formed by water movement over a sandstone bed, as unidirectional flow, currents or both (Collinson et al., 2006). Grains begin to move as the water velocity exceeds a specific critical value and asymmetrical ripples start to form almost instantly with widespread movement of grains finer than 0.6 mm (Collinson et al., 2006). Fine-grained layers may have been deposited during a late stage of channel abandonment, when the river is flooded and has a high water level. The accommodation is usually low at this point and fine-grained sediments settle out of suspension (Rust, 1977).

FA 2 may be interpreted as channel fill deposits or a transverse bar (Figure 4.1) deposited by a braided river environment. Channel fill deposits from braided rivers may be characterized by sedimentation in one stream channel or may represent several channels due to avulsions or cut-off processes. Channel switching may be caused by sudden abandonment of the whole of a channel course or by sediments filling up the channel due to increasing sedimentation rate and reduction in depth and hence accommodation decreases (Lunt et al., 2004). It seems most likely that FA 2 represents a development over time with deposits from several channels rather than one channel deposit of 15 meters. Braided streams are characterized by high width: depth ratios and the channels are seldom very deep (Miall, 1977).

Another possibility is that FA 2 represents a transverse bar deposited in a braided fluvial environment. Transverse bars form by sediments aggrading due to an equal rate of sedimentation and accommodation (Smith, 1971). The grain sizes on active bar surfaces tend to decrease downstream due to a decrease in depth and velocity, where small-scale structures tend to form (Smith, 1971). Transverse bar deposits are predominantly characterized by sandy material which is typically well sorted (Lunt et al., 2004). The sedimentary log of FA 2, shows well sorted sandstone units with small amounts of thin, fine-grained beds. These observations in addition to the sedimentary structures present through FA 2 may point to a transverse bar deposit (Figure 4.1).

The sedimentary successions of FA 2 are coarse and show an upwards fining trend. Sediments with an upwards fining trend are, according to Reineck and Singh (1975), most commonly well developed in channel fill sequences. The coarse grain sizes also point towards a braided depositional environment. FA 2 contains pebbles in the lowest beds of each FA 2 sequence (Figure 3.9), which is common for channel-floor deposits. This suggests that the sedimentary succession of FA 2 may be a channel fill deposit rather than a transverse bar.

4.1.3 FA 3

FA 3 is composed of several sandstone units of facies 2, with no or minor variations in grain size (Figure 3.9). Parallel lamination, cross-beds and randomly distributed pebbles occur in several sandstone units, but structureless sandstones are most frequently observed in FA 3. Structureless sandstone units dominate in the lowest part of FA 3, but can also be observed at the top of FA 3 (Figure 3.9). The depositional mechanisms that create the structureless, parallel laminated and cross-bedded sandstone unit have already been described in chapter 4.1.1 above and have been interpreted to represent fluvial systems. The pebbly sandstone units may have been deposited by saltation at the channel floor, which has been described in more detail above, in chapter 4.1.2.

The FA 3 log displays an aggradational stacking pattern which implies that the sedimentation rate is approximately equal to the accommodation. The sandstone units are well sorted and contains small-scale structures as described above. These observations may point to FA 3 being a transverse bar deposit (Figure 4.1). The formation and deposition of transverse bars are described above in chapter 4.1.2.

4.1.4 FA 4

FA 4 consists of the matrix supported and poorly sorted breccia of facies 4. The matrix of the breccia is very coarse-grained sand with a dark grey towards green color. The clasts in the breccia are mainly composed of K-feldspar and vary from angular to sub-rounded. Based on the poor sorting and shape of the clasts this deposit can be interpreted as a tillite, quite similar to the Moelv tillite in the Hedmark Group. A comparison of these two deposits will be given in chapter 4.5.1.

4.1.5 Braided river depositional environment

The lithologies of braided fluvial deposits are mostly made up of conglomerates, coarse-grained sandstones and varying amounts of fine-grained material (Selley, 1996). Sedimentary sequences deposited by braided rivers displays an upwards fining trend, which may be caused by gradual channel abandonment or by falling flood stage (Nemec and Steel, 1984). The entire sedimentary log from Rundemellen shows upwards fining sequences, with conglomerates, coarse sandstones and thin fine-grained sandstone beds. Such upwards fining sequences are typical for fluvial successions, and the coarse grain size point to a braided

fluvial depositional environment. The sedimentary structures as cross-bedding, trough cross-bedding, parallel lamination, ripples and pebbly sandstone units observed at Rundemellen may also point to a fluvial depositional environment. The fluvial depositional mechanisms that create such structures have been described above, in chapter 4.1.1 and 4.1.2.

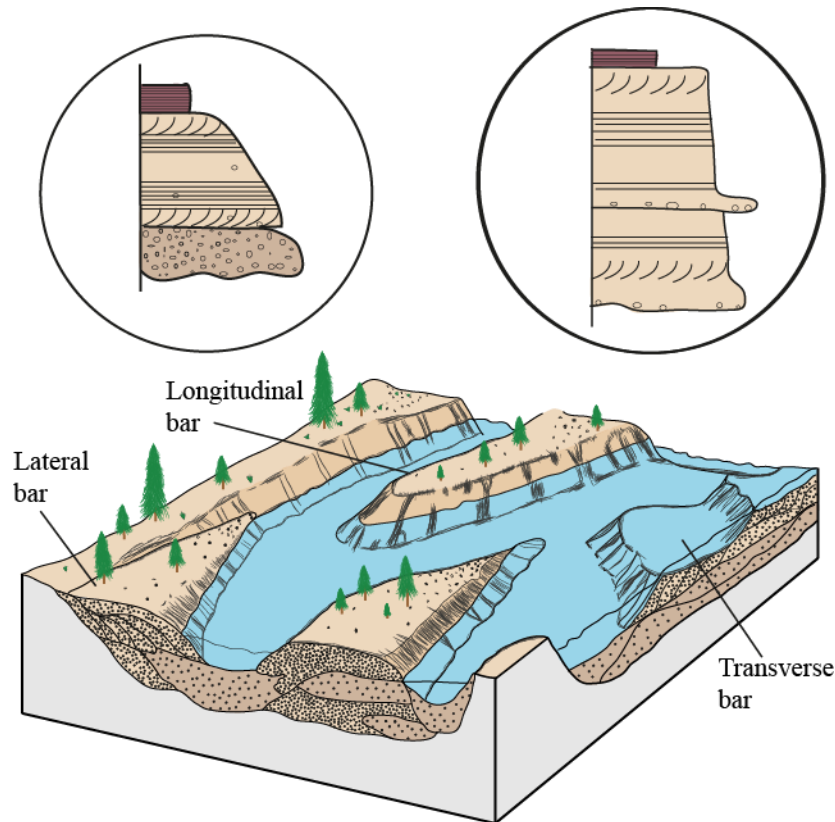


Figure 4.1: Depositional model of the braided stream environment with logs displaying longitudinal (left circle) and transverse bars (right circle) (Modified from Galloway and Hobday, 1983).

Streams with coarse bedload normally show highly variable patterns with bars and channels. In braided systems longitudinal bars are elongated parallel to flow and tend to split the stream into several branches. At the flat bar tops deposition takes place where coarse bedload might lodge in an imbricate packing. At the downstream end of the bar, avalanching may give rise to cross-bedding (Collinson et al., 2006). In deeper areas of the channels, the coarsest bedload is often deposited, but this may not be disguised when the bed becomes sub-aerially exposed and fine-grained material settles during low-water stages (Collinson et al., 2006). It seems likely that some units of the Rundemellen section display such longitudinal bar deposits as described by Collinson et al., (2006).

The sedimentary sequences with upwards fining development are also common in sedimentary successions deposited by turbidity currents (Doeglas, 1962). There are several reasons why it is not very likely that the sedimentary successions at Rundemellen were deposited by such processes. The beds have a red color which is not very common for turbidites, and no signs of Bouma sequence were observed (Doeglas, 1962). Red beds are however, common in braided deposits where the color often is a result of red iron oxide cement and may reflect early, sub-aerially alteration (Selley, 1996). The total absence of vegetation at the time of deposition favors a braided environment of the fluvial models, since channel banks are not cohesive and there is almost nothing that hinders run-off.

4.2 Mineralogical observations

This chapter will present and discuss different mineralogical observations from thin sections and heavy mineral analysis. Quartz/total feldspar ratios will be discussed in chapter 4.3.1: Transport and maturity.

Mineral precipitation

Mineral precipitation was seen as thin bands with a darker pink to red color occurring in the sandstones at Rundemellen. Due to the stronger red color it is possible that these bands are enriched in hematite. According to Loeschke (1967), the red color of the Valdres Group sandstones at Mellane may be result of hematite rather than high concentrations of K-feldspar.

Formation of sericite

Sericite is formed by low-grade metamorphic processes and sericitization of plagioclase (Que and Allen, 1996; Dunoyer de Segonzac, 1970). These two processes will further be described. Sericitization is the process in which feldspars are altered to sericite by the reaction of hydrothermal fluids with feldspar grains. This process takes place when hydrothermal fluids react with the grain surfaces in the pores, resulting in replacement of feldspar by sericite. This often results in a more sodic composition of the remaining feldspar grains (Que and Allen, 1996). Sericite can also form by low-grade metamorphic processes when muscovite is altered to sericite by replacement of Al by Mg and Fe²⁺ (Dunoyer de Segonzac, 1970).

The presence of sericite in the Rundemellen samples seems to have been formed by metamorphic processes rather than sericitization of feldspar grains. There is no evidence of sericite replacing the feldspar grains, nor is sericite found to occur within the feldspar grains.

Perthites

The perthites observed in the Rundemellen samples are mainly composed of K-feldspar with lamellas of albite. The absence of basic plagioclase in the Rundemellen samples can be explained by weathering processes which allow only the most durable plagioclase minerals (albite and orthoclase) to be transported over a longer time period (Loeschke, 1967). These perthites are characteristic for the Jotun area and have been suggested to originate from the Jotun rocks (Loeschke, 1967; Turner and Whitaker, 1976).

Heavy minerals

The heavy minerals found in the Rundemellen samples heavily dominated by zircon with only minor amounts of phosphates, orthosilicates and rutile (Table 3.2 and Appendix D). The zircons will therefore be the main focus. In one sample (Rund 1-5-16) zircon grains were found to have overgrowths of xenotime which according to Morton and Hallsworth (1999) is associated with intense leaching. Zircons with xenotime overgrowths have also been observed in fluvial Carboniferous and Jurassic sandstones in England, where they indicated an intense acidic groundwater leaching (Morton and Hallsworth, 1999). The zircons in the samples from Rundemellen were in addition fractured and metamict. This may indicate that the heavy minerals were formed in a hydrothermal environment before they were transported and deposited with the coarse clastic sediments which make up the sedimentary successions at Rundemellen.

Other features observed

The mineralogical analysis showed that quartz is the dominating mineral in almost every sample, where undulatory quartz was most common (Appendix B). This implies that most of the quartz grains have been somewhat deformed and exposed to a variety of pressure and temperature conditions. Many grains are also fractured, where some have been crushed and lost their original grain shape. These observations reflect the tectonic history of the rocks of the Valdres Group.

4.3 Environmental setting

This chapter will present a discussion on the maturity development and transport distance of the Valdres Group at Rundemellen. A brief discussion on the tectonic settings for the Valdres Group deposits and a short interpretation of possible provenance areas will also be presented.

4.3.1 Transport and maturity

The Rundemellen sedimentary successions are highly dominated by quartz, with varying amounts of K-feldspar and plagioclase (Figure 4.2, Appendix B and C). The plagioclase content is generally very low or not present at all. The ratio between quartz and feldspar may serve as a maturity indicator for sediments. This is because the quartz grains are more stable and resistant to erosion and weathering during transport than feldspars. The relationship between K-feldspar and plagioclase may also provide information about maturity since K-feldspar is more stable and resistant to weathering and erosion than plagioclase (Parsons, 2010). Hence, a high quartz/total feldspar ratio is expected for mature sediments, which

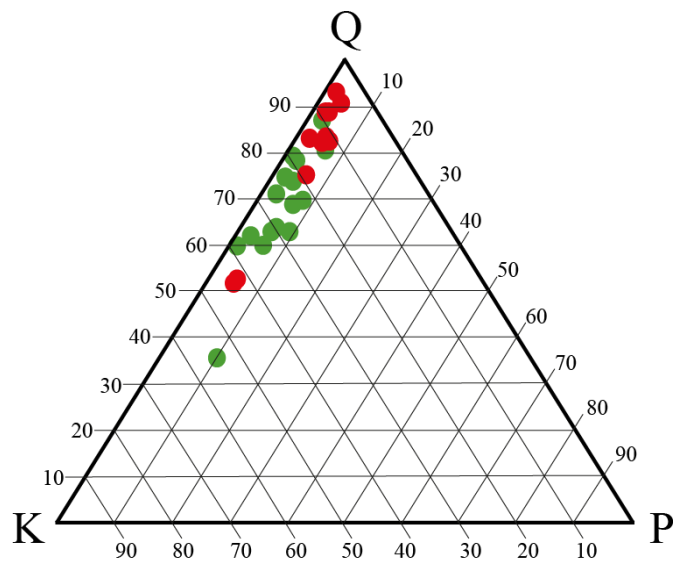


Figure 4.2: Displays the relationships between quartz, K-feldspar and plagioclase in the Rundemellen samples. The percentages are calculated from the point counting results shown in red (Appendix B) and XRD results in green (Appendix C). Two samples plot outside main assemblage (red dots), one is the breccia sample and the other one is a fine-grained sandstone sample. XRD results also show that the breccia sample plot outside the main assemblage.

is the case for most Rundemellen samples (Figure 3.21). This may imply that the sedimentary rocks at Rundemellen are mature and were transported for a relatively long distance before deposition. However, if the provenance rocks were mature, the sedimentary deposits will also be mature independent of transport distance.

The grain shape and sorting of sediments is generally a function of transport distance and reworking of sediments. Rounded grains and well sorting indicates a long transport distance and mature sediments. The sandstones at Rundemellen are mostly well sorted with grain shapes varying from sub-rounded to sub-angular (Appendix A). The sorting may imply a long transport distance while the grain shape may indicate a somewhat shorter transport distance. Sedimentary deposits from braided rivers are usually poorly sorted, since braided rivers tend to develop in areas with high relief close to the source (Miall, 1977). This may indicate that the provenance rock is mature rather than maturity caused by a long transport distance.

The results from the heavy mineral analysis revealed that the Valdres Group at Rundemellen is overwhelmingly dominated by zircon, with only minor amounts of other heavy minerals (Table 3.2 and Appendix D). Mechanisms operating during transport, deposition and diagenesis may have a large impact on the composition of heavy mineral assemblages in sandstones (Morton and Hallsworth, 1994). During transport minerals are subjected to abrasion processes which may affect the assemblage of mechanically stable minerals. However, several studies of large river systems with long transport distances found no evidence of decreasing heavy mineral assemblage or diversity downstream due to abrasion processes (Morton and Hallsworth, 1999).

Studies point to hydraulic and diagenetic processes being important controls on the diversity and assemblages of heavy minerals in sedimentary deposits. Heavy minerals behave differently than quartz and feldspar grains during transport and deposition because they have a higher density (Morton and Hallsworth, 1999). Rubey (1933) suggested that grains with the same settling velocity are deposited together, thus smaller heavy mineral grains can be deposited together with larger and less dense grains. Heavy minerals react sensitively to energy changes during transport due density differences. Low-energy conditions, such as flood plain environments, may deposit different heavy minerals than higher-energy environments (Morton and Hallsworth, 1999). Petrographical analysis showed that the fine-grained sandstone samples were found to contain a larger variety of heavy minerals than coarser sandstone samples.

Diagenetic processes influence the heavy mineral assemblages by dissolution of unstable phases and secondary growth of other minerals (Morton and Hallsworth, 1999). The degree of mineral depletion is affected by the amount of time a sedimentary deposit has been

exposed to pore-fluid movements and higher temperatures. During burial sediments are exposed to an increase in pore fluid temperature and the most unstable minerals starts to dissolve. They include calcic amphiboles, pyroxene, olivine and titanite to mention some. The most stable minerals as zircon, monazite, apatite and TiO_2 –minerals will remain even at burial depths of 4000 meters (Morton and Hallsworth, 1999).

The heavy mineral results show that the Valdres Group at Rundemellen is depleted in different heavy minerals, and is overwhelmingly dominated by zircon (Table 3.2 and Appendix D). Since the sedimentary succession is of Precambrian age and subjected to tectonic deformation, it seems reasonable that the low diversity of heavy minerals is caused by diagenetic and/or tectonic processes rather than abrasion during transport. The heavy minerals found in the samples are among the most stable ones, and the zircons are fractured and metamict.

4.3.2 Rift-controlled basin

The Valdres Basin is a continental rift basin where the sedimentary rocks of the Valdres Group were deposited by braided streams. The sedimentary successions observed at Rundemellen today were probably tectonically reduced to its present thickness during the Caledonian Orogeny.

Several rifting episodes after the initial Valdres Basin was created resulted in basin expansion and creation of increased accommodation during the deposition of the Valdres Group. The fluvial Rendalen Formation in the eastern part of the Hedmark Basin possesses similar trends with large-scale upwards fining units. They have been interpreted to be tectonically controlled either by variations in subsidence and accommodation within the basin, or movements along marginal faults (Nystuen, 1987). During rifting, accommodation is created in the basin and highland areas are often formed along the corresponding basin margins. The SW basin margin of the Valdres Basin probably represents a high created by footwall uplift during basin formation. It is possible that this high acted as a sediment source area and transported coarse sediments into the Valdres Basin. This assumption is based on the paleocurrent measurements at Rundemellen, indicating a transport direction from WNW towards ESE for the Valdres Group. As the basin began to fill, accommodation decreased and hence the relief became reduced. This led to deposition of fine grained material if no new

accommodation was created to obtain the sedimentation rate. Since the Hedmark- and the Valdres basins were located close to each other during deposition of the Valdres Group, it can be assumed that also the Valdres Group was tectonically controlled and represents syn-rift sediments. Reconstruction of the basin geometry in the Valdres Basin is difficult because the basin margins are not preserved due to erosion (pers. com. J. P. Nystuen, 2017).

4.3.3 Provenance area

Sedimentary basin deposits carry records of the surrounding bedrock formations, both proximal and distal (Lamminen et al., 2015). The sedimentary successions seen today have been influenced by processes from weathering of the source rock, to deposition and post-depositional alteration (transport, sediment storage, depositional environment and paleoclimate).

As a result of the formation of Rodinia during Mesoproterozoic time (Figure 1.2) the Sveconorwegian Orogen were created (Lamminen et al., 2015). This mountain belt acted as a sediment source for the basins formed at the western Baltoscandian margin, during the break-up of Rodinia in Neoproterozoic time (Figure 1.3). The Hedmark Group sedimentary deposits have been interpreted to have an Sveconorwegian source by Lamminen et al. (2015). This is probably also the case for the Valdres Group rocks, since both basins were located close to each other at the western margin of Baltoscandia (Figure 1.5).

Jotun rocks have been suggested as a possible source for the Valdres Group by several authors based on the presence of Jotun perthites (Loeschke, 1967; Turner and Whitaker, 1976). However, this theory is questionable because there are only small amounts of such perthites in the Valdres Group (Loeschke, 1967). According to Loeschke (1967), other perthite types occur more frequently than the Jotun perthites in the Valdres Group and other source areas should be taken into consideration.

The conglomerates at Rundemellen contain rhyolite-, granite- and quartzite clasts. These clasts may originate from the Mesoproterozoic volcanic and sedimentary rocks in the Telemark area called the “Telemark Supracrustals” or volcanic rocks from Hallingdal and Numedal (Loeschke, 1967). The volcanic sources were composed of rhyolite and basalt while the sedimentary supracrustal sources consisted of quartzites, sandstones, conglomerates and

breccia (Bingen et al., 2005b). The rhyolite in the Telemark area is a possible source for the rhyolite clasts seen in the conglomerates at Rundemellen. Several sedimentary formations in the Telemark area are composed of mature sedimentary rocks (Lamminen and Köykkä, 2010) and may have acted as a source for the Valdres Group sandstones. According to Loeschke (1967), possible sources for the Valdres Group are only abundant in the Precambrian successions in Telemark, Hallingdal and Numedal.

The paleocurrent measurements imply that sediments were transported from WNW towards ESE direction (Figure 4.4), which may point to a source area in WNW. The streams in a braided river are highly variable and transport directions may vary with 180 degrees in a braided stream environment (pers. com. J. P. Nystuen, 2017). This is due to the rapid fluctuations and channel switching in the river.

These theories are however only based on analysis of the sedimentary rocks found at Rundemellen and comparison to the published Precambrian history of Norway. If dating analysis of zircons in the Valdres Group were available, it could be possible to propose a provenance area with more certainty.

4.4 Correlation with Skarvemellen

Great compositional variations can occur within a braided river system influx; several streams shift channels and may have sediment influences from different areas. Variations in mineralogy between Rundemellen and Skarvemellen can occur but the distance between them are very short and the source area might have been the same.

The Skarvemellen samples generally contain more plagioclase and less quartz than the Rundemellen samples (Figure 4.3). Two Rundemellen samples plot outside the main clusters; these are the breccia sample and a fine-grained sample. They contain more K-feldspar and less quartz than the other samples (Figure 4.3). The breccia and the fine-grained samples are not as well sorted as the sandstone samples, and may be less mature. The Skarvemellen breccia sample contains less K-feldspar clasts and more quartz and plots in the cluster. Despite small differences the main mineralogical development of the samples from Rundemellen and Skarvemellen is relatively similar.

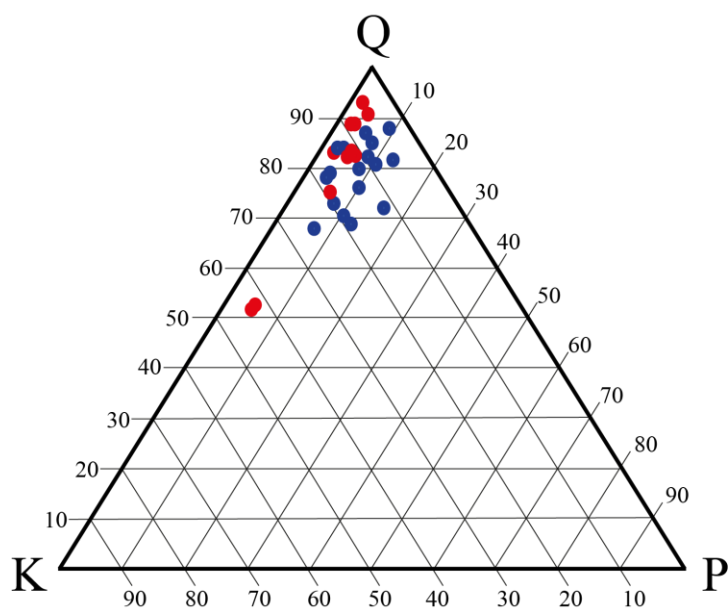


Figure 4.3: QAPF plot of the Rundemellen samples (Red) and the Skarvemellen samples (blue). The ratios are calculated from point counting results (Appendix B).

The analyzed Rundemellen samples generally contain more quartz, less plagioclase, more zircon and less apatite than the Skarvemellen samples. The degree of rounding is generally better at Skarvemellen than at Rundemellen and indicates a possible longer or more powerful transport for sedimentary successions at Skarvemellen (Appendix A). The differences are minor and braided rivers may have great variations in mineralogical composition within a single system. These differences may be caused by great mineralogical variations over short distances in the provenance area, leading to a difference in sediment composition from one channel to another. Mineralogical differences between channels can also occur if sediment is transported from different directions and only into some of the channels in the braided river.

Slight differences in paleocurrent measurements were measured at the two sites; Rundemellen displays an E-SE direction and the succession logged at Skarvemellen E-NE transport direction (Figure 4.4). As described above, great variations may occur within a single braided system, both with respect to mineralogy and transport directions. It is likely to assume that the sedimentary rocks at Rundemellen and Skarvemellen were deposited in two separate channel systems based on the paleocurrent measurements and the mineralogical differences.

Paleocurrent measurements

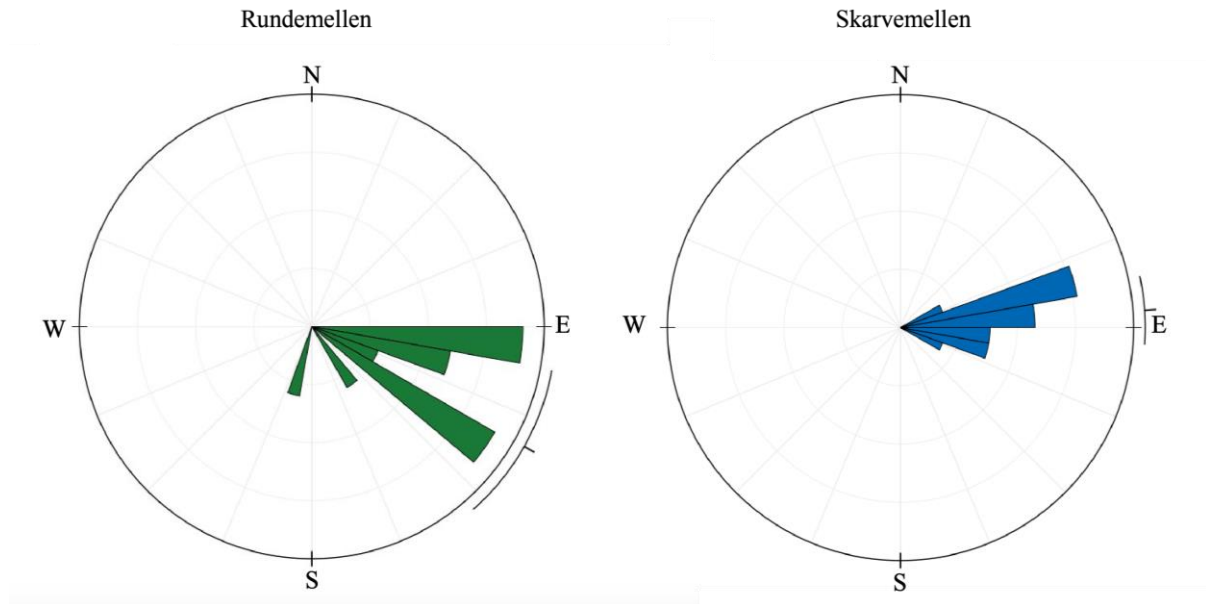


Figure 4.4: Paleocurrent measurements from Rundemellen (green) and Skarvemellen (blue). The Rundemellen rose diagram displays an ESE sedimentary transport direction while the Skarvemellen diagram displays an ENE transport direction.

The distance between Rundemellen and Skarvemellen today is approximately 2 km in straight line. The Valdres Group is overturned at both localities and may imply that they were situated at the same limb of the Skarvemellen recumbent anticline formed during the Caledonian Orogeny. If they were positioned in the same flank of the anticline, their distance would have been approximately the same before thrusting. If they were positioned at different limbs of the anticline, the distance between the two localities would have been greater and the directions twisted prior to Caledonian thrusting.

At Rundemellen the breccia was not observed as solid rock, which was the case at Skarvemellen. The breccia occurring at both localities has been interpreted as a tillite deposited during the Varanger glaciation, and can therefore be correlated (Figure 4.6). The tillite has been interpreted to be an equivalent to the Moelv tillite in the Hedmark Basin, an important surface for both local and regional correlation.

In the petrographic analysis it is observed that the tillite at Rundemellen contains more K-feldspar and matrix than the tillite at Skarvemellen. From thin section analysis it is seen that the Rundemellen sample has several large clasts composed of K-feldspar, while the Skarvemellen sample does not. The XRD results (Appendix C) also show a larger amount of K-feldspar in the tillite at Rundemellen. This can be caused by the larger clast variations in the sample. The Skarvemellen sample has a high amount of small quartz grains in the matrix which have been counted as matrix and contributes to differences between point counting- and XRD- results (Appendix B and C). The Skarvemellen sample may be more representative for the matrix, while the Rundemellen sample has several clasts of K-feldspar leading to a difference in mineralogical composition. Despite several small differences, the main characteristics are the same. Both samples are poorly sorted and matrix supported, with angular clasts floating in a coarse matrix. However, only one sample of the breccia was taken from Rundemellen and two samples from Skarvemellen which lead to uncertainties.

Correlation of the conglomerate unit shown in Figure 4.5 and 4.6 is based on similarities in field occurrences. Figure 4.5 shows that both conglomerate units have small clasts in a pink matrix. Both conglomerates are grain-supported and seem to have the same mineralogical composition at both localities. Rund 1-13-16 and Ska 2-8-16 represent the conglomerates, at Rundemellen and Skarvemellen respectively. The petrographical analysis confirms that the two conglomerates have the same mineralogical composition, but the Rundemellen conglomerate contains more quartz and less matrix than the conglomerate at Skarvemellen.

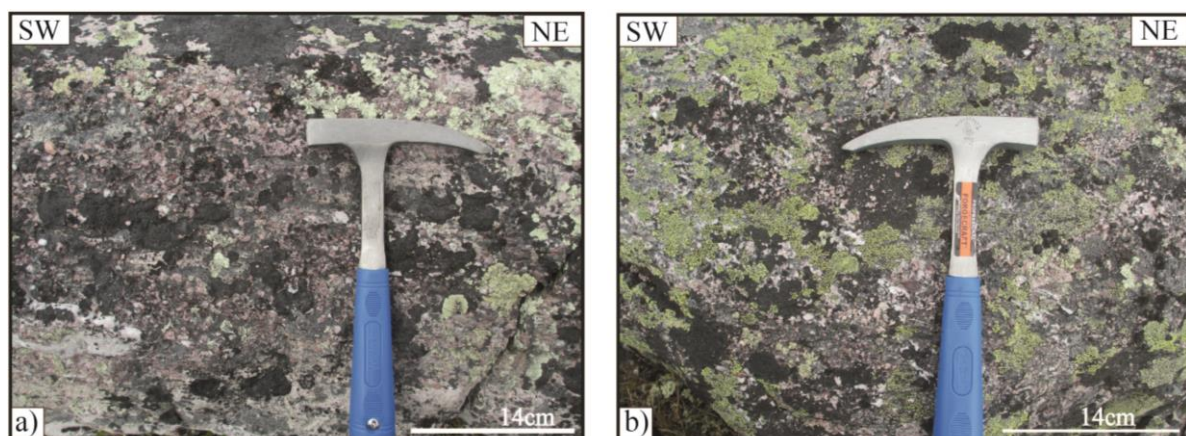


Figure 4.5: Grain supported conglomerates with small clasts in a pink, coarse-grained matrix. a) Conglomerate observed at Skarvemellen shows great similarities with one of the conglomerate units observed at Rundemellen (b). Vegetation makes it difficult to see the conglomerates clearly, but to the left of the hammer in both a) and b), it is possible to see that both conglomerates consist of small clasts in a red matrix.

S

N

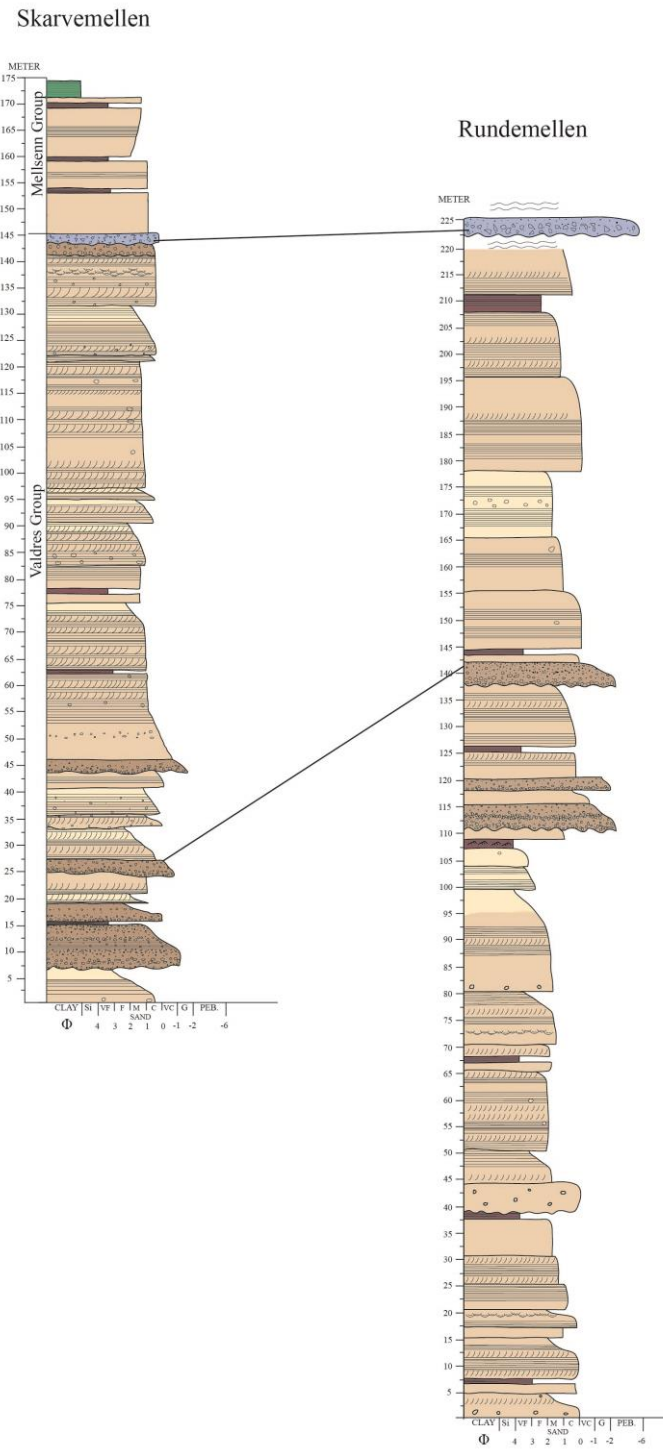


Figure 4.6: Correlation of the sedimentary logs from Rundemellen and Skarvemellen. The Skarvemellen log is from Småkasin (2017).

The Valdres Group at both Rundemellen and Skarvemellen has been interpreted to represent braided stream environments in a central part of the Valdres Basin (Figure 4.7). The sedimentary succession at Skarvemellen contains more sedimentary structures than the sedimentary successions at Rundemellen (Figure 4.6). This can imply that there have been more frequent energy-changes in the channels of Skarvemellen.

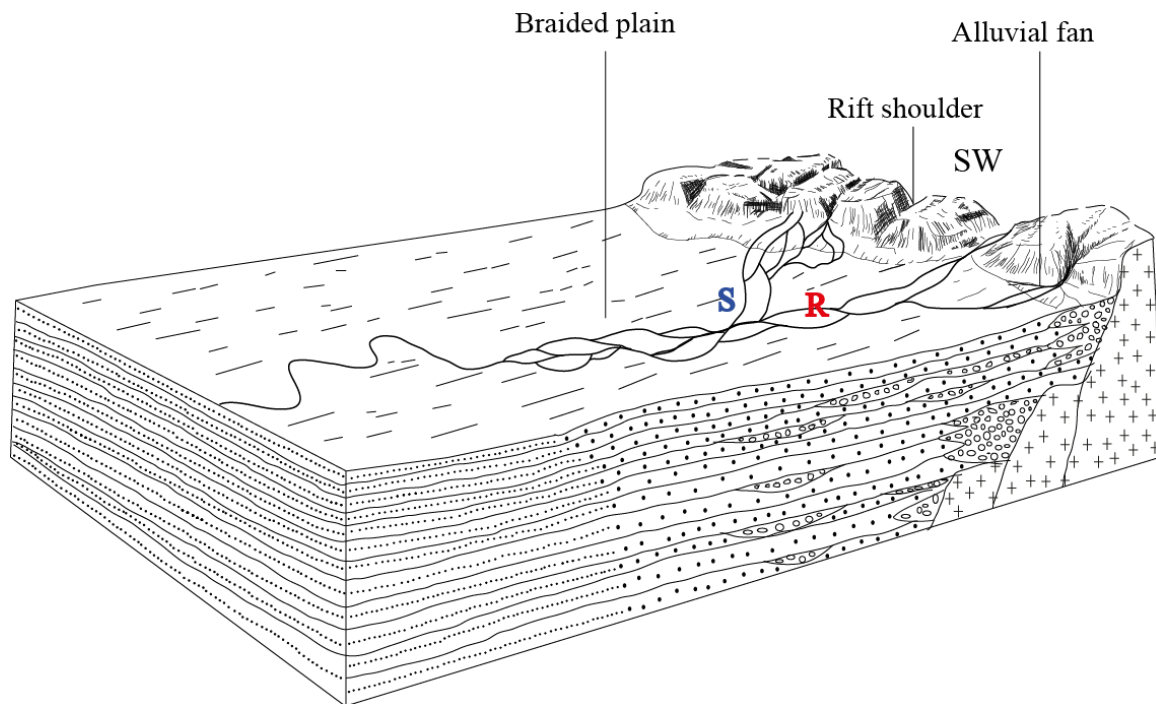


Figure 4.7: A possible model for the continental Valdres Basin. The position of Rundemellen (R) and Skarvemellen (S) is suggested in a central part of the basin (Modified from Nystuen, 1982).

4.5 Correlation with the Hedmark Group

4.5.1 Correlation with the Ring Formation

One sandstone sample from the Ring Formation has been studied in thin section and SEM. The results show pore-filling chlorite in the Ring Formation sandstone, while at Rundemellen the pore-filling mineral in the sandstones is muscovite and sericite. This may indicate that the Ring Formation have been exposed to different metamorphic regime than the Valdres Group. Another possibility is that the sediment source is different for the two formations. The

mineralogical composition in the Valdres Group sandstones from Rundemellen and the sandstone in the Ring Formation is otherwise quite similar, with quartz and K-feldspar being the dominant minerals.

The heavy mineral analysis shows that the Ring Formation contains large amounts of apatite, whereas the Valdres Group at Rundemellen is dominated by zircon (Appendix D). The two formations generally contain the same heavy minerals, but the amount varies (Appendix D).

Glacial deposits of Late Neoproterozoic age have been recorded on most continents, also at low latitudes which imply that the Earth was affected by a global glaciation (Bingen et al., 2005a). This Neoproterozoic glacial deposit occurs as tillites in the Hedmark Basin and in the Valdres Basin (Nystuen and Lamminen, 2011). Both tillites are composed of siltstone and sandstone matrix of compositions comparable to the overlying Ekre- and Vangsås formations (Nystuen and Lamminen, 2011). The tillite in the Valdres Basin is composed of lithologies similar to the Moelv Formation in the Hedmark Basin. The stratigraphic characteristics are also quite similar and support the interpretation that this unit is a glacier deposit (Nystuen and Lamminen, 2011). In the Valdres Basin the tillite reflects glaciation on top of a continental rift-basin succession with coarse-clastic alluvial fans and thick clastic fluvial succession in the central part of the basin. In the Ormtjernkampen area the tillite was deposited on top of an alluvial fan succession and on crystalline basement rocks, whereas in the Mellene area it was deposited on top of thick, fluvial successions (Nystuen and Lamminen, 2011). This may imply that the Valdres Group at Mellane was deposited in the central part of the Valdres Basin.

Sveconorwegian sediment sources have been suggested for sedimentary successions of the Hedmark Basin and for the Valdres Group at Rundemellen (Lamminen et al., 2015; Loeschke, 1967). Extensive research in the Hedmark Basin sedimentary rocks suggests several source areas. Zircon ages show that the sedimentary material in the NW part of the Hedmark Basin likely to be of Sveconorwegian origin (Lamminen et al., 2015). The NE part of the Hedmark Basin was possibly sourced from the TIB (Trans-Scandinavian Igneous Belt) indicated by the zircon ages (Lamminen et al., 2015).

4.5.2 Correlation with the Rendalen Formation

The development of the Rendalen Formation in the eastern, continental part of the Hedmark Basin seems comparable to the development in the continental Valdres Basin. The Rendalen Formation was deposited by fluvial systems in Late Proterozoic time (Nystuen, 1982).

As seen in Figure 4.8, the Rendalen Formation is composed of several upwards fining units. The figure also shows how a braided environment can vary within a single system. The sedimentary log from Rendalsølen contains coarse sandstone units and may display overall upwards fining and coarsening trends (Figure 4.8). The sedimentary log of the Rendalen Formation at Brennhammaren is only composed of several upwards fining units consisting of coarse sandstone. In the Salsfjellet location, the Rendalen Formation contains several units of fine-grained sandstone in between the coarse upwards fining sandstone units (Figure 4.8).

There are great similarities between the sedimentary successions from Rundemellen and those of the Rendalen Formation (Figure 4.6 and 4.8). They are all composed of coarse sediments with upwards fining trends. The sedimentary log of the Rendalen formation from Salsfjellet has several thin layers of fine-grained sandstone occurring in between coarse sandstone. This can also be seen in the log from Rundemellen. The Rendalen Formation contains sedimentary rocks with coarser grain sizes than the Rundemellen succession. The Rendalen Formation and the Valdres Group had different sediment sources, and coarser sediments were transported into the eastern part of the Hedmark Basin than in the Valdres Basin.

The Rendalen Formation and the Valdres Group were deposited in Late Proterozoic time (Nystuen 1982). The two formations were deposited by comparable depositional environments in separate basins that were closely positioned at that time. This makes it possible to correlate the two formations by depositional environment.

RENDALSØLEN

BRENNHAMMAREN

SALSFJELLET

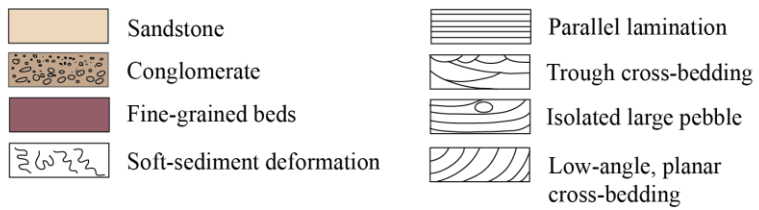


Figure 4.8: Sedimentary logs of the Rendalen Formations from Rendalsølen, Brennhammaren and Salsfjellet (Modified from Nystuen, 1982).

5 Conclusion

The Valdres Basin was created during the break-up of the continent Rodinia in Neoproterozoic time and was located at the western margin of Baltoscandia. During the early stages the shallow rift was dominated by coarse clastic fluvial sedimentation. These sedimentary deposits are today known as the Valdres Group.

The environment resulting in the deposition of the Valdres Group at Rundemellen has been interpreted to be characterized by braided rivers in the central part of the Valdres rift basin. The lithologies observed at Rundemellen are composed of conglomerates, coarse-grained sandstones and varying amounts of fine-grained material. The sedimentary sequences display an overall upwards fining trend, which may be caused by gradual channel abandonment or by falling flood stage.

A Sveconorwegian sediment source has been suggested both for the Valdres Group and the Hedmark Group. As a result of the formation of Rodinia the Sveconorwegian Orogen were created and later acted as a sediment source for the basins formed along the western Baltoscandian margin. Paleocurrent measurements from Rundemellen imply that sediments were transported from WNW towards ESE direction. This may point to a source area in WSW, and the SW flank of the Valdres Basin may be a possible sediment source. The Telemark supracrustals have also been suggested as a possible sediment source for the Valdres Group at Rundemellen. The volcanic sources in the Telemark area consisted of rhyolite and basalt and been suggested as a source for the conglomerate clasts. The sedimentary supracrustals in Telemark consisted of quartzites, conglomerates, sandstones and breccia and could have been a possible source for the Valdres Group at Mellane. Zircon datings have not been carried out for the Valdres Group at Mellane. Such analysis and related age-correlation can further improve our understanding of the provenance area.

Mineralogical differences between the Skarvemellen- and Rundemellen samples have been suggested to be a result of variations in mineralogical composition in the source area. The paleocurrent measurements may indicate that deposition took place in two separate river channels, which also could have contributed to light mineralogical variations.

References

- Bingen, B., Griffin, W. L., Torsvik, T. H. & Seaeed, A. 2005a. Timing of Late Neoproterozoic glaciation on Baltica constrained by detrital zircon geochronology in the Hedmark Group, south-east Norway. *Blackwell Publishing Ltd*, 250-258 p.
- Bingen, B., Skår, Ø., Marker, M., Sigmond, E. M. O., Nordgulen, Ø., Ragnhildstveit, J., Mansfeld, J., Tucker, R. D. & Liégeois, J.-P. 2005b. Timing of the continental building in the Sveconorwegian orogen, SW Scandinavia. *Norwegian Journal of Geology*, 85, 87-116 p.
- Bjørlykke, K., Elvsborg, A. & Høy, T. 1976. Late Precambrian sedimentation in the central sparagmite basin of south Norway. *Norsk Geologisk Tidsskrift*, 56, 233-290 p.
- Bjørlykke, K. O. 1905. Det centrale Norges fjeldbygning. *Norges Geol. Unders*, 39, 595 p.
- Bockelie, J. F. & Nystuen, J. P. 1985. The southeastern part of the Scandinavian Caledonides. *In: Gee, D. G. & Sturt, B. A. (eds.) The Caledonide Orogen- Scandinavia and Related Areas*. John Wiley & Sons Ltd, Chichester, 69-88 p.
- Bruker. 2011. Diffrac. Suite. User Manual. Original Instructions. *Bruker AXS GmbH*, 162 p.
- Collinson, J. D., Mountney, N. P. & Thompson, D. B. 2006. *Sedimentary Structures, third edition*, Hertfordshire, England, Terra Publishing, 292 p.
- Compton, R. R. 1962. Manual of Field Geology. *Soil Science*. New York: Wiley, 295 p.
- Doeglas, D. J. 1962. The structure of sedimentary deposits of braided rivers. *Sedimentology*, 1, 167-190 p.
- Dunoyer De Segonsac, G. 1970. The transformation of clay minerals during diagenesis and low-grade metamorphism: A review. *Sedimentology*, 15, 281-346 p.
- Esmark, J. 1829. Reise fra Christiania til Tronhjem. *Christiania (Oslo)*, 81 p.
- Fossum, K. 2012. *Sedimentology, petrology and geochemistry of the Kilimatinde Cement, central Tanzania*. Master Thesis, University of Oslo, 129 p.
- Galloway, W. E. & Hobday, D. K. 1983. Fluvial systems. *In: Galloway, W. E. & Hobday, D. K. (eds.) Terrigenous Clastic Depositional Systems*. US: Springer-Verlag, 51-79 p.
- Goldschmidt, V. M. 1916. Konglomeraterne inden høifjeldskvartsen. *Norges Geol. Unders*, 77, 61 p.
- Goldstein, J., Newbury, D. E., Joy, D. C., Lyman, C.E, Echlin, P., Lifshin, E., Sawyer, L. & Michael, J. R. 2003. Scanning electron microscopy and X-ray microanalysis. Springer.
- Google Maps. 2017. *Kartdata* [Online]. Available: <https://www.google.no/maps/@61.6859716,9.612721,7z?hl=en> [Accessed 13.05 2017].
- Hartz, E. H. & Torsvik, T. H. 2002. Baltica upside down: A new plate tectonic model for Rodinia and the Iapetus Ocean. *Geological Society of America*, 30, 255-258 p.
- Heim, M., Schäfer, U. & Milnes, A. G. 1977. The nappe complex in the Tyin-Bygdin-Vang region, central southern Norway. *Norsk Geologisk Tidsskrift*, 57, 171-178 p.
- Hillier, S. 2000. Accurate quantitative analysis of clay and other minerals in sandstones by XRD: comparison of a Rietveld and a reference intensity ratio (RIR) method and the importance of sample preparation. *Clay Minerals*, 35, 291-302 p.
- Holtedahl, O. 1959a. Noen iakttagelser fra Grønsennknipa i Vestre Slidre, Valdres. *Norges Geol. Unders*, 205, 90-106 p.
- Holtedahl, O. 1959b. Noen iakttagelser fra Grønsennknipa i Vestre Slidre, Valdres. *Norges Geol. Unders*, 90-106 p.

- Hossack, J. R. 1968. Pebble deformation and thrusting in the Bygdin area (Southern Norway). *Tectonophysics- Elsevier Publishing Company, Amsterdam*, 5, 315-339 p.
- Hossack, J. R. & Cooper, M. A. 1986. Collision tectonics in the Scandinavian Caledonides. *In: Coward, M. P. & Ries, A. C. (eds.) Collision Tectonics*. Geological Society Special Publications, 19, 287-304 p.
- Hossack, J. R., Garton, M. R. & Nickelsen, R. P. 1985. The geological section from the foreland up to the Jotun thrust sheet in the Valdres area, south Norway. *In: Gee, D. G. & Sturt, B. A. (eds.) The Caledonide Orogen- Scandinavia and Related Areas*. John Wiley & Sons Ltd, Chichester, 443-446 p.
- Kartverket. 2017. *Norgeskart* [Online]. Available: http://www.norgeskart.no/?_ga=2.44021100.813259395.1494610268-1929000086.1494610268#!?project=seeiendom&layers=1002,1014&zoom=12&lat=6787841.28&lon=189935.03&sok=rundemellen [Accessed 13.05 2017].
- Kjerulf, T. 1873. Sparagmittfjeldet. *Universitetsprogram for andet Halvaar, Christiania*, 85 p.
- Kjerulf, T. 1879. Udsigt over det sydlige Norges geologi. *Christiania, W. C. Fabritius*, 262 p.
- Kjerulf, T. & Dahl, T. 1866. Geologisk kart over det søndenfjeldske Norge, optaget 1858-1865. *Christiania*.
- Kulling, O. 1961. On the age and tectonic position of the Valdres sparagmite. *Geol. Fören. Stockholm. Förh.*, 102, 531-550 p.
- Kumpulainen, R. & Nystuen, J. P. 1985. Late Proterozoic basin evolution and sedimentation in the westernmost part of Baltoscandia. *In: Gee, D. G. & Sturt, B. A. (eds.) The Caledonide Orogen- Scandinavia and Related Areas* John Wiley & Sons Ltd, Chichester, 213-232 p.
- Lamminen, J., Andersen, T. & Nystuen, J. P. 2015. Provenance and rift basin architecture of the Neoproterozoic Hedmark Basin, South Norway inferred from U-Pb ages and Lu-Hf isotopes of conglomerate clasts and detrital zircons. *Geol. Mag.*, 152, 80-105 p.
- Lamminen, J. T. & Köykkä, J. 2010. The provenance and evolution of the Rjukan Rift Basin, Telemark, South Norway: The shift from a rift basin to an epicontinental sea along a Mesoproterozoic supercontinent. *Precambrian Research*, 181, 129-149 p.
- Loeschke, J. 1967. Zur Stratigraphie und Petrographie des Valdres-Sparagmites und der Mellsenn-Gruppe bei Mellane/Valdres (Süd-Norwegen). *Norges Geol. Unders.*, 243, 5-66 p.
- Loeschke, J. & Nickelsen, R. P. 1968. On the age and tectonic position of the Valdres Sparagmite in Slidre (Southern Norway). *N. Jb. Geol. Paläont.*, , 131, 337-367 p.
- Lunt, I. A., Bridge, J. S. & Tye, R. S. 2004. A quantitative, three-dimensional depositional model of gravelly braided rivers. *Sedimentology*, 51, 377-414 p.
- Miall, A. D. 1977. A Review of the Braided-River Depositional Environment. *Earth-Science Reviews*, 13, 1-62 p.
- Moore, D. M. & Reynolds, R. C. 1997. X-Ray Diffraction and the Identification and Analysis of Clay Minerals. *Oxford: Oxford University Press*, 378 p.
- Morton, A. C. 1985. Heavy minerals in provenance studies. *In: Zuffa, G. G. (ed.) Provenance of Arenites*. D. Reidel Publishing Company, 249-277.
- Morton, A. C. & Hallsworth, C. 1994. Identifying provenance-specific features of detrital heavy mineral assemblages in sandstones. *Sedimentary Geology*, 90, 241-256 p.
- Morton, A. C. & Hallsworth, C. 1999. Processes controlling the composition of heavy mineral assemblages in sandstones. *Sedimentary Geology*, 124, 3-29 p.
- Nemec, W. & Steel, R. J. 1984. Alluvial and coastal conglomerates: their significant features and some comments on gravelly mass-flow deposits. *In: Koster, E. H. & Steel, R. J.*

- (eds.) *Sedimentology of Gravels and Conglomerates*. Canadian Society of Petroleum Geologists, 10, 1-31 p.
- Nickelsen, R. P. 1967. The Structure of Mellene and Heggeberg, Valdres. *Norges Geol. Unders*, 9-121 p.
- Nickelsen, R. P., Hossack, J. R. & Garton, M. R. 1985. Late Precambrian to Ordovician stratigraphy and correlation in the Valdres and Synnfjell thrust sheets of the Valdres area, southern Norwegian Caledonides; with some comments on sedimentation. In: Gee, D. G. & Sturt, B. A. (eds.) *The Caledonide Orogen- Scandinavia and Related Areas*. John Wiley & Sons Ltd, Chichester, 369-378 p.
- Nystuen, J. P. 1982. Late Proterozoic Basin Evolution on the Baltoscandian Craton: The Hedmark Group, Southern Norway. *Norges Geol. Unders, Bulletin 67*, 375, 1-74 p.
- Nystuen, J. P. 1985. The southeastern part of the Scandinavian Caledonides. In: G, G. D. & Sturt, B. A. (eds.) *The Caledonide Orogen- Scandinavia and Related Areas*. John Wiley & Sons Ltd.
- Nystuen, J. P. 1987. Synthesis of the tectonic and sedimentological evolution of the late Proterozoic-early Cambrian Hedmark Basin, the Caledonian Thrust Belt, southern Norway. *Norsk Geologisk Tidsskrift*, 67, 395-418 p.
- Nystuen, J. P. 2013. Urtidskontinentet brytes opp. In: Ramberg, I. B., Bryhni, I., Nøttvedt, A. & Rangnes, K. (eds.) *Landet blir til*. 2 ed.: Norsk Geologisk Forening. 120-148 p.
- Nystuen, J. P. & Lamminen, J. 2011. Neoproterozoic glaciation of South Norway: from continental interior to rift and pericratonic basins in western Baltica. *Geological society of London*, 36, 613-622.
- Oberhardt, N. 2013. *Granite weathering, saprolitization and the formation of secondary clay particles, SW Bornholm*. Master Thesis, University of Oslo, 102 p.
- Parsons, I. 2010. Feldspars defined and described: a pair of posters published by the mineralogical society. Sources and information. *Mineralogical Magazine*, 74 (3), 529-551 p.
- Powers, M. C. 1953. A New Roundness Scale for Sedimentary Particles. *Journal of Sedimentary Petrology*, 23 (2), 117-119 p.
- Que, M. & Allen, A. R. 1996. Seritization of plagioclase in the Rosses Granite Complex, Co. Donegal, Ireland. *Mineralogical Society*, 60, 927-936 p.
- Reading, H. G. & Levell, B. K. 1996. Controls on the sedimentary rock record. In: Reading, H. G. (ed.) *Sedimentary Environments*. 3 ed.: Blackwell Publishing company, 704 p.
- Reineck, H. E. & Sing, I. B. 1975. *Depositional Sedimentary Environment*, Springer-Verlag, 439 p.
- Rubey, W. W. 1933. The Size-Distribution of Heavy Minerals Within a Water-Laid Sandstone. *Journal of Sedimentary Petrology*, 3, 3-29 p.
- Rust, B. R. 1977. Depositional models for braided alluvium. *Canadian Society of Petroleum Geologists*, 5, 605-623 p.
- Selley, R. C. 1996. *Ancient sedimentary environments and their sub-surface diagnosis, fourth edition*, Chapman & Hall, 300 p.
- Sietronics. 2013. *Siroquant version 4* [Online]. Available: <http://www.siroquant.com/> [Accessed 28.05 2017].
- Smith, N. D. 1970. The Braided Stream Depositional Environment: Comparison of the Platte River with Some Silurian Clastic Rocks, North-Central Appalachians. *Geological society of America Bulletin*, 81, 2993-3014 p.
- Smith, N. D. 1971. Transverse Bars and Braiding in the Lower Platte River, Nebraska. *Geological society of America Bulletin*, 82, 3407-3420 p.
- Småkasin, R. Ø. 2017. *The Eocambrian Valdres Group at Skarvemellen, Mellane- field observations and petrographical analysis*. Master thesis, University of Oslo.

- Strand, T. 1959. Valdres-sparagmittens stratigrafiske stilling. *Norges Geol. Unders.*, 205, 184–198 p.
- Turner, P. & Whitaker, J. H. 1976. Petrology and provenance of Late Silurian fluvial sandstones from the Ringerike Group of Norway. *Sedimentary Geology*, 16, 45-68 p.
- Törnebohm, A. E. 1873. Ueber die Geognosie der schwedischen Hochgebirge. *Kongl. Svenska Vetenskapsakad. Handl. Bih.*, 1, 59 p.
- Törnebohm, A. E. 1882. Om Vemdalsquartsiten och öfriga quartsitiska bildningar i Sveriges sydliga fjälltrakter. *Geol. Fören. Stockholm. Förh.*, 6, 274-294 p.
- Törnebohm, A. E. 1888. Om fjällproblemet. *Geol. Fören. Stockholm. Förh.*, 6, 274-294 p.
- Walker, J. D., Geissman, J. W., Bowring, S. A. & Babcock, L. E. 2012. *GSA Geologic Time Scale* [Online]. The Geological Society of America, Inc. Available: https://www.geosociety.org/GSA/Education_Careers/Geologic_Time_Scale/GSA/timescale/home.aspx [Accessed 19.03 2017].
- Wentworth, C., K 1922. A scale of grade and class terms for clastic sediments. *Journal of the Geological Society* 27, 377-392 p.

Appendix A (Thin sections)

Table 1: Thin section observations of facies 1 and 2 of the Rundemellen samples.

Facies	Sample	Lithology	Dominating framework configuration	Average size of the 10 largest grains (mm)	Average grain size	Most common grain shape	Sorting	Mineral content		Feldspar preservation		Remarks/Comments
								1.	2.	K-fsp.	Plag.	
1	Rund 1-13-16	Conglomerate	Grain supported	1,82	Coarse sand	Sub-rounded	Poorly-moderate	Quartz K-fsp. Plag. Mica Hem.	Seric. Opaq.	II/III	II/III	Coarse clastic conglomerate. Quartz is the most abundant mineral, and also represents the largest grains in the matrix. Rock fragments are present in the matrix together with K-feldspar, plagioclase and mica. Traces of hematite.
	Rund 1-14-16	Conglomerate	Grain supported	4,04	Very coarse	Angular to sub-rounded	Poorly sorted	Quartz K-fsp. Plag. Mica Hem.	Opaq.	II	II/III	Coarse clastic conglomerate. Quartz is the most abundant mineral, and also represents the largest grains in the matrix. A large amount of the quartz grains are polycrystalline. Rock fragments are present in the matrix together with K-feldspar, plagioclase and mica. Traces of hematite.
	Rund 1-15-16	Conglomerate	Grain supported	5,26	Gravel	Sub-angular	Very poorly sorted to poorly sorted	Quartz K-fsp. Plag. Mica Hem.	Seric. Opaq.	IV	V	Coarse clastic conglomerate. Quartz is the most abundant mineral and represents the largest grains in the matrix. Rhyolite, quartzite and granite make up a large part of the clasts in the conglomerate together with K-feldspar. Rock fragments are present in the matrix together with K-feldspar, plagioclase and mica. Traces of hematite.
2	Rund 1-6-16	Sandstone	Grain supported	1,05	Medium sand	Sub-angular to sub-rounded	Well sorted	Quartz K-fsp. Plag. Mica	Seric. Opaq.	III	II	
	Rund 1-7-16	Sandstone	Grain supported	1,05	Coarse sand	Sub-angular to sub-rounded	Well sorted	Quartz K-fsp. Plag. Mica Hem.	Seric. Opaq.	III	III	

Table 2: Thin section observations of Rundemellen samples representing facies 2.

Facies	Sample	Lithology	Dominating framework configuration	Average size of the 10 largest grains (mm)	Average grain size	Most common grain shape	Sorting	Mineral content		Feldspar preservation		Remarks/Comments
								1.	2.	K-fsp.	Plag.	
2	Rund 1-8-16	Sandstone	Grain supported	0,93	Medium to coarse sand	Sub-angular to sub-rounded	Well sorted	Quartz K-fsp. Plag. Mica	Seric. Opaq.	II/III	II/III	
	Rund 1-9-16	Sandstone	Grain supported	1,21	Coarse sand	Sub-angular to sub-rounded	Very well sorted	Quartz K-fsp. Plag. Mica	Opaq.	III	III	
	Rund 1-10-16	Sandstone	Grain supported	1,07	Coarse sand	Sub-rounded	Well sorted	Quartz K-fsp. Plag. Mica	Seric. Opaq.	III	II/III	
	Rund 1-12-16	Sandstone	Grain supported	2,84	Very coarse sand	Sub-angular	Moderately sorted	Quartz K-fsp. Plag. Mica		IV	IV	
	Rund 2-1B-16	Sandstone	Grain supported	1,12	Coarse sand	Sub-angular to sub-rounded	Well sorted	Quartz K-fsp. Plag. Mica	Seric. Opaq.	II	III	
	Rund 2-2-16	Sandstone	Grain supported	1,01	Coarse sand	Angular to sub-angular	Well sorted	Quartz K-fsp. Plag. Mica	Seric. Opaq.	III	III	
	Rund 2-5-16	Sandstone	Grain supported	0,93	Medium sand	Sub-angular to sub-rounded	Well sorted	Quartz K-fsp. Plag. Mica	Seric. Opaq.	II	III	
	Rund 2-6-16	Sandstone	Grain supported	1,00	Coarse sand	Angular to sub-angular	Moderately to well sorted	Quartz K-fsp. Plag. Mica	Seric. Opaq.	III	III	

Table 3: Thin section observations of samples representing facies 2,3 and 4 from Rundemellen.

	Sample	Lithology	Dominating framework configuration	Average size of the 10 largest grains (mm)	Average grain size	Most common grain shape	Sorting	Mineral content		Feldspar preservation		Remarks/Comments
								1.	2.	K-fsp.	Plag.	
2	Rund 2-8A-16	Sandstone	Grain supported	1,01	Medium sand	Sub-rounded	Moderately sorted	Quartz K-fsp. Plag. Mica	Seric. Opaq.	II	II	
	Rund 2-8-16	Sandstone	Grain supported	1,17	Coarse sand	Sub-angular	Well sorted	Quartz K-fsp. Plag. Mica	Seric. Opaq.	II/III	II	
3	Rund 1-11-16	Sandstone	Matrix supported	0,82	Fine-grained sand	Sub-rounded	Moderately sorted	Quartz K-fsp. Plag. Mica Hem.	Seric. Opaq.	II/III	II/III	High content of mica and sericite, which makes up large parts of the matrix. The largest grains in the sample are quartz, mostly undulating. High content of opaque grains.
	Rund 2-3-16	Sandstone	Matrix supported	0,69	Fine-grained sand	Angular to sub-angular	Poorly sorted	Quartz K-fsp. Plag. Mica Hem.	Seric. Opaq.	II/III	II/III	High content of mica and sericite, which makes up large parts of the matrix. The largest grains in the sample are quartz, mostly undulating. High content of opaque grains.
	Rund 2-7B-16	Sandstone	Matrix supported	0,61	Fine-grained sand	Sub-angular to sub-rounded	Very poorly to poorly sorted	Quartz K-fsp. Plag. Mica Hem.	Seric. Opaq.	II/III	II/III	High content of mica, which makes up large parts of the matrix. The largest grains in the sample are quartz, mostly undulating. High content of opaque grains.
4	Rund 1-5-16	Breccia	Matrix supported	4,53	Gravel to very coarse sand	Angular	Very poorly sorted	Quartz K-fsp. Plag. Mica Hem.	Seric. Opaq.	II/III	II	Matrix supported breccia with K-feldspar clasts of varying size. The matrix consists of mica and small grains of quartz, K-feldspar, plagioclase and hematite. Opaque mineral grains are abundant.

Table 4: Thin section observations of samples representing facies 1 from Skarvemellen (Småkasin, 2017).

Facies	Sample	Lithology	Dominating framework configuration	Average of the 10 largest grains	Average grain size (mm)	Most common grain shape	Sorting	Mineral content		Feldspar preservation		Remarks/Comments
								1.	2.	K-fsp.	Plag.	
1	Ska 11-16	Conglomerate	Grain supported	2.27 mm	Coarse 0.65 mm	Sub-rounded	Poor	Qtz. K-fsp. Plag. Mica Seric.	Hem. R.F	III	II	Rock Fragments: Rhyolite, Granite and quartzite. Rock fragments are the largest grains in the sample. Mica is pore filling.
	Ska 10-16	Conglomerate	Grain supported	1.48 mm	Coarse 0.88 mm	Sub-rounded	Well	Qtz. K-fsp. Plag. Mica	Hem. R.F	III	III	Rock Fragments: Rhyolite, Granite and quartzite. Small amounts of pore filling mica. Fractured grains, filled with epoxy, mica or polycrystalline quartz.
	Ska 2-9-16	Conglomerate	Grain supported	1.22 mm	Coarse 0.55 mm	Sub-rounded to rounded	Well	Qtz. K-fsp. Plag. Mica	Hem. R.F	III	III	Rock Fragments: Rhyolite, Granite and quartzite. Mica is pore filling.
	Ska 2-8-16	Conglomerate	Grain supported	4.84 mm	Very coarse 1.94 mm	Sub-rounded to rounded	Poor	Qtz. K-fsp. Plag.	Opq. R.F			Rock Fragments: Rhyolite, Granite and quartzite. Largest rock fragments are the quartzites in this sample. Rhyolite and granite occur as small grains in the matrix
	Ska 2-7-16	Conglomerate	Grain supported	0.54 mm	Medium 0.46 mm	Sub-rounded	Well	Qtz. K-fsp. Plag. Mica	Hem.	III	III	Represents the conglomerate matrix.
	Ska 2-5-16	Conglomerate	Grain supported	4.47 mm	Very coarse 1.16 mm	Sub-rounded	Moderate	Qtz. K-fsp. Plag. Mica	R.F Hem	II/III	II	Rock fragments of rhyolite, granite and quartzite are the largest grains in the sample.

Table 5: Thin section observations of Skarvemellen samples representing facies 2 (Småkasin, 2017).

Facies	Sample	Lithology	Dominating framework configuration	Average of the 10 largest grains	Average grain size (mm)	Most common grain shape	Sorting	Mineral content		Feldspar preservation		Remarks/Comments
								1.	2.	K-fsp.	Plag.	
2	Ska 9-16	Arkose	Grain supported	2.315 mm	Coarse 0.58 mm	Sub-rounded	Moderate	Qtz. K-fsp. Plag. Mica	Hem.	II	II	Fracturing of the grains, especially the quartz grains.
	Ska 8-16	Arkose	Grain supported	0.61 mm	Medium 0.41 mm	Sub-angular to sub-rounded	Moderate	Qtz. K-fsp. Plag. Mica Seriz.	Hem. R.F	III	III	Fracturing of the grains. Mica is pore filling.
	Ska 6-16	Arkose	Grain supported	0.71 mm	Medium 0.5 mm	Sub-angular	Well	Qtz. K-fsp. Plag. Mica Seriz.	R.F. Hem.	III	II	The grains are fractured.
	Ska 4-16	Arkose	Grain supported	1.11 mm	Medium 0.46 mm	Sub-rounded	Well	Qtz. K-fsp. Plag. Mica Seriz.	Hem.	III	II	Deformation cracks, filled with polycrystalline quartz.
	Ska 2-13-16	Arkose	Grain supported	1.00 mm	Coarse sand	Angular	Well	Qtz. K-fsp. Plag. Mica Seriz.	Hem. R.F	II/III	III	
	Ska 2-12-16	Arkose	Grain supported	1.01mm	Coarse 0.54 mm	Sub-rounded to rounded	Well	Qtz. K-fsp. Plag. Mica Seriz.	R.F	II/III	II/III	Mica is pore filling.

Table 6: Thin section observation of Skarvemellen samples representing facies 3 and 4 (Småkasin, 2017).

Facies	Sample	Lithology	Dominating framework configuration	Average of the 10 largest grains	Average grain size (mm)	Most common grain shape	Sorting	Mineral content		Feldspar preservation		Remarks/Comments
								1.	2.	K-fsp.	Plag.	
3	Ska 7-16	Sandstone	Grain supported	0.74 mm	Medium 0.4 mm	Sub-rounded	Moderate	Qtz. K-fsp. Plag. Mica Seriz.	Hem. R.F	III	II	Mica is pore filling. Zone with mica and heavy minerals.
	Ska 5-16	Sandstone	Matrix supported	0.52 mm	Medium 0.29 mm	Angular to sub-angular	Poor	Qtz. K-fsp. Plag. Mica Seriz.	Hem.	II/III	II/III	Fractured grains where some are filled with mica. Mica is pore filling.
	Ska 2-11-16	Sandstone	Matrix supported	0.71 mm	Medium 0.37 mm	Sub-rounded to rounded	Moderate to poor	Qtz. K-fsp. Plag. Mica Seriz.	Hem.	II/III	II/III	Mica is pore filling. Quartz grains are more rounded and larger than the feldspar grains.
	Ska 2-4-16	Sandstone	Matrix supported	0.87 mm	Fine 0.25 mm	Sub-angular	Very poor	Qtz. K-fsp. Plag. Mica	Hem.	III	II	Mica occur in zones with an enrichment of hematite.
	Ska 2-2-16	Sandstone	Matrix supported	0.72 mm	Fine 0.20 mm	Sub-rounded	Poor	Qtz. K-fsp. Plag. Mica	Hem.	III	III	Alternating zones of fine-grained and coarser material.
4	Ska 13-16	Breccia	Matrix supported	3.54 mm	Very coarse	Sub-angular to angular	Poor	Qtz. K-fsp. Plag. Mica	R.F	II	III	Rock fragments of quartzite.
	Ska 10-9-16	Breccia	Grain supported		Coarse – very coarse	Sub-angular to sub-rounded	Poor	Qtz. K-fsp. Plag. Mica	R.F	II	II	Large amounts of polycrystalline quartz. Rock fragments of quartzite.

Appendix B (Point counting)

Table 7: Point counting results of Rundemellen samples sorted according to facies (Und= undulatory extinction, Qtz= quartz, K-fsp= K-feldspar, Fsp= feldspar, R. F= rock fragment, HM= heavy minerals, Opaque=opaque minerals).

		Monocrystalline		Polycrystalline	Feldspar									
	Samples	Und.	Non. Und.	Undulatory	Total Qtz.	K-fsp.	Plagioclase	Total Fsp.	R.F	Matrix	Hematite	HM/OPQ	Porosity	Other
Facies 1	Rund 1-13-16	57.0	6.0	7.7	70.7	6.5	2.5	9.0	2.0	17.2	0.0	0.2	0.2	0.5
	Rund 1-14-16	59.5	10.0	15.5	85.0	4.7	0.2	4.9	5.0	3.7	0.0	0.2	1.2	0.0
Facies 2	Rund 1-7-16	43.5	6.3	7.0	56.8	9.0	3.2	12.2	7.0	21.5	0.0	1.5	0.0	0.2
	Rund 1-10-16	52.5	7.3	15.5	75.3	7.2	1.5	8.7	2.5	13.0	0.0	0.5	0.0	0.0
	Rund 1-11-16	37.5	6.5	3.5	47.5	12.0	3.7	15.7	1.2	33.5	0.0	0.2	1.7	0.2
	Rund 2-8-16	45.3	7.8	17.7	70.8	10.2	2.0	12.2	0.5	16.5	0.0	0.0	0.0	0.0
	Rund 2-6-16	43.0	8.0	6.5	57.5	8.1	3.0	11.1	6.7	22.0	0.0	2.5	0.2	0.0
	Rund 2-5-16	51.2	3.3	6.0	60.5	3.5	2.5	6.0	3.2	27.7	0.7	1.2	0.5	0.2
	Rund 2-2-16	52.5	7.7	7.7	67.9	12.0	2.2	14.2	3.5	14.2	0.0	0.2	0.0	0.0
Facies 3	Rund 2-7B-16	9.4	2.4	0.2	11.8	9.5	0.7	10.2	0.2	70.2	0.7	6.2	0.7	0.0
	Rund 2-3-16	15.8	4.2	0.7	20.7	3.2	1.0	4.2	0.7	66.7	0.0	7.7	0.0	0.0
Facies 4	Rund 1-5-16	17.0	4.0	12.5	33.5	26.6	2.7	29.3	2.5	24.0	0.3	9.7	0.7	0.0

Table 8: Point counting results of Skarvemellen samples sorted according to facies (Und=undulatory extinction, K-fsp= K-feldspar, Qtz=quartz, Fsp=feldspar, R.F=rock fragment, HM=heavy minerals, OPQ= opaque minerals, M= Melssenn Group) (Småkasin, 2017).

	Samples	Monocrystalline		Polycrystalline	Total Qtz.	Feldspar		Total Fsp.	R.F	Matrix	Hematite	HM/OPQ	Porosity	Other
		Und.	Non. Und.	Undulatory		K-fsp.	Plagioclase							
Facies 1	Ska 10-16	32,0	15,0	19,5	66,50	5,0	5,3	10,3	9,0	14,3	0,0	0,0	0,0	0,0
	Ska 2-9-16	52,5	5,0	8,8	66,3	7,5	7,5	15,0	2,3	12,8	1,5	1,3	0,8	0,3
	Ska 2-8-16	34,3	3,0	19,3	56,5	7,8	2,5	10,3	0,5	25,3	3,3	3,8	0,5	0,0
	Ska 2-7-16	26,0	8,0	9,0	43,0	11,3	3,8	15,0	6,3	31,3	1,5	2,8	0,0	0,3
	Ska 2-5-16	36,5	1,5	24,3	62,3	6,5	6,3	12,8	4,5	20,5	0,0	0,0	0,0	0,0
Facies 2	Ska 18-16 (M)	26,8	1,5	43,5	71,8	16,8	3,3	20,0	3,8	4,5	0,0	0,0	0,0	0,0
	Ska 16-16 (M)	22,5	5,0	35,3	62,8	13,5	3,8	17,3	1,5	18,3	0,3	0,0	0,0	0,0
	Ska 9-16	29,8	10,5	5,8	46,0	17,0	4,0	21,0	2,5	29,8	0,0	0,0	0,8	0,0
	Ska 8-16	44,8	11,0	6,5	61,8	2,8	6,0	8,8	7,8	19,0	1,5	0,0	1,0	0,3
	Ska 7-16	24,8	14,8	10,5	50,0	8,8	7,8	16,5	1,3	31,3	1,0	0,0	0,0	0,0
	Ska 6-16	37,0	13,0	5,3	55,3	5,3	3,8	9,0	5,5	25,3	1,8	2,0	1,0	0,3
	Ska 4-16	31,3	5,5	11,8	48,5	8,3	9,5	17,8	4,3	27,0	0,5	0,8	0,5	0,8
	Ska 2-13-16	12,8	37,8	14,0	64,5	10,0	5,8	15,8	6,3	12,3	0,0	0,0	0,8	0,5
Ska 2-12-16	39,8	8,3	10,0	58,0	10,5	6,8	17,3	5,8	14,8	0,3	2,5	1,3	0,3	
Facies 3	Ska 5-16	16,0	5,8	1,0	22,5	5,8	3,5	9,3	0,5	64,0	1,3	1,0	1,5	0,0
	Ska 2-11-16	28,0	3,8	4,0	35,8	3,0	2,5	5,8	2,0	54,0	1,3	1,0	0,5	0,0
	Ska2-4-16	17,8	5,8	0,8	24,3	1,8	3,5	5,3	1,0	45,3	22,3	1,5	0,0	1,0
Facies 4	Ska 13-16	20,0	1,0	11,0	32,0	9,0	5,3	14,0	6,0	44,8	0,3	3,0	0,0	0,0

Appendix C (XRD)

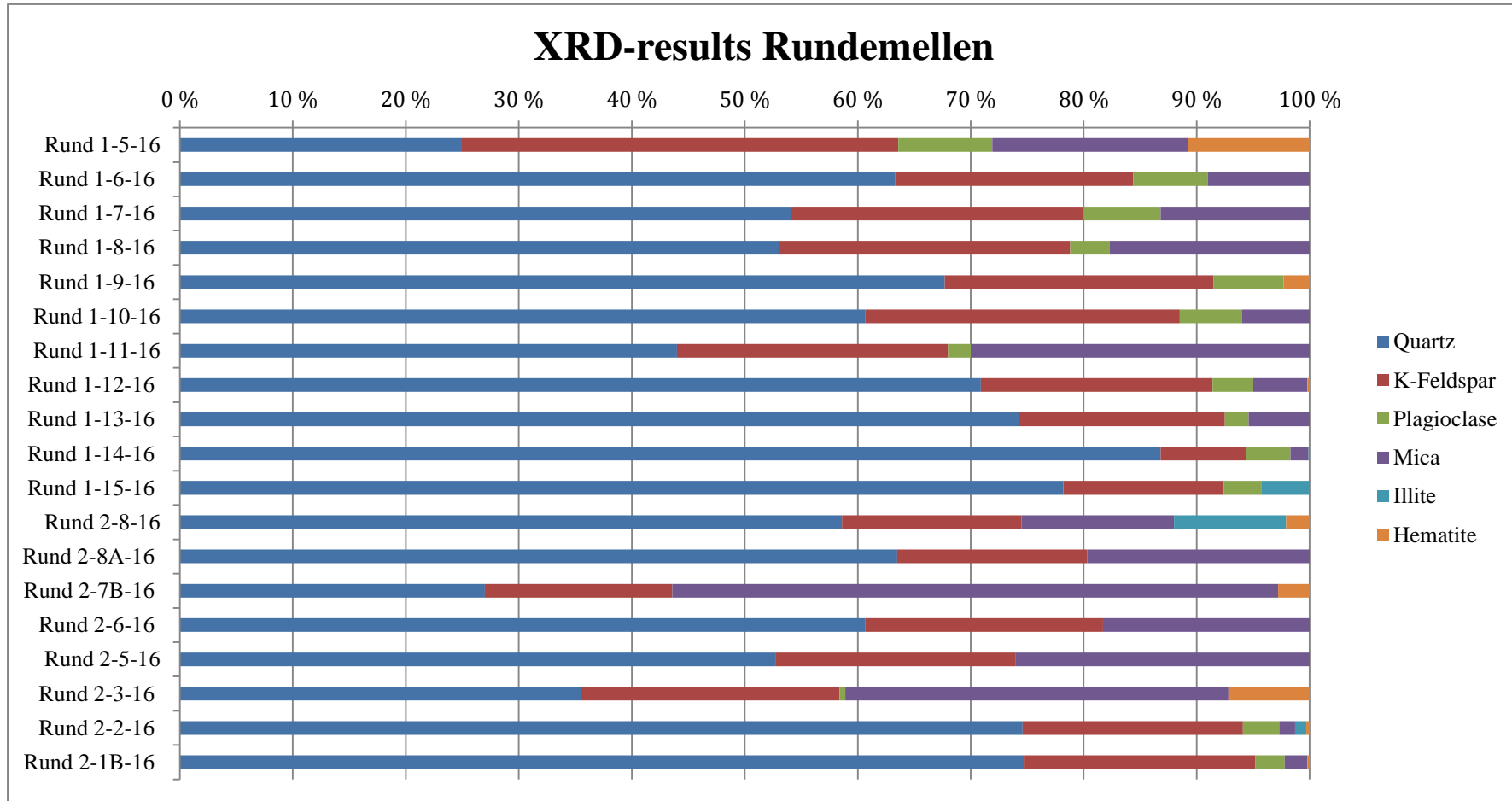


Figure 1: XRD-results of samples from Rundemellen shown in XRD%. The samples are in stratigraphic order.

Table 9: XRD results provided from the semi-quantitative analysis. The values are given in XRD% and the samples are arranged in stratigraphic order.

Sample	Quartz	K-Feldspar	Plagioclase	Mica	Illite	Hematite
Rund 1-5-16	24.9	38.7	8.3	17.3	0.0	10.8
Rund 1-6-16	63.3	21.1	6.6	9.0	0.0	0.0
Rund 1-7-16	54.1	25.9	6.8	13.2	0.0	0.0
Rund 1-8-16	53.0	25.8	3.5	17.7	0.0	0.0
Rund 1-9-16	67.7	23.8	6.2	0.0	0.0	2.3
Rund 1-10-16	60.7	27.8	5.5	6.0	0.0	0.0
Rund 1-11-16	44.0	24.0	2.0	30.0	0.0	0.0
Rund 1-12-16	70.9	20.5	3.6	4.8	0.0	0.2
Rund 1-13-16	74.3	18.2	2.1	5.4	0.0	0.0
Rund 1-14-16	86.8	7.6	3.9	1.6	0.1	0.0
Rund 1-15-16	78.2	14.2	3.3	0.0	4.3	0.0
Rund 2-8-16	58.6	15.9	0.0	13.5	9.9	2.1
Rund 2-8A-16	63.5	16.8	0.0	19.7	0.0	0.0
Rund 2-7B-16	27.0	16.6	0.0	53.6	0.0	2.8
Rund 2-6-16	60.7	21.0	0.0	18.3	0.0	0.0
Rund 2-5-16	52.7	21.3	0.0	26.0	0.0	0.0
Rund 2-3-16	35.5	22.9	0.5	33.9	0.0	7.2
Rund 2-2-16	74.6	19.5	3.2	1.4	1.0	0.3
Rund 2-1B-16	74.7	20.5	2.6	2.0	0.0	0.2

XRD-Results Skarvemellen

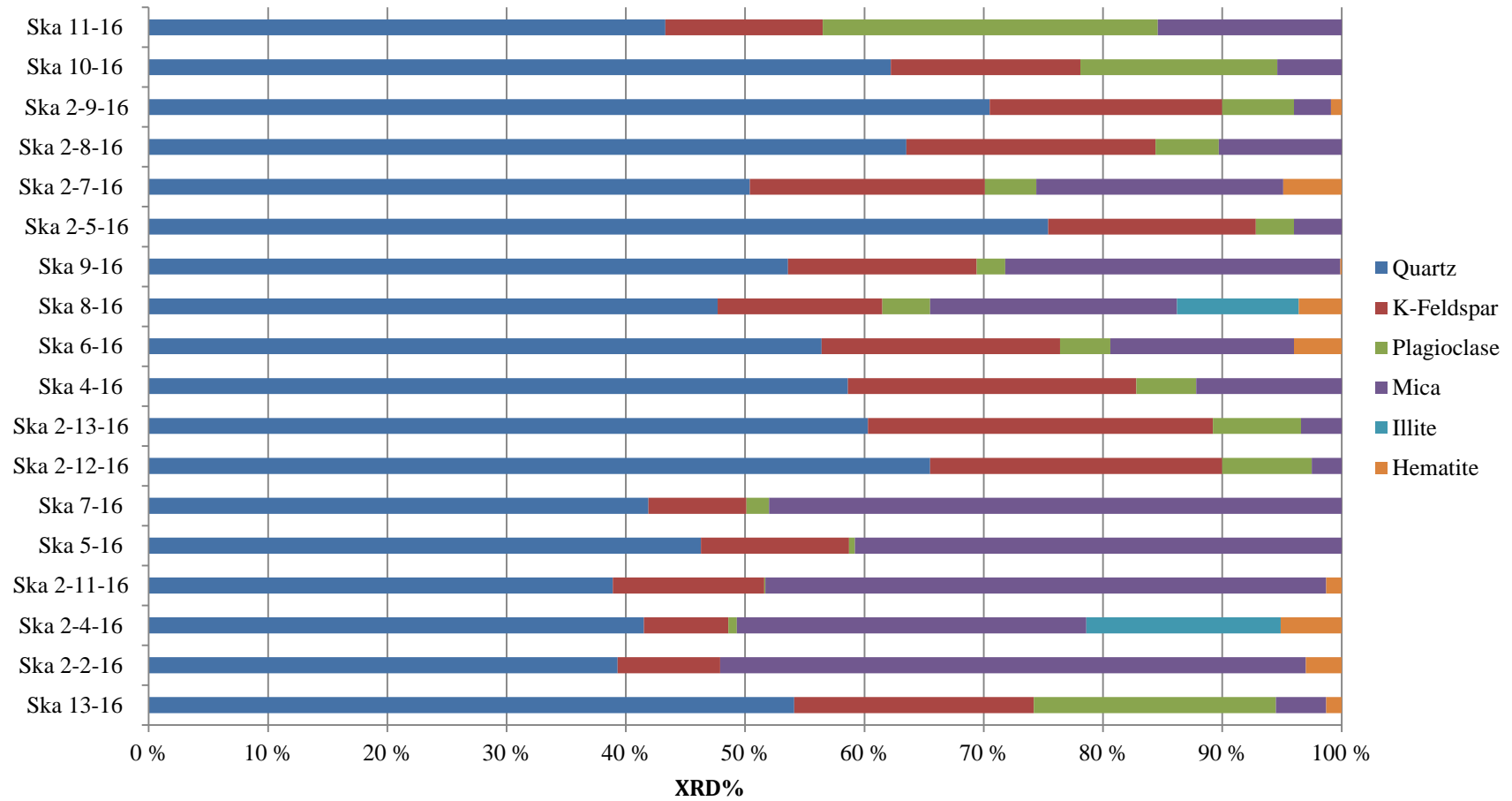


Figure 2: Barplot of XRD-results of Skarvemellen samples, given in XRD% (Småkasin, 2017).

Table 10: XRD-results of the Skarvemellen samples from the semi-quantitative analysis. The values are given in XRD% (Småkasin, 2017)

Sample	Quartz	K-Feldspar	Plagioclase	Mica	Illite	Hematite
Ska 13-16	54,1	20,1	20,3	4,2	0	1,3
Ska 2-2-16	39,3	8,6	0	49,1	0	3
Ska 2-4-16	41,5	7,1	0,7	29,3	16,3	5,1
Ska 2-11-16	38,9	12,7	0,1	47	0	1,3
Ska 5-16	46,3	12,4	0,5	40,8	0	0
Ska 7-16	41,9	8,2	1,9	48	0	0
Ska 2-12-16	65,5	24,5	7,5	2,5	0	0
Ska 2-13-16	60,3	28,9	7,4	3,4	0	0
Ska 4-16	58,6	24,2	5	12,2	0	0
Ska 6-16	56,4	20	4,2	15,4	0	4
Ska 8-16	47,7	13,8	4	20,7	10,2	3,6
Ska 9-16	53,6	15,8	2,4	28,1	0	0,1
Ska 2-5-16	75,4	17,4	3,2	4	0	0
Ska 2-7-16	50,4	19,7	4,3	20,7	0	4,9
Ska 2-8-16	63,5	20,9	5,3	10,3	0	0
Ska 2-9-16	70,5	19,5	6	3,1	0	0,9
Ska 10-16	62,2	15,9	16,5	5,4	0	0
Ska 11-16	43,3	13,2	28,1	15,4	0	0

Appendix D (Heavy minerals)

Table 11: Heavy mineral results of samples from Rundemellen, Skarvemellen and the Hedmark Group. Hedmark Group: Ring 0= Ring Formation, Rin 2-15=Brøttum Formation, BK 1: Biri chalk (Biri Formation), MB 1= tillite from Moelv Brygge. Valdres Group: Ska= samples from Skarvemellen, Rund= Samples from Rundemellen. At= anatase, Ap=apatite, Ca= calcic amphibole, Cp=clinopyroxene, Ep=epidote, Gt=garnet, Mo=monazite, Op=orthopyroxene, Ru=rutile, Sp=spinel, To=tourmaline, Zr=zircon.

Sample	At	Ap	Ca	Cp	Ep	Gt	Mo	Op	Ru	Sp	To	Zr	Total	Count
Ska 2-4-16		27,5							0,5			72,0	100,0	200
Ska 6-16		1,0									R	99,0	100,0	200
Ska 8-16		17,0									5,0	78,0	100,0	200
Ska 10-9-16		21,5	R	R							2,5	76,0	100,0	200
Ska 2-12-16									4,5			95,5	100,0	22
Ska 16-16												(8)	0,0	8
Rund 1-5-16		2,0				0,5			1,5			96,0	100,0	200
Rund 2-5-16			0,5	0,5	1,0		R					98,0	100,0	200
Rund 2-6-16		2,0	1,0					1,0			0,5	95,5	100,0	200
Rund 1-7-16		4,0									0,5	95,5	100,0	200
Rund 1-8-16					2,9	1,0						95,1	100,0	105
Rund 2-8-16					1,8							98,2	100,0	55
Ring 0		73,5				1,5	0,5		R	R	1,0	23,5	100,0	200
Rin 2-15		49,0									1,0	50,0	100,0	200
BK 1		32,4	5,9						2,9		32,4	26,4	100,0	34
MB 1	0,5	75,5		R		R	R		0,5		0,5	23,0	100,0	200

Appendix E (Field measurements)

Table 12: Strike/dip measurements from Rundemellen.

No. of measurements	Strike/Dip
1.	260/88
2.	263/80
3.	265/82
4.	267/77
5.	267/78
6.	255/80
7.	260/60
8.	264/66
9.	265/58
10.	265/63
11.	261/70
12.	267/72
13.	259/60
14.	263/70
15.	260/83
16.	250/67
17.	255/70
18.	255/51
19.	259/50
20.	258/80
21.	259/65
22.	249/68
23.	258/67
24.	250/40
25.	254/60
26.	254/63
27.	261/52
28.	247/49

Table 14: Strike/dip measurements from Skarvemellen (Småkasin, 2017).

No. of measurements	Strike/Dip
1.	243/38
2.	248/33
3.	250/31
4.	253/35
5.	260/38
6.	250/32
7.	247/30
8.	256/30
9.	250/33
10.	250/33
11.	248/30
12.	254/32
13.	248/35
14.	247/30
15.	254/31
16.	355/32
17.	252/30
18.	253/34
19.	250/30
20.	252/30
21.	252/32
22.	260/32

No. of measurements	Strike/Dip
23.	255/36
24.	258/33
25.	256/33
26.	257/33
27.	258/29
28.	262/30
29.	253/34
30.	270/30
31.	258/32
32.	258/35
33.	248/41
34.	255/38
35.	250/42
36.	260/45
37.	252/35
38.	260/54
39.	256/30
40.	247/31
41.	263/54
42.	260/60
43.	257/38